Mag.pharm. Diana Kienberger

Investigation of coating properties of lipids with focus on their stability using hot melt coating

MASTERARBEIT

zur Erlangung des akademischen Grades

Diplom-Ingenieurin

Masterstudium Chemical and Pharmaceutical Engineering

eingereicht an der

Technischen Universität Graz

Betreuer

Prof. Andreas Zimmer

Pharmazeutische Wissenschaften

Graz, August 2014

EIDESSTATTLICHE ERKLÄRUNG

AFFIDAVIT

Ich erkläre an Eides Statt, dass ich die vorliegende Arbeit selbstständig verfasst, andere als die angegebene Quellen/Hilfsmittel nicht benutzt, und die den benutzen Quellen wörtlich und inhaltlich entnommenen Stellen als solche kenntlich gemacht habe. Das TUGRAZonline hochgeladene Textdokument ist mit der vorliegenden Masterarbeit identisch.

I declare that I have authored this thesis independently, that I have not used other than the declared sources/resources, and that I have explicitly indicated all material which has been quoted either literally or by content from the sources used. The text document uploaded to TUGRAZonline is identical to the present master's thesis.

Danksagung

Zunächst möchte ich mich an dieser Stelle bei allen Personen bedanken, die mich während der Anfertigung dieser Arbeit unterstützt haben.

Ein besonderer Dank gilt meinem Betreuer, Herrn Prof. Andreas Zimmer, für das Bereitstellen dieses interessanten Themas der Diplomarbeit und meiner Zweitbetreuerin Dr. Sharareh Salar-Behzadi, die stets für mich ansprechbar war und trotz ihres vollen Terminkalenders Zeit fand, sich um meine Anliegen und Fragen zu kümmern.

Daneben gilt mein Dank auch allen Mitarbeitern des RCPE, die mit Ihrer Arbeit und ihren Vorschlägen zum Gelingen der Arbeit beigetragen haben, besonders Karin Becker, Neira Dzidic, Diogo Gomes Lopes und Julia Haring standen mir mit Rat und Tat zur Seite.

Großer Dank gebührt meiner Familie, insbesondere meinen Eltern, die mir mein Studium ermöglicht und mich in all meinen Entscheidungen unterstützt haben.

Ebenfalls bedanken möchte ich mich bei meinem Freund, DI Martin Reithmeier, der immer ein offenes Ohr für mich hatte.

Kurzzusammenfassung

Die Lagerstabilität von Arzneimitteln spielt eine wichtige Rolle in der Produktentwicklung bei der pharmazeutischen Industrie. Im Zuge dieser Masterarbeit wird die Stabilität eines Coatingmaterials bestehend aus Lipid und Emulgator, welches zum Überziehen des Arzneistoffes und zur Herstellung von sogenannten „direct to mouth granules“ verwendet wird, untersucht.

Die verwendeten Lipide sind Dynasan® 116 und Dynasan® 118, gemischt mit unterschiedlichen Mengen des Emulgators Tween® 65. In einer früheren Arbeit wurde das Freisetzungsprofil des N-Acetyl Cystein gecoatet mit einer Mischung von Dynasan® 116 bzw. Dynasan® 118 und Tween® 65 nach der Produktion bzw. nach der Lagerung unter Raum Temperatur (25 °C) und 40°C untersucht. Dabei wurde festgestellt, dass Granulate mit einem höheren Emulgatoranteil nach Lagerung bei 40°C eine schnellere Arzneistofffreisetzung zeigen, wenn es sich um einen Arzneistoff mit einer glatten Oberfläche (wie N-Acetylcystein) handelt. Deshalb wird vermutet, dass eine Phasenseparation des Lipid/Emulgatorgemisches stattfindet und dadurch mehr Emulgator an der Oberfläche vorhanden ist, was zu einer schnelleren Freisetzung führt. Im Gegensatz dazu zeigt eine Darreichungsform mit rauer Oberfläche (z.B. Granulate) langsamere Freisetzung, der Emulgator dringt in die Poren ein, sodass weniger davon an der Oberfläche vorhanden ist. Um diese vermutete Phasenseparation nachzuweisen, wurden verschiedene Labormethoden wie Röntgenstrukturanalyse, Differential Scanning Calorimetry, FT-IR und Kontaktwinkelmessungen durchgeführt.

Zusammenfassend kann gesagt werden, dass die Ergebnisse den starken Verdacht der Phasenseparation bestätigten. In der Röntgenstrukturanalyse kann ein zusätzliches Signal genau dort beobachtet werden, wo auch das Tween® 65-Signal liegt. Bei Proben mit niedrigem Emulgatoranteil ist dieses Signal nur nach Lagerung bei 40°C zu sehen, wenn der Emulgatoranteil erhöht wird, lässt er sich auch bei Raumtemperatur beobachten.

Der Kontaktwinkel ist bei Proben mit hohem Anteil an Tween® 65 nach Lagerung bei 40°C deutlich erniedrigt, im Gegensatz zur Lagerung bei Raumtemperatur, wo keine signifikanten Unterschiede zur initialen Messung vorhanden sind. Für diese Messungen wurden Objektträger mit den Mischungen von Lipid und verschiedenen Prozentanteil an Emulgator gecoated. Die Objektträger sollen einen Arzneistoff mit glatter Oberfläche repräsentieren, eine Phasenseparation führt in diesem Fall zu einer besseren Benetzbarkeit durch den Emulgator an der Oberfläche und dadurch zu einem niedrigeren Kontaktwinkel.

Auch die FT-IR Messungen zeigen Veränderungen wie Signalverschiebungen, aber diese Effekte treten wahrscheinlich wegen Veränderungen der polymorphen Form der Lipide auf.

Andere chemische Prozesse wie die Abspaltung von Stearinsäure können durch Röntgenstrukturanalyse und DSC Messungen ausgeschlossen werden.

Die Kombination aller Ergebnisse zeigt deutliche Veränderungen des Coatingmaterials, und bestätigt den Verdacht einer Phasenseparation.

Abstract

The storage stability of formulations plays an important role in the product development in pharmaceutical industry. In this thesis, the stability of coating material (=lipid and emulsifier) used for coating of API and producing direct-to-mouth granules, is investigated after storage.

The lipids are Dynasan® 116 and Dynasan® 118, mixed with different amounts of emulsifier Tween® 65. Previously, the release profile of N-Acetylcystein coated with mixtures of Dynasan® 116 or Dynasan® 118 with Tween® 65 was investigated via dissolution tests after storage at room temperature (25°C) and 40°C. Samples with higher amount of emulsifier in the coating (25%) showed an accelerated release after storage. It was assumed, that the phase separation of the mixture of Tween® 65 and Dynasan® causes the faster release of API. Due to the smooth surface of API (N-Acetylcystein), it was also assumed that Tween® 65 accumulated in the surface and caused the faster release profile after storage. In comparison a formulation with a rough surface (for instance granules) showed slower release after storage. The emulsifier penetrates into the pores, therefore, less emulsifier is existent in the surface.

The aim of this work is to declare a phase separation of lipid and emulsifier, therefore, different methods such as small and wide angle X-ray scattering (SWAX), Differential Scanning Calorimetry (DSC), Fourier Transmissions Spectroscopy (FT IR) and the measurement of the contact angle are conducted.

In summary, a strong indication of phase separation could be observed. The X-ray scattering showed an extra signal at the area of the Tween® 65 signal, which was observed with low amounts of emulsifier after storage at 40°C. By increasing the amount of Tween 65®, this extra signal could also be observed after storage of samples at room temperature. The contact angle measured on coated plain glass microscope slides with the lipid and different percentages of Tween 65 clearly decreases after storing at 40°C. In comparison samples stored at room temperature did not show significant changes. The plain glass microscope slides were chosen to represent a smooth surface of API, in this case a phase separation leads to an increasing amount of emulsifier in the surface, and therefore the contact angle is decreasing.

The FT-IR measurements show an extra signal and signal shifting, but probably this occurs due to changes in the polymorphism of Dynasan® 116 and Dynasan® 118 during the storage.

Other chemical processes like cleavage of stearic acid from the Tween® 65 molecule could be precluded using SWAXS and DSC measurements.

In conclusion, the obtained results confirmed the theory of phase separation during the storage.

Table of contents

Danksagung 3

Kurzzusammenfassung 4

Abstract 6

Table of contents 7

I. Introduction 1

II. General part 2

1. Polymorphism of lipids 2

1.1 Polymorphism of Dynasan® 116 3

1.2 Polymorphism of Dynasan® 118 4

2. Manufacturing process 5

2.1 Fluid Bed 5

2.2 Coating 8

2.3. Hot melt coating 9

3. Analytical methods 10

3.1 X-ray scattering 10

3.2 Differential Scanning Calorimetry 15

3.3 Contact angle measurements 18

3.4. FT-IR 19

4. Sample preparation 21

4.1 Cryomill 21

III. Material and Methods 23

1. The formulation 23

1.1 Active pharmaceutical ingredient 23

1.2 Coating formulation 24

2. Mixture of excipients 27

2.1 X-ray scattering 27

2.2 Differential Scanning Calorimetry 28

2.3 Contact angle measurement 29
2.4 FT-IR 30
IV. Results and Discussion 31
1. X-ray scattering 31
1.1 Storage of mixtures of Dynasan® 116 or Dynasan® 118 with Tween® 65 38
1.2 Physical mixture 43
2. Differential Scanning Calorimetry 45
2.1 Storage of mixtures of Dynasan® 116 or Dynasan® 118 with Tween® 65 50
3. Contact angle measurement 54
3.1 Measurement on plain glass microscope slides 54
3.2 Measurement on porous plate 62
4. FT-IR 64
4.1 Dynasan® 116 66
4.2 Dynasan® 118 68
V. Conclusion 72
Bibliography 73
VI. Appendix 75
List of Illustrations 75
Table of equations 76
Table of figures 76
Table of tables 79
List of abbrevations 80

I. Introduction

This thesis deals with the investigation of the coating properties of mixtures of lipids and different amounts of emulsifier (=coating material) with focus on their stability. These coating formulations were used for producing direct-to-mouth granules, manufactured in a fluid bed hot melt coating device. The active pharmaceutical ingredients are N-Acetylcysteine coated with different types and amounts of lipids and various percentages of emulsifying agents. Due to the different polymorphic behaviour of lipids, the influence of different amounts of emulsifying agent on the transition of less stable alpha polymorh to the more stable beta has been also investigated.

The used lipids are tristearin (Dynasan® 118) and tripalmitin (Dynasan® 116), the emulsifier is polysorbat 65 (Tween® 65). Previously, the release profile of coated API has been investigated via dissolution tests after production and after storage at room temperature (25°C) and 40°C. Samples with higher amount of emulsifier Tween® 65 in the coating (25%) showed accelerated release of N-Acetylcystein after storage at 40°C for one month. It was assumed, that the phase separation of the mixture of Tween® 65 and Dynasan® 118 or 116 causes the faster release of API. The aim of this diploma thesis is the investigation of coating layers after preparation and after storage via different analytical methods, i.e. SWAXS, DSC, FT IR and the measurement of the contact angle.

II. General part

1. Polymorphism of lipids

Every long chain compound shows polymorphism, especially fats and lipids are known for this attribute. The chemical structure of triacylglycerols (TAG) is presented in Figure 1, which comprises a glycerol with three fatty acid moieties (R_1/ R_2/ R_3). If fatty acids are the same (R_1=R_2=R_3), the structure called monoacid TAG. In a mixed acid TAG the fatty acids are of different kind. Tripalmitin and tristearin are monoacid TAGs, with three palmitic and three stearic acid moieties, respectively.

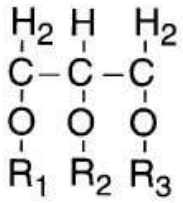

Figure 1. Triacylglycerol molecule.

[1]

A TAG normally has three polymorphic forms. The crystallization behaviour, i.e. the crystallization rate, crystal morphology, crystal sizes and their network, depends on the polymorphic form.

The polymorphism is affected by external factors, i.e. impurities, temperature, rate of crystallization, solvent or pressure. The chemical characteristics are influenced by the nature and properties of the three fatty acids rests of the TAG molecule. The three existing polymorphic forms are α, β´ and β, they are defined by subcell structures, which are based on cross-sectional packing modes of the zigzag aliphatic chain, as it can be observed in Figure 2.

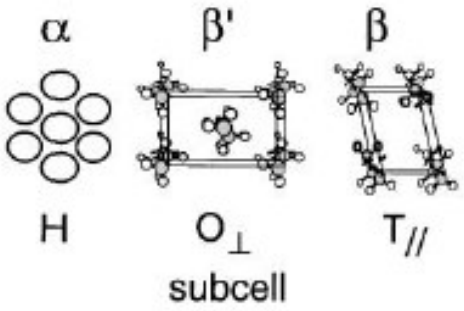

Figure 2. Polymorphism of a triacylglycerol molecule. [1]

An iterative sequence of the acyl chains included in a unit cell lamella along the long-chain axis is generated by the chain length structure. If the chemical characteristics of the three fatty acid moieties are the same or very related, a double chain length structure is generated, if the properties are different, a triple chain length is generated. The difference between a double and a triple chain length structure can be seen in Figure 3 [1].

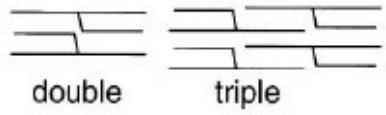

Figure 3. Chain length structure. [1]

According to the fatty acid compositions of the three moieties, the topic can be more complex, for example if they are heterogeneous TAGs. In several mixed-acid TAGs, no β form is available, so β´ becomes most stable, or two β forms are existing [1].

1.1 Polymorphism of Dynasan® 116

The molecular structures of the three polymorphs of Dynasan® 116 are described as disordered aliphatic chain conformation in α, intermediate packing in β´ and most dense packing in β, as it can be seen in Figure 4.

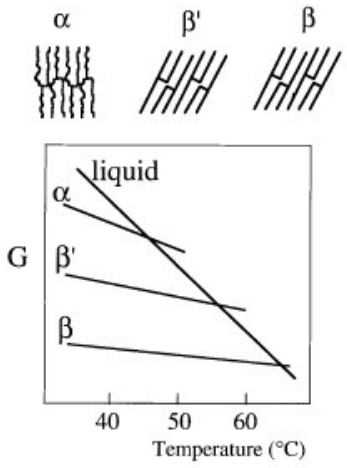

Figure 4. Molecular structures and Gibbs energy (*G*)-temperature relation of Dynasan® 116.
[1]

The highest Gibbs free energy (*G*) is observed in α, an intermediate energy in β´ and the lowest energy is observed in β. In Figure 4, a G-T (temperature) relationship can be seen. According to the

rate of crystallization and the related impact of the molecular structures, the crystal morphology is amorphous- like for α, tiny bulky shape for β´ and needle shape for β [1]. The stable polymorph is the β form, the melting point of each polymorph can be observed in Table 1.

Polymorph	Melting point [°C]
A	45
β´	57
B	66

Table 1. Melting points of Dynasan® 116.

[2]

1.2 Polymorphism of Dynasan® 118

The polymorphic properties of Dynasan® 118 are basically common to those in the other fats, i.e. Dynasan® 116. It has three polymorphic forms, α, β´ and β, where β is the most stable polymorph. The α and β´ form are monotropic, β has a triclinic crystal lattice. The α-polymorph forms a hexagonal crystal lattice, where the hydrocarbon chains are perpendicular to the basic level. The hydrocarbon chains are tilted to the basic level, providing a β-polymorph. The β´-polymorph has the same arrangement of hydrocarbon ions, but an orthorhombic crystal lattice is formed [3].

The melting points and corresponding enthalpies of fusion can be seen in Table 2.

Polymorph	Melting point [°C]	Enthalpy of fusion [kJ.mol^{-1}]
A	54	145
β´	63,5	143
B	72	203

Table 2. Melting points and corresponding enthalpies of fusion.

[3] [4]

2. Manufacturing process

2.1 Fluid Bed

The fluid bed process is an air suspension process, which is widely used in chemical engineering and pharmaceutical manufacturing such as mixing, granulation and coating [5].
Basically, using fluid bed technology, material to be processed is placed into a process chamber and held in the fluidized state using an airflow, which is blown upwardly and through a perforated base plate into the process chamber. In principle, a fluid bed keeps particles in suspension in a close area by blowing air through the particle bed. Air velocity and particle characteristics are parameters that influence the state of the bed. Coating in fluid beds is achieved by spraying the coating liquid onto the particles. Fluid beds are used in pharmaceutical manufacturing for granulation, drying and coating processes, as for agglomeration and drying processes [6] [7].
Fluid bed technology has the following advantages in comparison to other granulation and coating technologies such as pan coating and using drums and mixers: because of the high rates of heat and mass transfer, a uniform temperature distribution within the bed can be reached and short processing times are possible. In addition, shearing forces occurring in fluid beds help to avoid the formation of agglomerates. Moreover, a continuous flow of particles through the spray zone, which is fundamental for constant product quality, can be achieved [8].
Fluid beds exist in different scales, with a volume of the container from 1.5 l up to more than 3000 l.
The air flow rate differs from less than 750 m^3/h in smaller systems up to 14 000 m^3/h in big devices.
The accelerated air is warmed in a heater and then brought in the process chamber. Thereby the particles are held in motion and the kind of movement is controlled by various construction of base plate or processing chamber.
According to the position of the nozzle (Bottom spray, Top spray and Tangential spray) and depending on the operating conditions (continuous, batch), different types of process exist [5] [6].
Using these methods enables application of various processes such as granulation, pelleting, drying, coating and layering [7].

Bottom spray, Top spray and Tangential spray method will be discussed below. In Figure 5 a schematic diagram of a fluid bed equipment using top spray can be seen.

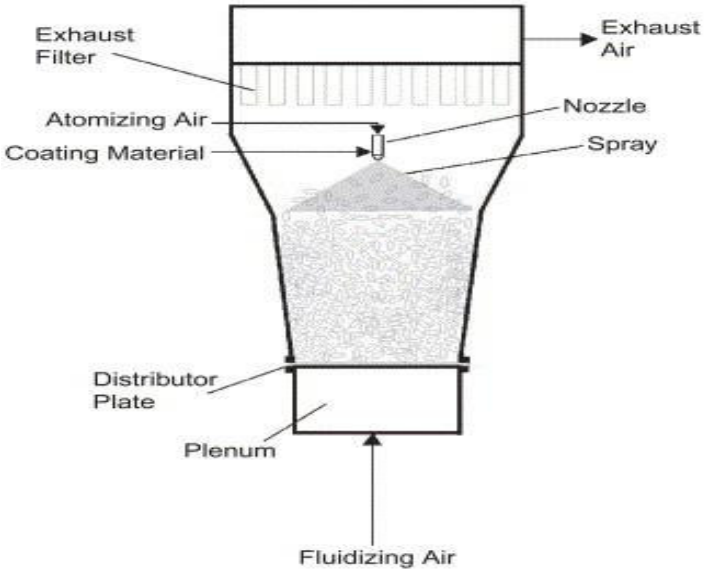

Figure 5. Schematic diagram of a fluid bed coating equipment (top spray)
[9]

2.1.1 Top Spray

In a top spray process, the spray nozzle is installed at the upper part of the process chamber, above the fluidized bed. The liquid is sprayed counter currently onto the fluidized particles. This technique is widely used in the food and feed industry, as well as in the fine chemical industry. In general, this method is more adequate for granulation. According to the uncontrolled fluidized bed, which does not assure optimal distribution of coating liquid on the bed, the conventional top spray method is not convenient for preparing dosage forms with modified release profiles [7] [10].

2.1.2 Bottom Spray

In bottom spray processing, the nozzle is installed at the bottom of the processing chamber and sprays upwards, concurrently into the fluidized bed. Due to this bottom spray method, Wale Wurster presented the wurster method in 1959. His construction includes a small inner column (the so-called wurster), which is fixed above the center of the air distribution base plate surrounding an upwards-directed nozzle. In the center, the perforations in the air distribution base plate are larger, smaller towards the periphery, and larger again along the outermost circle. According to this configuration, strong air stream and an upwards-directed core movement inside the wurster and a drop of the cores outside the wurster are enabled. Pressing cores to the container wall can be prevented by an elevated air stream near the edge of the container [7].

A constant residence time of particles in the spraying zone may be lead to a homogenous coating. The high speed of the particles results in a high kinetic energy, which avoids sticking of the wet particles. Therefore also small particles can be coated without agglomeration [5].

2.1.3 Tangential Spray

Using tangential spray process or rotor method, the particles are forced into a rotating movement by a rotating disc plate or by a particular construction of the air distribution base plate and the resulting air/gas flow or. The fluidizing air/gas gets in the process chamber through a ring gap between a rotating disc and the process chamber wall. According to this design, the circular motion of the feed material is guaranteed, while the coating liquid is sprayed tangentially through the bed. In the recent past, possibilities to combine the rotational movement of a core bed with the bottom spray method have been facilitated, the rotor method could also be seen as sub-category of bottom spray processing [7]. Similar to bottom spray process, the particle movement is considered to be homogenous. However, the kinetic energy is even higher than in bottom spray technique, which can lead to coating problems of very small particles and particles that are not spherically, they can be destroyed [10].

Suitable substances for fluid bed processing must have a sufficient hardness to avoid abrasion, due to the strong mechanical impact [5].

2.1.4 Fluid bed equipment with modified construction

In the recent years modifications in the construction of fluid bed devices, especially in the construction of base plate and spraying nozzle have been undertaken to improve the bed flow and thus to perform a more homogeneous particle movement and homogeneous distribution of spraying liquid to the bed.

One of these approaches is the Ventilus® system constructed by INNOJET HERBERT HÜTTLIN, Germany.

This construction, Innojet® Laboratory System Ventilus® V-2.5/1 with an Innojet® Hot-Melt-Device IHD-1. Ventilus® V-2.5/1 has been used for coating trials in this work. The construction of Ventilus system is described below:

The air distribution base plate is built up of a concentric arrangement of overlapping guiding plates. According to this design of the guiding plates, a radial airflow moving the bed radially towards the

wall of the process chamber, then upwards along the wall and then back to the center of chamber, is possible. This uniform circulation of the bed is sustained without friction between the core bed and the wall of the processing chamber. In the center of the overlapping guiding plates, a multimedia nozzle is located. Due to this design, the fluidization of the bed as well as the distribution of the spraying liquid are improved, a more homogeneous coating and better coating quality can be achieved [7].

2.2 Coating

In recent years the process of coating to achieve taste masking of multiparticulate systems has become more important. There are many reasons for this, as a patient centric product design to fulfil the requirements of patients, is desired. This happens in order to increase the adherence to medication, by masking of the unpleasant taste of API or by providing modified release profiling. Moreover, the multiparticulate systems improve the adherence of geriatric and paediatric population with difficulties in swallowing to medication.

Using fluid bed technology, every time a particle is flowing through the coating zone, low amount of coating material is added until the entire surface has been covered, this process is illustrated in Figure 6. Coating material can be solved or dispersed in a liquid, which is sprayed on the surface of particles. The main procedures are droplet formation, contact, spreading, coalescence and evaporation, they nearly happen at the same time during the process. By constant repeat of this procedures, film thickness can be continuously increased [11].

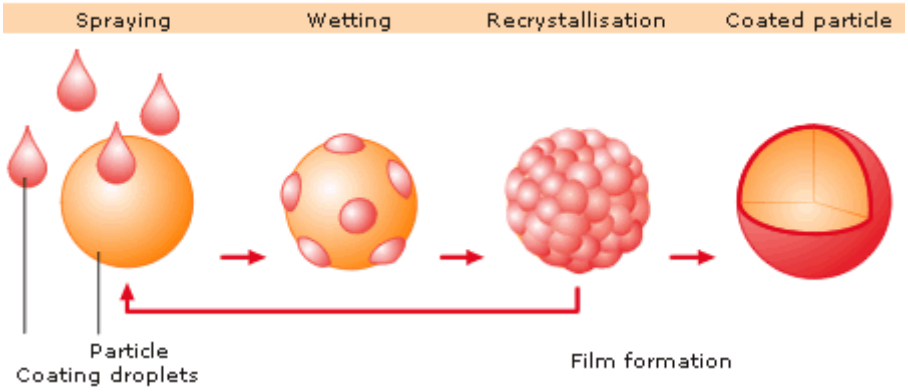

Figure 6. Formation of a coated particle during a coating process.

[12]

2.3. Hot melt coating

Hot-melt coating is a flexible and low cost technology which can be used for microencapsulation, pelletisation, coating of tablets and so on. It is flexible because a conventional fluid bed can be modified to spray molten lipid-based formulations avoiding solvents and therefore the intensive cost of organic solvents, and the high temperatures and long drying treatments of aqueous solvents. Moreover, this technology is environment friendly since coating excipients are lipids being naturally occurring and digestible compounds. Other advantages are the reduced processing time and the decreased risk of microbial contamination, according to the water-free manufacturing step. Furthermore, a good taste masking quality can be guaranteed and a controlled release profile can be provided, whereby the number of daily dose can be decreased.

The main lipid excipients used for hot melt coating are waxes, vegetable oils, polyoxylglyceride, fatty acids and partial glycerides. They are selected according to their influence on drug release, the cabability to protect against degradation, the cabability to mask unpleasant taste and due to a number of physicochemical characteristics, as thermal or rheological behaviour and polymorphism [13].

3. Analytical methods

3.1 X-ray scattering

3.1.1 Small angle X-ray scattering (SAX)

SAX is a method to analyse structural characteristics of colloidal dimension. The particle size is inversely proportionate to the scattering angle, this is shown by the reciprocity law, which describes every scattering process. According to the big scale of colloidal dimensions compared to the smaller X-ray wavelength, the angular range of cognoscible scattering is small. X-rays are basically scattered by electrons, thus, X-Ray small angle scattering is always monitored. But it is only monitored, if electron density heterogeneities of colloidal size occur in the sample. Due to the fact that incoherent scattering is low at small angles, following explanations are limited to coherent scattering.
The scattering process can be described by electrons, which oscillate with the frequency of the X-rays going through the samples and give out coherent secondary waves. These waves influence each other. Figure 7 demonstrates this phenomenon.

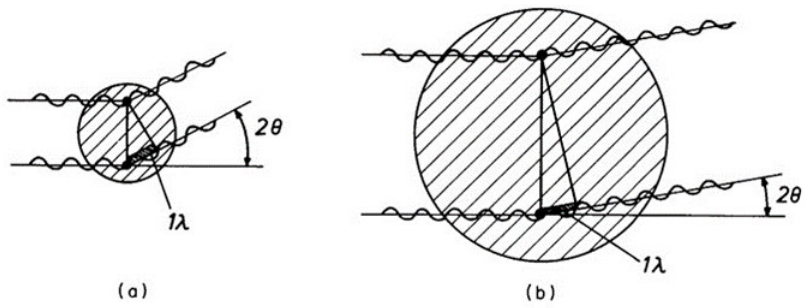

Figure 7. A small and a bigger spherical particle

[14]

A spherical particle is seen in Figure 7 a, it is supposed that the waves scattered from the two points shown to an angle 2Θ have a phase difference of 1λ. Because of destructive influence, no scattering in the direction 2Θ will be observed if scattering from all points is involved. Smaller scattering angles reveal smaller path differences, thereby the waves mutually reinforce one another. In the direction of zero scattering angle all the waves are in phase, there the highest signal of scattering can be found.

In Figure 7 b, a bigger particle can be seen. According to a smaller scattering curve, the phase difference of 1λ can be observed at smaller scattering angles. In conclusion it can be said that particles, that are big in comparison to the wavelength, can be analysed with X-ray small angle scattering. So the knowledge about the scattering curve is important. Figure 8 shows different types of scattering curves, where the y axis represents I, the Fourier Inversion.

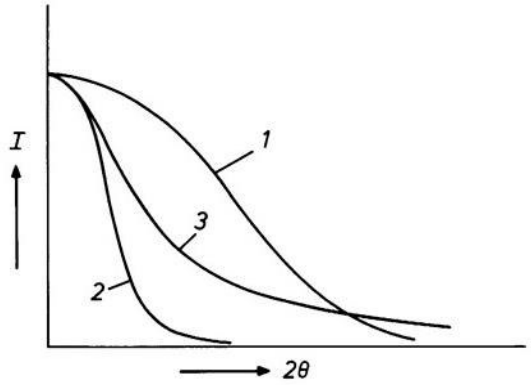

Figure 8. Different types of scattering curves

[14]

For the small particle, shown in Figure 7 a, the observed scattering curve will be like curve 1. For bigger particles, as shown in Figure 7 b, the curve will be narrower, like curve 2. Different techniques to calculate such scattering curves exist.

One method uses the distance distribution function of the electrons $p(r)$. Fourier inversion, the scattering curve I can be calculated.

Equation 1:

$$I(h) = 4\pi \int_0^\infty p(r) \frac{\sin hr}{hr} \cdot dr$$

$$I(h) = Fourier\ Inversion$$

$$p = \ electron\ density$$

$$h = \frac{4\pi \sin \theta}{\lambda}$$

$\lambda =$phase difference

$$2\theta = scattering\ angle$$

If electrons are shifted within a particle by small distances in comparison to the complete particle dimension, the small angle scattering curve will stay basically uninfluenced. Thereby, particles that are less inhomogeneous can be seen with consistent electron density distribution.

Until now, an isolated particle was observed. For homodisperse, adequate dilute solutions, the sum-up of intensities of every particle leads to the result. It is very difficult to estimate the size, shape, mass and actually the electron density distribution from the scattering curve. A model particle that corresponds to the particle in solution, so that the scattering curve is identical, should be detected. If the curve detected is precisely and the angular range is large, the issue of analysis is more demanding and more rewarding. If completive maxima can be observed in addition to the main maximum of the curve, the latter is especially true. These additional maxima are often very low, but small variations in the model can influence their position, height and shape. An entire solution for the challenge of finding an adequate model needs multiple cycles of estimation, sometimes just experiment and error.

A number of information can be obtained from the scattering curve, offering the background for every analysis.

One of these parameters is the radius of gyration, R, which is the root mean square of the distances of every electron from its balance point. Thus, R is a unit for the areal expansion of the particle, it is proportionate to the square root of the fall of the tangent in the limit $2\Theta \rightarrow 0$, seen in a plot of $\ln I \; vs \; (2\Theta)^2$ (Guinier plot). In case of rod shaped particles, multiplication of the scattering curve by 2Θ results in the cross-section factor. This factor is a curve, which is only depending on size, shape and electron density distribution inside the cross-section R_c.

If particles are plate-like structured, multiplication by 2Θ gives the thickness factor that is depending on the particle thickness and electron density distribution vertical to the particle plane.

For particles with consistent electron density distribution, the parameter $Volume\, V$ can be computed, as can be seen in Equation 2.

Equation 2:

$$V = K - \frac{I_0}{\int_0^\infty I(2\Theta) * (2\Theta)^2 * d(2\Theta)}$$

$$V = Volume$$

$$I = Fourier\ Inversion$$

$$K = \frac{\lambda^3 * a^2}{4\pi}$$

$a =$ distance sample

$$d = diameter$$

$$2\Theta = scattering\ angle$$

For a known concentration, the value of the integral is not depending on the degree of dispersion. According to the increase of intensity and volume with the particle weight, the equation for V implies the quotient of I_0.

The quotient of scattering intensity and primary intensity are the "absolute intensity", if this factor is known, the $particle\ molecular\ weight$ can be received. Due to this, the small angle scattering can be utilized to kind of "weight" particles. A special property of it is, that an identification of the mass per unit length for rod shaped particles and the mass per unit area for plate-like structured particles can be achieved.

The last parameter is the $distance\ distribution\ function\ p(r)$, which is received by Fourier inversion of the scattering curve, seen in Equation 3.

Equation 3:

$$p(r) = \frac{1}{2\pi^2} \int_0^\infty I(h) * hr * \sin hr * dh$$

$$I = Fourier\ Inversion$$

$$d = diameter$$

$$p = \ electron\ density$$

$$h = \frac{4\pi \sin \theta}{\lambda}$$

Summing up, theoretical scattering curves can be calculated for a model of known shape. A collection of scattering curves for scores of three-axial bodies is available, with this collection and the parameters explained above, estimations of size and shape can be made. Particularly biological macromolecules as proteins, nucleic acids, viruses and ribosomes have been analysed. For more extensive particle shapes, an approximation of the particle with a high amount of small spheres is suitable.

In place of comparing experimental and theoretical scattering curves, theoretical and experimental functions $p(r)$ can be compared too. Both ways are similar, the comparison of functions has some benefits, it is closer to human intuition and one particle parameter ($largest\ particle\ dimension$) can be deduced directly.

To further improve the small angle method, the electron density inhomogeneities within the particles can be determined. Especially if the particle is built up of different chemical compounds, this is important. Two approaches exist: The first one is the convolution square root technique. The calculation of the radial electron density from the distance distribution function is possible.

The second method is the “phase –contrast technique”, which does not depend on any particle symmetry. According to the modification of the electron density of the solvent, the difference between particle and solvent is changed and so the scattering. The goal is to find a solvent with equal electron density to the particle compounds. So the scattering of this compound disappears and information about the remaining parts of the molecule can be received. However, finding adequate solvents is the major challenge of this method.

The investigated particles are often biological macromolecules with identical shape and stable composition. In contrast, natural and synthetic chain molecules have a rapidly changing coil structure. The “persistence length” is a suitable parameter for the degree of coiling.

The small angle scattering technique is also useful for the investigation of dissolved particles that are no biological macromolecules, e.g. oligomers.

But not only colloidal particles in solution can be studied using small angle scattering, but also solids, e.g. natural and synthetic high polymers, metals, allays and glasses can be investigated [14].

3.1.1.1. Principles of diffraction

Scattering

Due to the interference of waves scattered by a subject, diffraction is created. If X-rays strike the subject, every electron gets the source of a scattered wave. According to the high energy of an X-ray photon that differs from the binding energy of an atom, the electrons act like free electrons.

Thus, all secondary waves have similar intensity, as seen in the Thomson formula in Equation 4.

Equation 4:

$$I_e(\theta) = I_p * 7{,}9 * 10^{-26} * \frac{1}{a^2} * \frac{1 + 2\theta cos^2}{2}$$

I_p= primary intensity

a= distance from the subject to the point of registration

$$2\theta = scattering\ angle$$

The scattering angle 2θ has only a weak influence on the intensity [14].

3.1.1.2 Interference

Incoherent scattering occurs as well as coherent scattering, but due to the investigated small angle only coherent scattering is viewed. It is talked about coherence, if the amplitudes are added. So the intensity is given by the absolute square of the resulting amplitude. The amplitudes differ in their phase φ that is dependent on the position of the electron in space. A single secondary wave is suitable illustrated as the complex form: $e^{i\varphi}$. The phase φ is calculated as $2\pi/\lambda$ time the difference between the optical path and an optional reference point.

It is also possible to measure extremely anisometric and composite particles, e.g. rod-like particles and flat particles. According to their special pattern in diffraction behaviour, this particles need specific treatment [14].

3.1.1.3 Instrumentation

Some special conditions must be present in an X-ray laboratory. First of all, complete darkness must be guaranteed, furthermore no strong vibrations, as caused by traffic are allowed. Another point is sufficient air conditioning, the temperature should be constant within ± 2°C, very high or low air humidity should be prevented [14].

3.1.2 Wide angle X-ray scattering

According to the position of the detector, which is closer to the sample, X-ray scattering can be observed at higher angles. Studying the WAXS region, information about secondary structures and their variations can be obtained. The evaluation of this data without high-definition models is difficult. Due to its high sensitivity, WAXS is used for the identification of structural affinities and description of structural fluctuations [15].

3.2 Differential Scanning Calorimetry

Calorimetry means the measurement of heat, and to measure heat, the exchange of heat has to take place. To quantify this heat exchange, the difference in temperature in a body can be used. Another possibility is to link the whole process to a heat flow which creates local differences in temperature. The production and consumption of heat can occur during chemical reactions or physical transitions, therefore calorimetry is a general technique to examine this processes. In a measuring equipment, a

precise known amount of heat is brought to a sample or emitted from the sample, the following modification of temperature is scaled [16].

The International Confederation for Thermal Analysis and Calorimetry (ICTAC) defines Differential Scanning Calorimetry as a process, in which the flow rate of heat to a sample is observed against time or temperature. The temperature of the sample is controlled [16].

Besides the determination of heat, DSCs can measure heat flow rates (power) and typical reaction and transition temperatures. The accurate determination of heat capacities has been enhanced over the last few years. Not only integral (total) heat of reactions or transitions can be measured, but also "partial heats" can be quantified using a certain temperature interval. This is important for kinetic determinations, evaluation of crystallinity and purity [16].

DSC measures the variation of an attribute (heat flow rate), which is connected to the change of the sample temperature. If no change of sample temperature occurs, no variation of heat flow can be observed. Therefore, a defined temperature program is always connected to a DSC measurement. In the event of thermally activated reactions or transitions, the temperature of the sample is changed due to inner procedures and causes the DSC signal. If the heat flow rate is not zero, a temperature difference between the sample and the reference is present, hence an alteration of the heat flow difference is connected to an alteration of the temperature [16].

Using a DSC, reaction heats and heats of transition or heat flow rates and their modifications at typical temperatures can be quantified. Small amount of sample (milligram range) is sufficient, it can be measured in wide temperature ranges and with high precision. DSC measurements are utilized in the following areas:

- characterization of samples
- reference measurements (quality control, identification of substances)
- stability testing
- determination of phase diagrams
- purity investigations
- kinetic evaluation
- safety research

DSC is also utilized together with other techniques for thermal analysis or other analytical methods, mostly in conjunction with Thermogravimetry (TG), less frequent in combination with Evolved Gas Analysis (EGA), Thermomicroscopy or Thermosonimetry.
The benefit of concurrent analysis is, that the sample is evaluated under similar conditions and that various information is received by using one measurement. But there are also disadvantages, as the lower sensitivity, the higher chance to failure, the increased time requirements and the higher equipment prices.

Summing up, DSC has been improved over the last few years, as now the following points are appropriate:

- the theoretical background and functioning of (heat-flux) DSC are better known and understood
- sources for mistakes and corrective measures are known
- according to suitable data treatment and efficient computers, the necessary quantifications can be made easily
- due to better calibration and measurement techniques the assurance of results is enhanced
- DSC is a fast and reliable technique with a broad area of use

3.2.1 Types of Differential Scanning Calorimeters

Two different types of DSCs exist, the heat flux DSC and the power compensation DSC. They distinguish in their structure and principle of measurement, but they are similar in their *differential method of measurement*. For both types it is determined as a technique of measurement, in which the scaled amount (sample) is compared with an amount of same kind. The known value differs minimally from the value of the sample, and the distinction between the values is measured. The typical properties of all Differential Scanning Calorimeters are the twin-type conformation and the direct in-difference contact of the two identical measuring systems. The benefit of this system is counterbalance of temperature alteration, when the distinction between the signals is generated. Thus, the temperature alteration cannot influence the systems. The fundamental property of each DSC equipment is the differential signal. Another property is the dynamic mode of operation, which means, that the temperature can kept constant or can be decreased or increased at a current rate. An indicative feature for both types of calorimeters is that the scaled signal is proportionate to a heat flow rate Φ and not to a heat. According to this, time-based dependences of a transfer to be investigated based on the $\Phi(t)$ curve can be made. So heat flow rates can be quantified directly and all Differential Scanning Calorimeters can solve problems occurring in a wide range of areas [16].

3.3 Contact angle measurements

At a contact angle θ, a liquid/vapour interface gets in contact with a solid surface. The surface free energies between the liquid, solid and surrounding vapour cause the contact angle. The contact angle provides information about the wettability of a solid by a liquid. So the measurement of the contact angle is utilized to specify the relative hydrophobicity or hydrophilicity of a surface. The unit, in which the value is expressed, are degrees.

In the event of complete wetting (spreading), the contact angle is 0°. If the contact angle lies between 0° and 90°, the solid is wettable, above 90° it is not wettable. In the event of ultrahydrophobic materials the contact angle approximates to 180°. The classification can be observed in Figure 9.

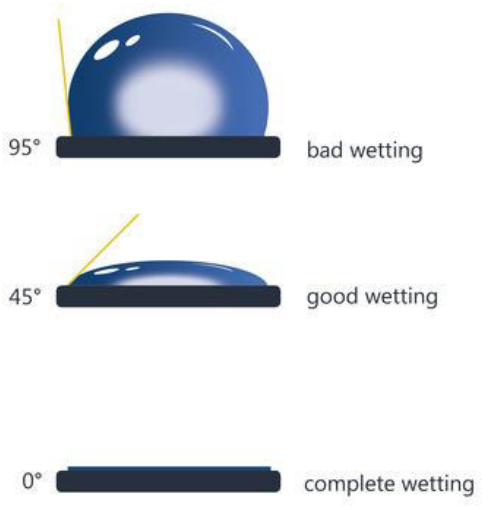

Figure 9. Contact angle of different samples.

[17]

For the determination of the contact angle, Young`s equation is utilized. Due to this equation, there is a link between the contact angle θ, the surface tension of the liquid σ_l, the interfacial tension γ_{sl} between liquid and solid and the surface free energy σ_s of the solvent, as it can be observed in Figure 10.

Equation 5:

$$\sigma_s = \gamma_{sl} + \sigma_l * \cos\theta$$

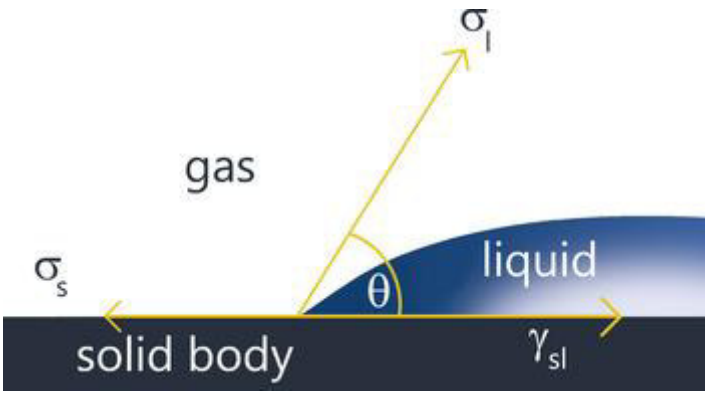

Figure 10. Diagram of the contact angle.

[17]

For the determination of the surface free energy, the contact angle measured with one or various liquids can be used.

The contact angle is used when the knowledge of the intensity of the phase contact between liquid and solid is important, e.g. coating, painting, printing, bonding or dispersing [17] [18].

For measuring the contact angle, different methods exist. If the contact angle is determined using the picture of a sessile drop at the point of intersection between the drop shape and the projection of the surface (baseline), it is called drop shape analysis (DSA). Determining the force acting in the tensile direction, when moving a plate-shaped solid perpendicular in a liquid, is the so-called Wilhelmy plate method. Surface tension and wetted length are associated with this force too. In the top-view distance method, the curve of the drop surface connected to the contact angle is defined. The gap between light points which are reflected from the highest point of the drop surface is measured [17].

3.4. FT-IR

Commonly, Infrared spectra are recorded by quantifying the admittance of light quanta with a continuous distribution of the sample. The frequencies of the absorption bands proportionate to the energy difference between the excited states and vibrational grounds. The absorptions bands according to the vibrational transitions are located in the wavelength region of λ=2.5...1000 µm. A non-linear molecule with *n* atoms causes normal vibrations, which only absorb infrared radiation if they modulate the molecular dipole moment [19].

Two unique molecules are not able to generate a similar spectrum, because the spectrum shows the molecular absorption and transmission, so a fingerprint of the sample is produced.

A further development is the Fourier-Transform Infrared spectroscopy (FT-IR). In this case, an interferogram (all frequencies are overlapping) is produced. By Fourier transformation, this interferogram is converted to a common IR spectrum [20] [21]. Interferometry generates a complex waveform that is an amount of contributions from all wavelengths emitted by a source. Wavelength differentiations originate from the characteristic that wavelength differentiations are modulated at various frequencies [22].

FT-IR has the following applications:

- Identification test
- Quality testing
- Quantitative analysis

In Figure 11, the setup of a Fourier-Spectrometer can be seen. For analysing a sample, infrared energy, which is emitted from a shining black body-source, goes through an aperture. This beam is produced by starting with a broadband light source, which is containing the full spectrum of wavelengths to be measured. The aperture examines, how much energy is presented to the sample and, as a consequence, to the detector. Afterwards the beam enters the Michelson interferometer, which is a specific arrangement of mirrors, one of which is moved by a motor. As this mirror moves, each wavelength of light in the beam is consistently blocked, transmitted, blocked, transmitted, by the interferometer, according to wave interference. Accordingly, the beam enters the sample, it is transmitted through the sample or reflected off the surface. Various wavelengths are modulated at various rates, so that at each moment, the beam coming out of the interferometer has a different spectrum. In the end, the beam goes to the detector for concluding measuring. Computer processing is used to turn the raw data into the required outcome by the algorithm of Fourier transformation [21] [22].

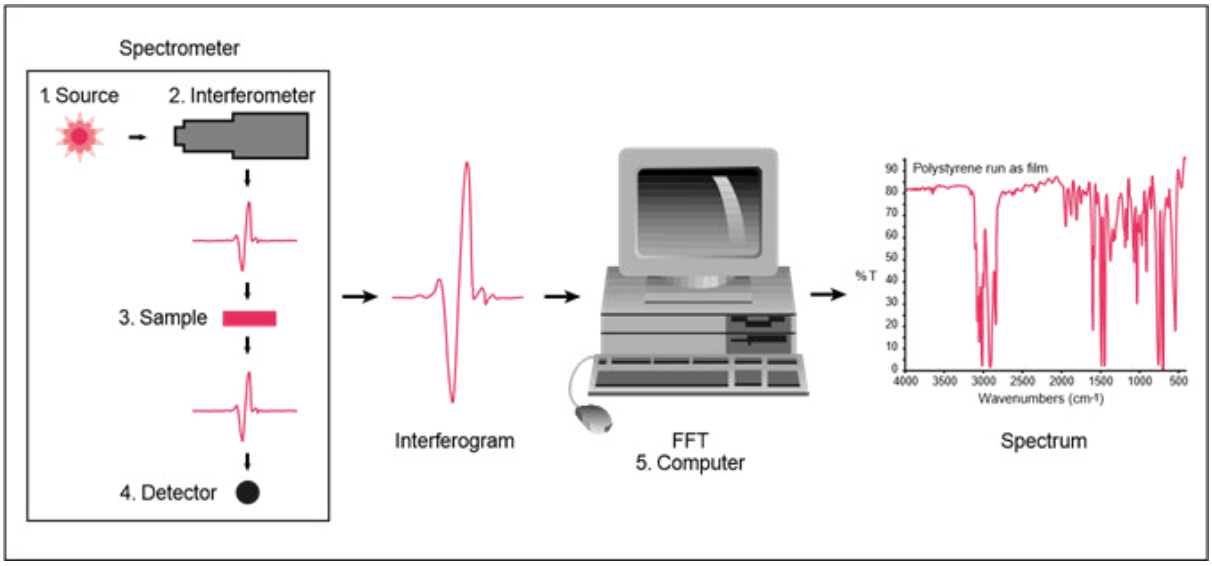

Figure 11. Setup of a Fourier-Spectrometer.

[21]

According to the necessity to have a relative scale for absorption intensity, it is important to measure a background spectrum without any sample in the beam and compare the measurements afterwards.

FT-IR shows some benefits over normal IR measurements, e.g. a faster measurement due to the simultaneously measured frequencies. Another point is the increased sensitivity, the used detectors are more sensitive and the optical throughput is higher. The mirror in the interferometer is the only movable component in the device, therefore the facility of damage is low [21].

4. Sample preparation

4.1 Cryomill

The Cryomill is especially designed for cryogenic grinding. The grinding jar is cooled before and during the grinding process using liquid nitrogen from the integrated cooling system. Thereby the sample gets rough and volatile components can be maintained. Using an auto fill system, the amount of liquid nitrogen, which is needed to keep the temperature at -196°C, is added. It is possible to use programmable cooling and grinding cycles, from 10 s to 99 min [23]. In Figure 12, a cryomill can be seen.

Figure 12. Picture of a Retsch® cryomill.

[23]

The cryomill has the following applications examples:

- Chemical products
- Tablets
- Tissue
- Foods
- Animal feeds
- Bones

It is used for size reduction, mixing, homogenization or cell disruption, in the fields of agriculture, biology, chemistry, construction materials, food, geology, medicine and pharmaceuticals. The feed material can be hard, medium-hard, soft, brittle, elastic or fibrous, the size can be reduced due to impact or friction [23] [24].

III. Material and Methods

1. The formulation

The pharmaceutical active ingredient (API) is N-Acetylcysteine (NAC). The API is directly coated via hot melt coating using fluid bed technology. Two different compositions containing tripalmitin (Dynasan® 116) or tristearin (Dynasan® 118) with Polysorbate 65 (Tween® 65) are used as coating formulation. The coating should provide a desired taste masking of NAC with immediate release profile. The immediate release profile is defined as releasing 85% of API within 15 minutes. The physico-chemical behaviour of NAC and the coating formulation are described below.

1.1 Active pharmaceutical ingredient

N-Acetylcysteine ($C_5H_9NO_3$, M_r = 163.2 g/mol) is an N-acetylated Cysteine. It is existent as a white, crystalline powder or as transparent crystals and it has an unpleasant smell of sulphur.

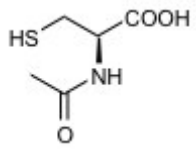

Figure 13. **Chemical structure of N-Acetylcysteine**
[25]

This active pharmaceutical ingredient (API) is an expectorant pharmaceutical drug. It is used in the treatment of respiratory diseases that come along with viscous secretion. Another indication for NAC is to handle a Paracetamol overdose.
The mucolytic effect happens due to the dissolving of disulphide-bonds in glycoproteins of the mucus, so the viscosity is decreased. The results of this effect, tested in clinical trials, are discussed contradictory, the effectiveness is not demonstrated definitely.
NAC gets hydrolysed in the liver to the active metabolite Cysteine, which is an amino acid. Diacetylcystine, Cystine und different Disulfides are also generated. Due to the high First-pass effect only 10% reach the systemic circulation. The active metabolites are eliminated through the kidneys.
As a prodrug of L-Cysteine, it is also anti-oxidative and works as a radical scavenger. Cysteine is a component of Gluthation, which is important to detoxify the toxic metabolite NAPQI (N-acetyl-p-benzoquinone imine) that is accumulated if you are intoxicated with Paracetamol.

The daily dosage of NAC for adults is determined at 600 mg. and for children at the age of 2 -12 years old is fixed at 300 mg (three times 100 mg). NAC is contraindicated for children younger than 2 years. NAC should be carefully applied if patients have a risk for gastrointestinal bleeding or suffer from Asthma bronchiale.

Part of the undesirable effects are nausea and vomiting, pyrosis, very rarely it can lead to urticaria, headache and temperature [25] [26] [27].

1.2 Coating formulation

1.2.1 Tween® 65

Tween® 65 is also known as Polysorbate 65, or in food industry as E 436. The IUPAC name is Polyoxyethylen(20)-sorbitan-tristearat.

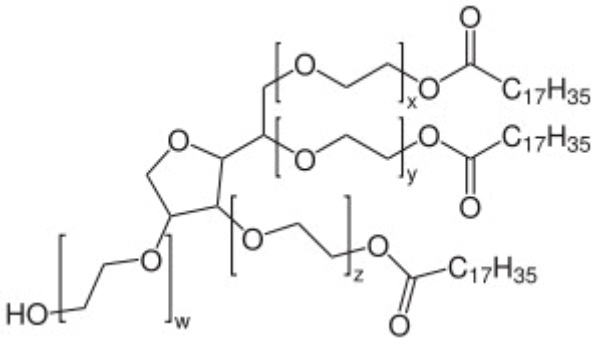

Figure 14. Chemical structure of Tween® 65
[28]

Tween® 65 is a solid, light yellow substance, which is soluble in alcohols and lipids. Tween® 65 is a synthetic produced surfactant. This excipient has a HLB-Value of 10.5, which is adequate for the manufacturing of water-in-oil emulsions. It is biodegradable. Tween® 65 is used as an emulsifying agent in our formulation. Emulsifiers are defined by the International Union of Pure and Applied Chemistry (IUPAC). They are surfactants that are lowering the interfacial tension when they are adsorbed positively at interfaces. Emulsifiers consist of both, hydrophilic as well as lipophilic parts, and they are able to form micellar aggregates.

In the European Union (EU) Tween® 65 is applied as a food additive for several foodstuffs. The Acceptable Daily Intake (ADI)-value is defined at 10 mg/kg body weight, and it is the same for all polysorbates.

The manufacturing process includes the transformation of an anhydride of sorbitol with ethylene oxide and a subsequent esterification with stearic acid [28] [29].

1.2.2 Triacylgycerides

Dynasans® are various types of microcrystalline triglycerides, esterified with fatty acids. They contain saturated, even numbered and unbranched fatty acids.

We used Tripalmitin (Dynasan® 116) and Tristearin (Dynasan® 118) as main components of coating formulation in our experiments.

Dynasan®116 ($C_{51}H_{98}O_6$) is Tripalmitin, it means that the triglyceride is esterified with three palmitic acid rests ($C_{16}H_{32}O_2$).

Dynasan® 118 is Tristearin ($C_{57}H_{110}O_6$), it is esterified with three stearic acid rests ($C_{18}H_{36}O_2$).

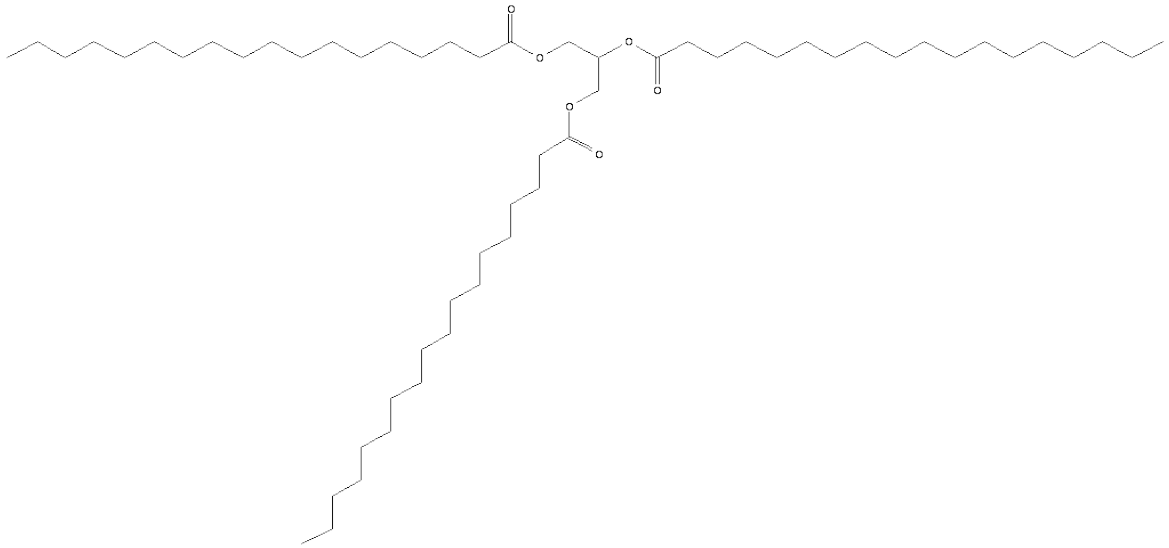

Figure 15. Chemical structure of Dynasan® 118

[30]

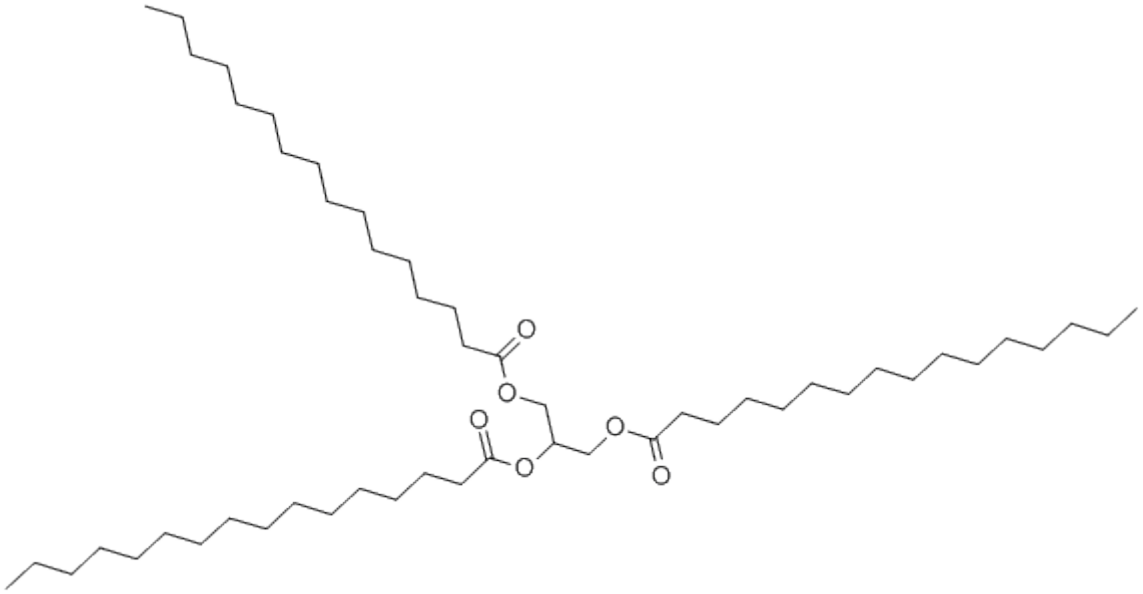

Figure 16. Chemical structure of Dynasan® 116

[31]

The components of Dynasan® appear in the human body, so they are toxicologically seen as unproblematic. The LD_{50}-value (=Letale Dosis) for the rat is higher than 5 g/kg body weight [31] [30].

1.2.3 Highly Dispersed Silicon Dioxide

Highly dispered silicon dioxide is also called colloidal silicic acid, Aerosil® and Silica colloidalis anhydrica, its molecular formula is SiO_2. It is a bluish-white, fine, airy and flaky crystalline powder with a size of primary particles around 15 nm. Due to clustering effects of the primary particles, agglomerates or aggregates with a diameter of 1-200 µm can be generated. As a result of the very low particle size, Aerosil® has a very low bulk density (50 g/l).

The silanol groups on the surface can build a three dimensional structure with neighbour groups by reason of hydrogen bonds. This leads to an increase of viscosity in non-polar systems, even in low concentrations. As a result of the hydrogen bonds to polar systems highly dispersed silicon dioxide has an excellent absorption capacity. It can absorb 40% moisture, without losing the texture of the dry powder. It is used as glidant, adsorbent, to make a surface more hydrophilic for a better disintegration of tablets, to stabilize suspensions and as a gel forming agent [5]. In the current study, Aerosil® with a concentration of 0.5% (W/W) was added to NAC to absorb moisture and to improve the flow characteristics.

2. Mixture of excipients

The following mixtures of Dynsasan® 116 or Dynasan® 118 with various amount of Tween® 65 are used for investigation of phase separation using different analytical methods (Table 3). Dynasan® 116 and Dynasan® 118 are purchased from Cremer Oleo GmbH & Co. KG, Hamburg, Germany, Tween® 65 is ordered from Croda GmbH, Nettetal, Germany

Dynasan® 116		**Dynasan® 118**		**Tween® 65**	
10% Tween® 65 25°C	10% Tween® 65 40°C	10% Tween® 65 25°C	10% Tween® 65 40°C	Tween® 65 25°C	Tween® 65 40°C
20% Tween® 65 25°C	20% Tween® 65 40°C	20% Tween® 65 25°C	20% Tween® 65 40°C		
30% Tween® 65 25°C	30% Tween® 65 40°C	30% Tween® 65 25°C	30% Tween® 65 40°C		
40% Tween® 65 25°C	40% Tween® 65 40°C	40% Tween® 65 25°C	40% Tween® 65 40°C		
50% Tween® 65 25°C	50% Tween® 65 40°C	50% Tween® 65 25°C	50% Tween® 65 40°C		
Dynasan® 116 25°C	Dynasan® 116 40°C	Dynasan® 118 25°C	Dynasan® 118 40°C		

Table 3. The investigated samples of Dynasan® 116, Dynasan® 118 and Tween® 65

2.1 X-ray scattering

2.1.1. Preparation of the samples

Different amounts of Dynasan® 116, respectively Dynasan® 118, are weighted in a beaker glass in an analytical balance with different ratios of Tween® 65 (Table 3). Then the mixture of lipid and emulsifying agent is molten at a temperature of around 95°C and stirred with a magnetic stir bar for homogenization. Afterwards the mixture of Dynasan® and Tween® 65 is filled in a glass capillary. Every sample is prepared twice, one capillary is stored at room temperature (25°C), and the other is stored in a drying chamber at 40°C.

To create a physical mixture, four samples, pure Dynasan® 116 compared with 10%, respectively 50% Tween® 65 and pure Dynasan® 118, compared with 10%, respectively 50% Tween® 65, are prepared in a cryomill (Retsch GmbH, Haan, Germany). Pure lipids are molten at a temperature of around 95°C and then solidified, afterwards solid lipid and solid emulsifier are weighted in a beaker glass in an

analytical balance and. The physical mixtures are then cryomilled, using two cycles to 5 minutes, respectively. Directly after milling the produced powder is filled in a capillary for X-ray measurement.

2.1.2 Implementation

The apparatus used is a Small and Wide Angle X-ray Scattering (SWAXS).The compact Kratky camera with line-focus optics (HECUS X-ray Systems, Graz, Austria) fixed on a sealed-tube X-ray generator (Seifert, Ahrensburg, Germany) is used at 30kV/0.4 mA The high brilliance microfocus X-r-ray source Cu has a wavelength of λ = 1.542A˚. Using a linear position-sensitive detector (PSD-50 M, HECUS X-ray Systems, Graz, Austria), the SAXS spectra are plotted in the angular range of 0.06° < 2Θ < 8°, with an independent detector the WAXS spectra are plotted in the angular range of 17° < 2Θ < 27°. SAXS and WAXS spectra are recorded at the same time. The samples are measured at room temperature with the X-ray exposure time of 1200 s.

2.1.3 Reference substance

As reference substances, pure Dynasan® 116, Dynasan® 118 and Tween® 65 are investigated using SWAXS. The preparation of these samples is as same as for lipid/emulsifier mixtures. The pure substance is molten, stirred with a magnetic stir bar and filled in the capillary. One of the capillaries is stored at room temperature, one is stored in a drying chamber at 40°C.

2.2 Differential Scanning Calorimetry

2.2.1 Preparation of the samples

Different amounts of Dynasan® 116, respectively Dynasan® 118, are weighted in a beaker glass in an analytical balance with different ratios of Tween® 65 (Table 3). Then the mixture of lipid and emulsifying agent is molten at a temperature of around 95°C and stirred with a magnetic stir bar for homogenization. Afterwards, 2-5 mg of each mixture is weighted in an analytical balance in a crucible using a pipette. Afterwards, the crucible (lower part) and the perforated lid are hermetically sealed. The pans consist of Aluminium and are ordered from NETZSCH GmbH, Selb, Germany. Every sample is prepared twice, one pan is stored at room temperature (25°C), and the other is stored in a drying chamber at 40°C.

2.2.2 Implementation

The pans are put in the Differential Scanning Calorimeter DSC 204 F1 Phoenix, (NETZSCH GmbH, Selb, Germany). According to preliminary work, the temperature programs, listed in Table 4, are used for the measurements.

	Starting point [°C]	**Heating rate [°C/min]**	**Endpoint [°C]**	**Cooling rate [°C/min]**	**Endpoint [°C]**
Dynasan® 116	10	40	90	10	10
Dynasan® 118	20	25	100	10	20

Table 4. DSC conditions for Dynasan® 116 and Dynasan® 118.

2.2.3 Reference substances

As reference substances, pure Dynasan® 116, Dynasan® 118 and Tween® 65 are investigated using DSC. The preparation of these samples is as same as for lipid/emulsifier mixtures. The pure substance is molten, stirred with a magnetic stir bar and filled in the DSC pans using a pipette. One of them is stored at room temperature; the other one is stored in a drying chamber at 40°C.

2.3 Contact angle measurement

2.3.1 Preparation of the samples

Different amounts of Dynasan® 116, respectively Dynasan® 118, are weighted in a beaker glass in an analytical balance with different ratios of Tween® 65 (Table 3). Then the mixture of lipid and emulsifying agent is molten at a temperature of around 95°C and stirred with a magnetic stir bar for homogenization. Afterwards an object slide, respectively a porous plate, is put in the molten mixture and pulled out so that its surface is covered with the sample. The object slide is purchased from Carl Roth GmbH + Co KG, Karlsruhe, Germany, the porous plate is a porous concrete called Ytong P2. Depending on the sample, it takes some time until the surface is getting solid on the object slide. One object slide is stored at room temperature (25°C), and the other is stored in a drying chamber at 40°C.

2.3.2 Implementation

The room is shaded to have a better contrast. The object slide, respectively the porous plate, is put in the device “Easy Drop”, purchased from A. Krüss Optronic, Hamburg, Germany. A special syringe (Hamilton Messtechnik GmbH, Höchst, Germany) is filled with ultrapure water and fixed in the

device. A drop of 1.5 µl of ultrapure water is put on the surface of the object slide and the contact angle is measured.
On every plain glass microscope slide, 10 measurements on different points are undertaken, three slides per sample are prepared

2.3.3 Reference substances

As reference substances, pure Dynasan® 116, Dynasan® 118 and Tween® 65 are investigated using the contact angle measurement. The preparation of these samples is as same as for lipid/emulsifier mixtures. The pure substance is molten, stirred with a magnetic stir bar and brought on the surface of the object slides. One of the object slides is stored at room temperature; the other one is stored in a drying chamber at 40°C.

2.4 FT-IR

2.5.1 Preparation of the samples

Different amounts of Dynasan® 116, respectively Dynasan® 118, are weighted in a beaker glass in an analytical balance with different ratios of Tween® 65 (Table 3). Then the mixture of lipid and emulsifying agent is molten at a temperature of around 95°C and stirred with a magnetic stir bar for homogenization. Afterwards the samples are filled in plastic cups, every sample is prepared twice, one plastic cup is stored at room temperature (20°C), and the other is stored in a drying chamber at 40°C.

2.4.2 Implementation

A small amount of sample is put in the sample holder of the FT-IR device, it is important to assure that the entire surface is covered with sample. The FT-IR used is the model Vertex 70, purchased from Bruker Corporation, Massachusetts, USA. The measurements are performed using 16 scans. Every sample is measured in triplicate.

2.4.3 Reference substances

As reference substances, pure Dynasan® 116, Dynasan® 118 and Tween® 65 are investigated using FT-IR. The preparation of these samples is as same as for lipid/emulsifier mixtures. The pure substance is molten, stirred with a magnetic stir bar and filled in the plastic cups using a pipette. One of the cups is stored at room temperature, one is stored in a drying chamber at 40°C.

IV. Results and Discussion

1. X-ray scattering

The X-ray scattering measurements are conducted to see a possible phase separation in the spectra. For this reason pure Dynasan® and Tween® 65 and different mixtures of them are investigated using SWAXS. These samples are filled in capillaries and then stored at room temperature (RT) at 25°C and in the drying chamber at 40°C for six months to observe the influence of storing conditions.
Additionally, physical mixtures of four samples are prepared using a cryomill for comparing their crystallinity to the molten mixtures.
Furthermore, the polymorphism of pure lipid and the impact of different amounts of Tween® 65 on the lipid polymorphism were studied. The storage time and the required ratio of Tween 65 for transforming of unstable α-from to β are listed in Table 5. It can be observed, that increasing the amounts of Tween® 65 lead to a faster transformation from α to β polymorphism. For example, in the case of pure Dynasan® 116 the the transformation of α-from to β-form was observed by the measurement of sample after one month storage at 40°C, while adding 30% Tween® 65 results in the immediate transform of α-from to β-form.

Amount of Dynasan ®118 [%]	Amount of Tween 65 [%]	β- form	Amount of Dynasan ®116 [%]	Amount of Tween 65 [%]	β- form
100	0	1 month 40°C	100	0	1 month 40°C
90	10	1 month 40°C	90	10	1 month RT
80	20	1 month RT	80	20	1 month RT
70	30	n.d.	70	30	Time 0
60	40	1 month RT	60	40	Time 0
50	50	1 month RT	50	50	Time 0

Table 5. Dynasan® 116 & 118: Transformation of α-from to β as response to temperature and adding emulsifier (Tween® 65)

The α form of Dynasan® 116 in WAXS is described by one strong reflection at about 4.15 Å, the β form is characterised by three dominant signals at 4.6 Å, and 3.85 Å and 3.7 Å [32]. In SAXS the α form of Dynasan® 116 is characterised by three signals at 15.33 Å, 22.78 Å and 44.59 Å, the three signals of the β polymorphism are shifted to 13.66 Å, 20.33 Å and 40.18 Å. The α form of Dynasan®

118 is described by one signal in WAXS at 4.2 Å [33]. In WAXS the α form is described by three signals at 17 Å, 25.4 Å and 50.7 Å, while the three signals for β are shifted to 15.15 Å, 22.65 Å and 44.85 Å. The WAXS and SAXS spectra of the pure substances (Dynasan® 116, Dynasan® 118 and Tween® 65) can be observed in the following figures.

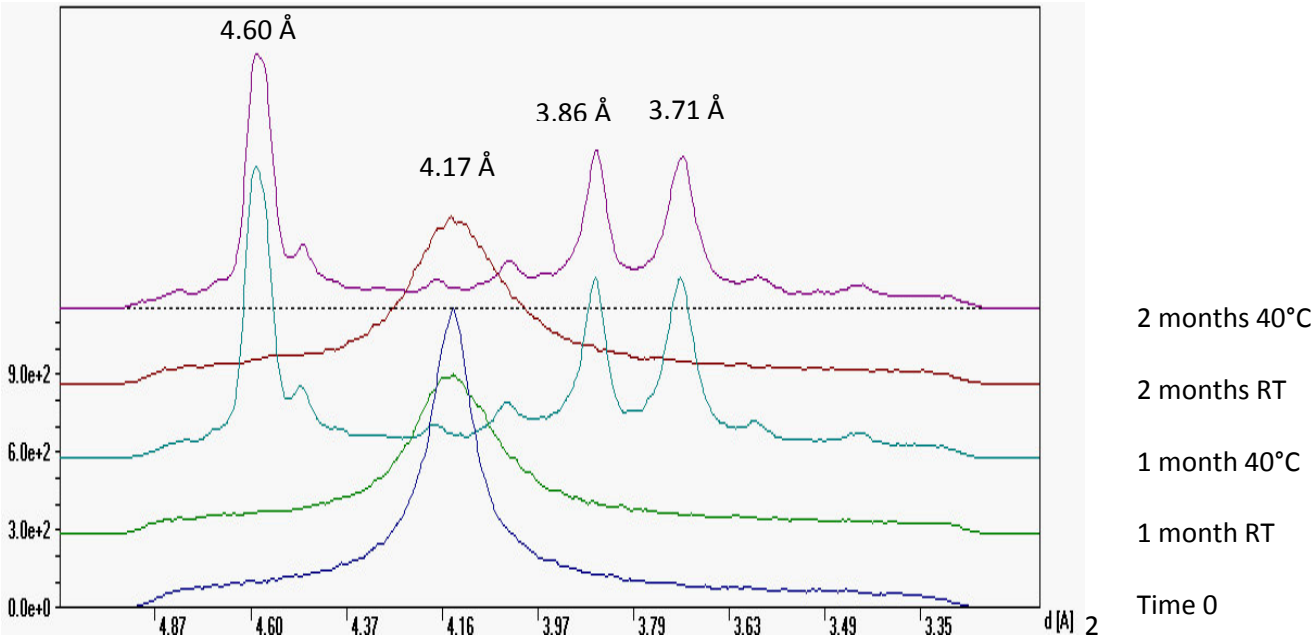

Figure 17. WAXS Spectra of pure Dynasan ® 116 after 1 and 2 months.

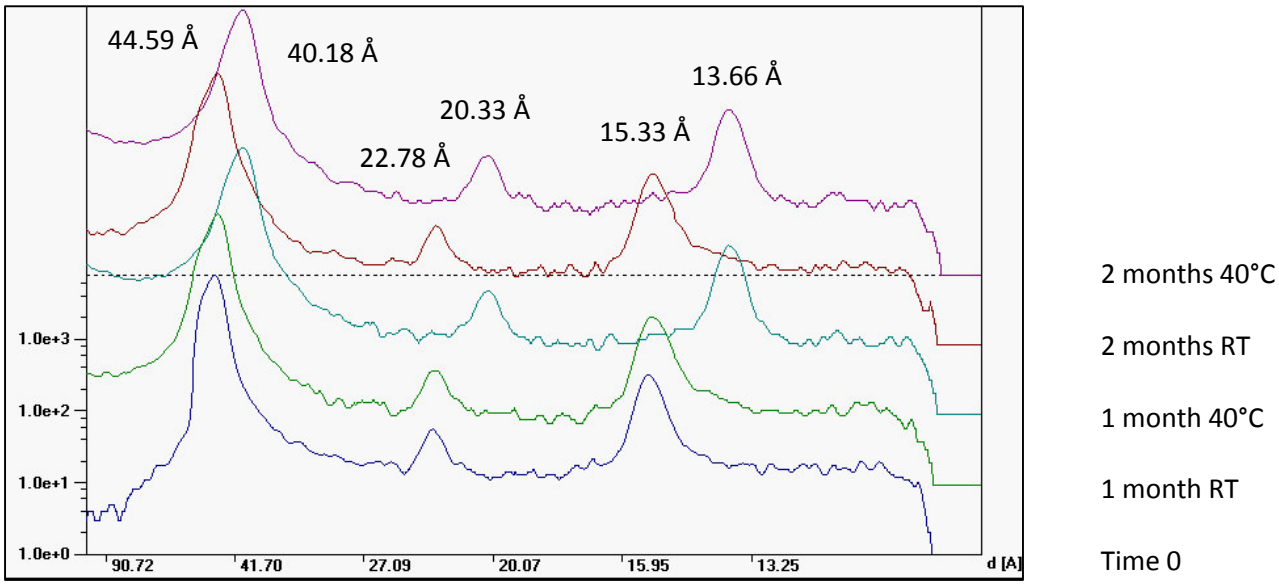

Figure 18. SAXS Spectra of pure Dynasan ® 116 after 1 and 2 months.

In Figure 17 and Figure 18, the spectra of pure Dynasan ® 116 after one and two months are seen. Directly after preparing and after storage at room temperature, the α polymorphism is existing. The β polymorphism is reached after storing for one month at 40°C in the drying chamber. As it can be

observed in Figure 19 and Figure 20, the β polymorphism is given after storage at 40°C in the drying chamber, after storage at room temperature, the α polymorphism is still dominant.

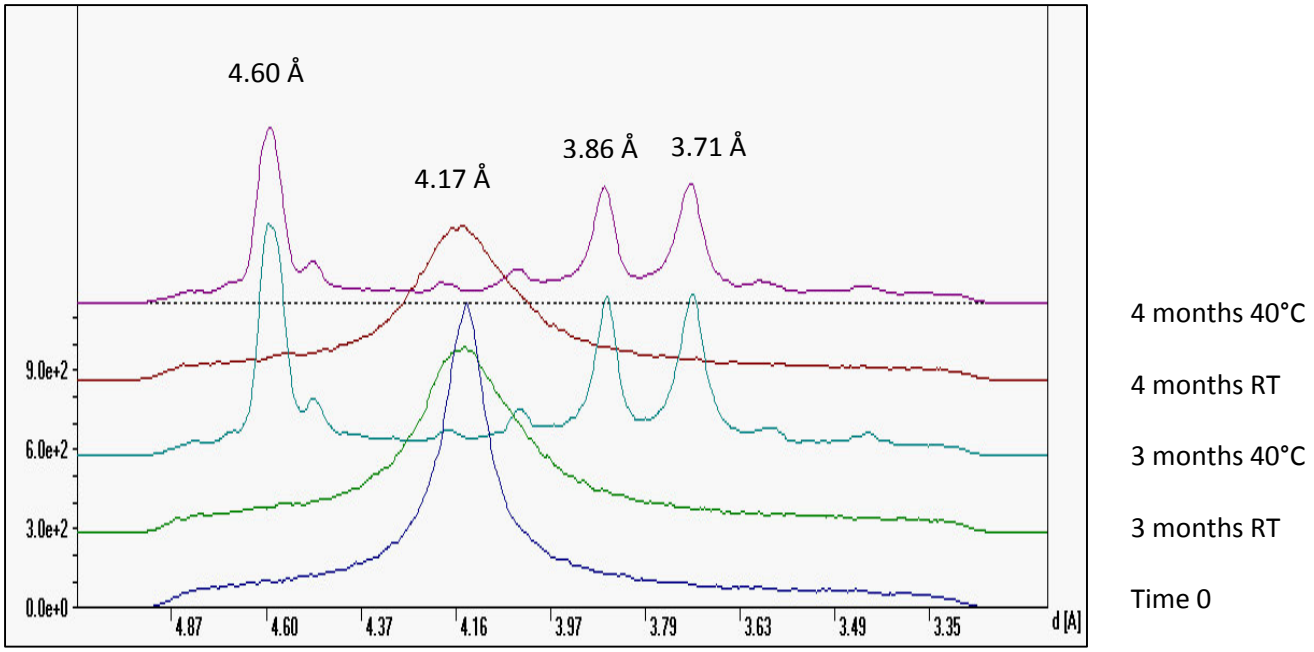

Figure 19. WAXS Spectra of pure Dynasan ® 116 after 3 and 4 months.

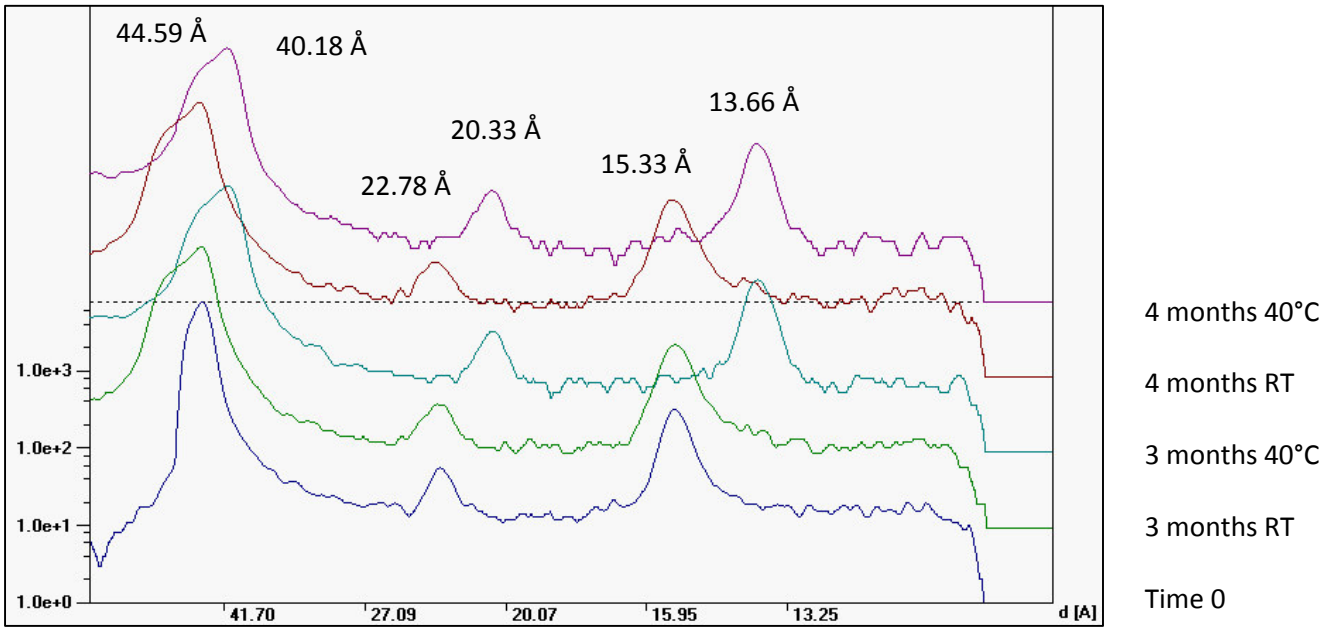

Figure 20. SAXS Spectra of pure Dynasan ® 116 after 3 and 4 months.

Figure 21 and Figure 22 show the spectra of pure Dynasan ® 118 after one and two months. It can be seen, that after storage at room temperature the α polymorphism is given, after storage at 40°C in the drying chamber, the α-form is completely transformed to β polymorphism.

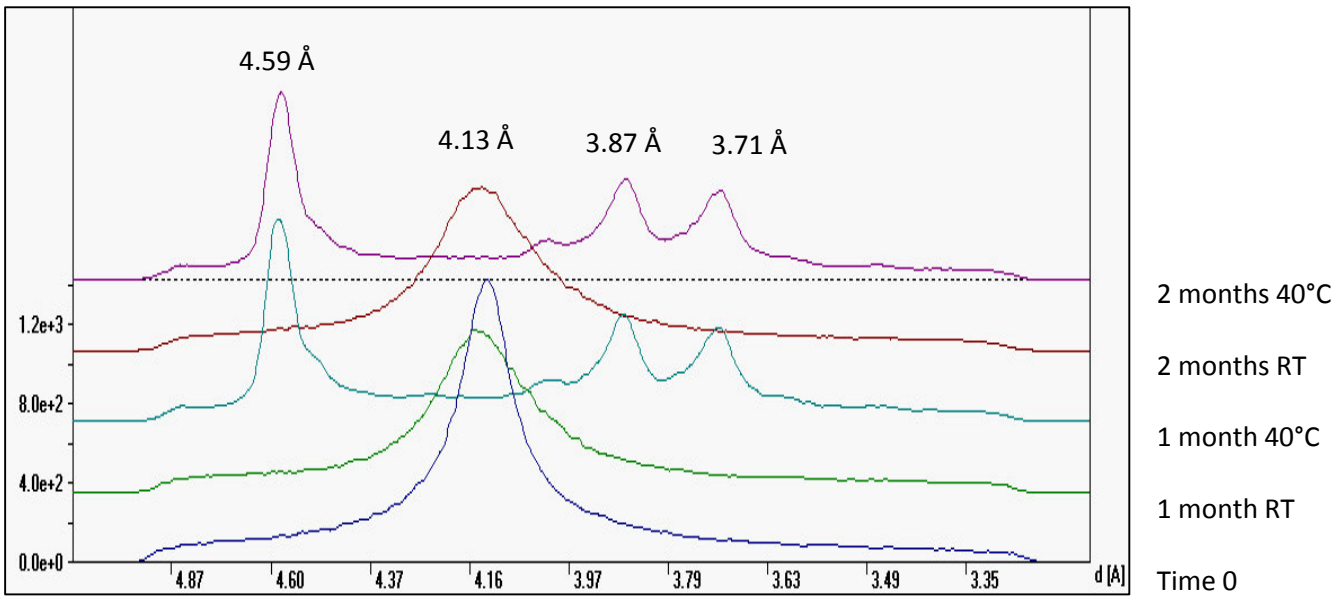

Figure 21. WAXS Spectra of pure Dynasan ® 118 after 1 and 2 months.

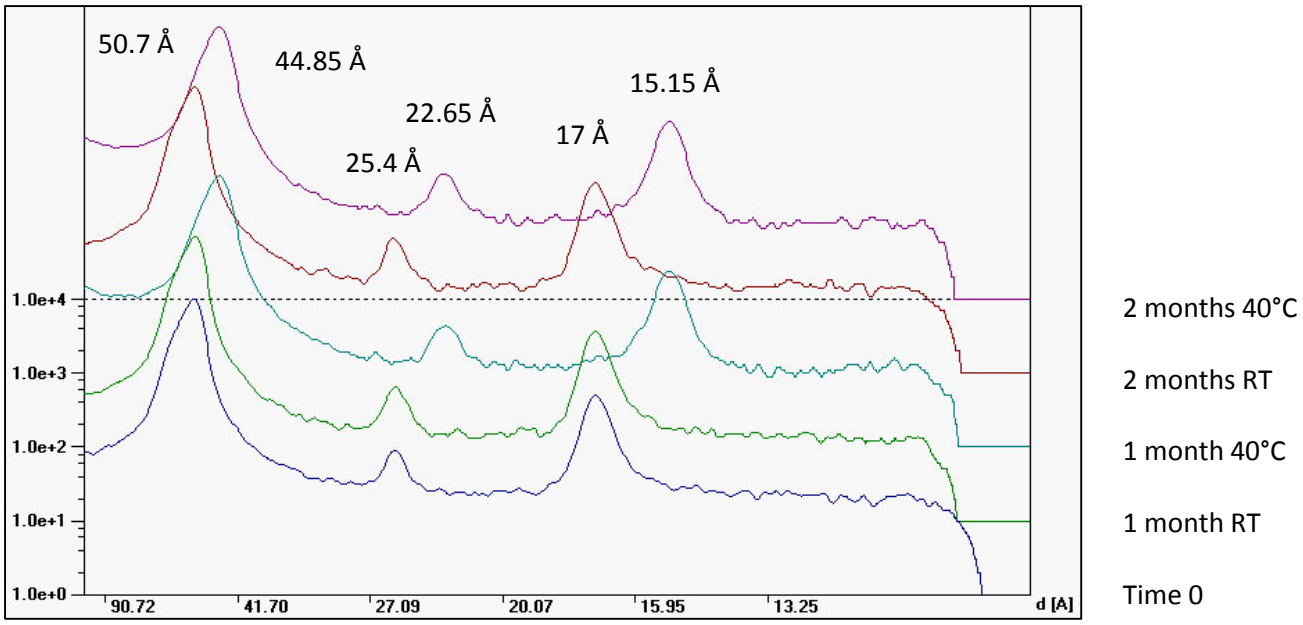

Figure 22. SAXS Spectra of pure Dynasan ® 118 after 1 and 2 months.

Even after storage in room temperature for four months, pure Dynasan ® 118 is still in α polymorphism, as it can be seen in Figure 23 and Figure 24.

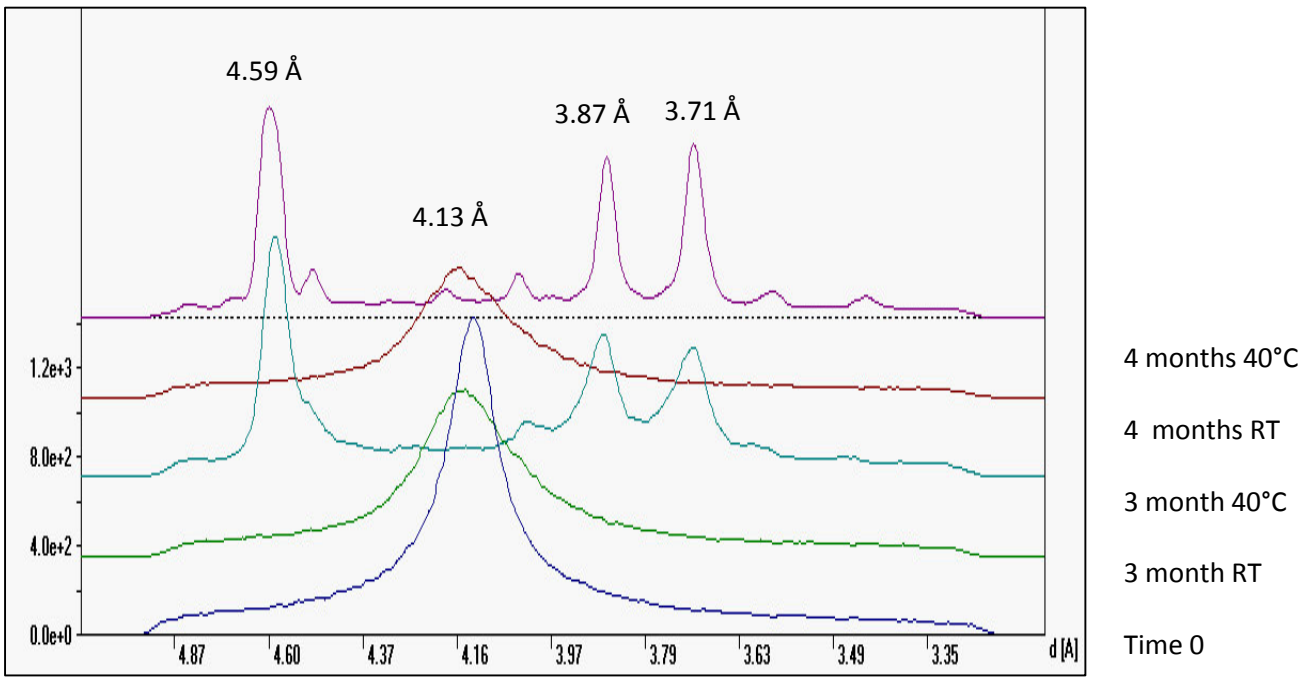

Figure 23. WAXS Spectra of pure Dynasan ® 118 after 3 and 4 months.

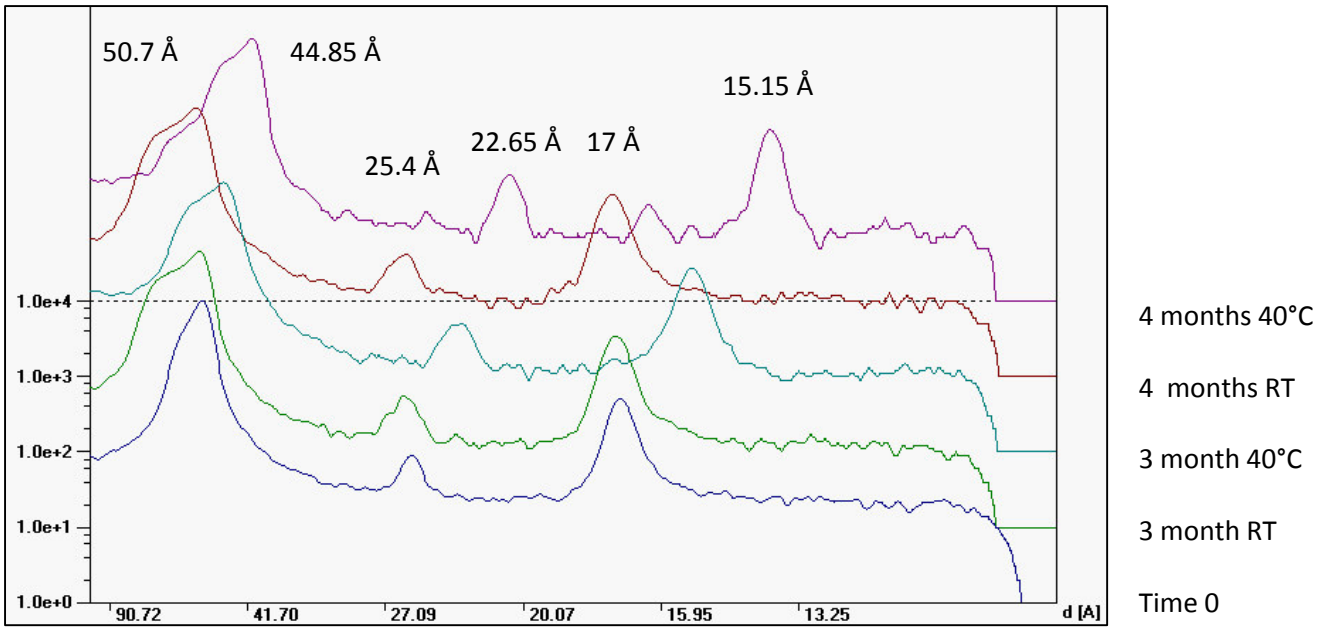

Figure 24. SAXS Spectra of pure Dynasan ® 118 after 3 and 4 months.

The crystallinity of pure Tween® 65 and its modification after storage at 25°C and 40°C is shown in Figure 25 to Figure 27. In the WAXS and SAXS spectra, Tween® 65 is characterised by a signal at 4.14 Å and 47 Å, respectively. The 4.14 Å signal in WAXS range remains stable during the storage time under both 25°C and 40°C. In the SAXS range, however, an extra signal at 68.5 Å occurs after two months storage at room temperature (Figure 26 and and Figure 29). During storage at 40°C, Tween® 65 is molten, so this signal only occurs after storage at room temperature. It is not exactly known what it shows, maybe a separation or a polymorphic form of the Tween®65 molecule, further investigation has to be done at this point.

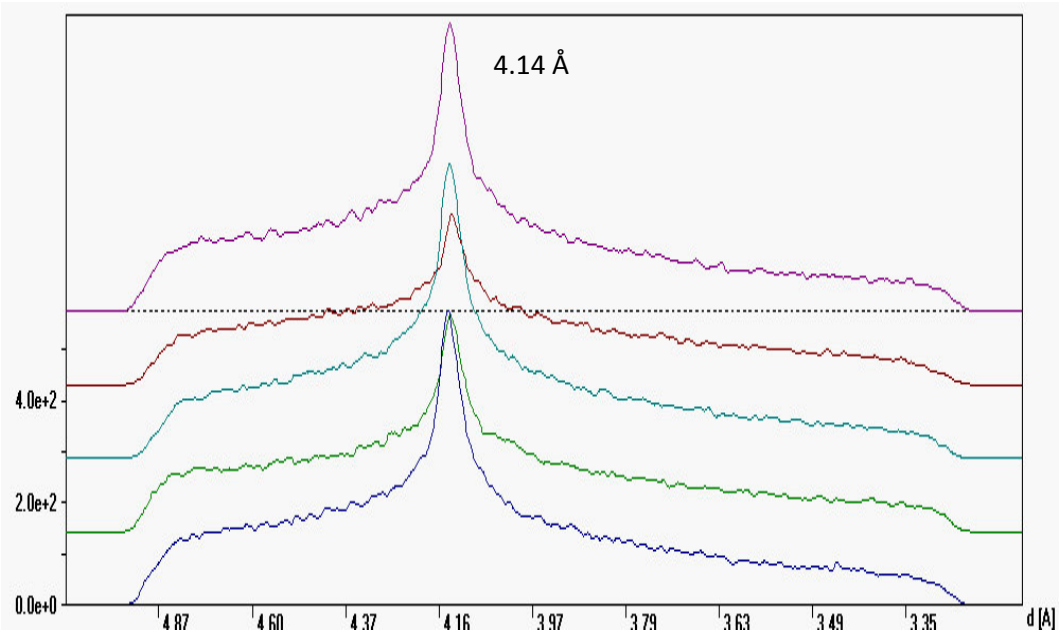

Figure 25. WAXS Spectra of pure Tween ® 65 and after 1 and 2 months storage at room temperature and 40°C.

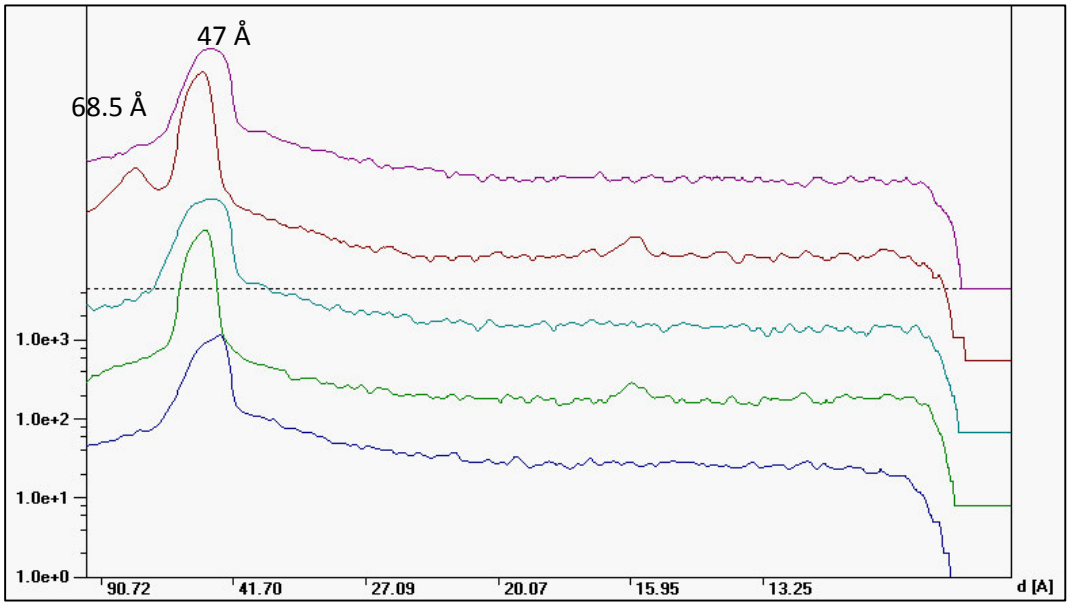

Figure 26. SAXS Spectra of pure Tween ® 65 and after 1 and 2 months storage at room temperature and 40°C.

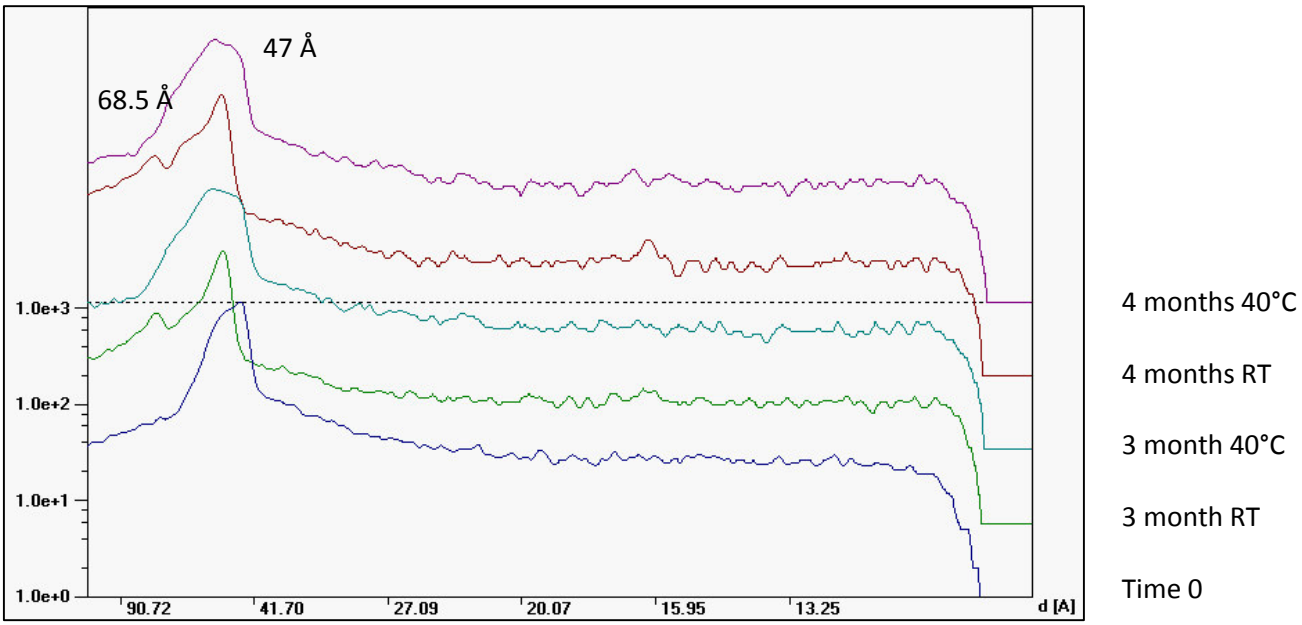

Figure 27. SAXS Spectra of pure Tween ® 65 and after 3 and 4 months storage at room temperature and 40°C.

To exclude, that the additional signal of 47 Å in SAXS is due to the cleavage of pure stearic acid from the Tween® 65 molecule, stearic acid was also screened via SWAXS (Figure 28 and Figure 29). Three signals of 4.35 Å, 4.16 Å and 3.76 Å are dominant for stearic acid in WAXS range, whereas the signal 4.16 Å was similar to the WAXS signal of Tween Tween® 65. In SAXS range tristearin shows three signals at 40.82 Å, 20.49 Å and 13.64 Å. The additional signal in Tween® 65 after storage at room temperature (68.5 Å) is not observed for stearic acid, so the cleavage can be precluded.

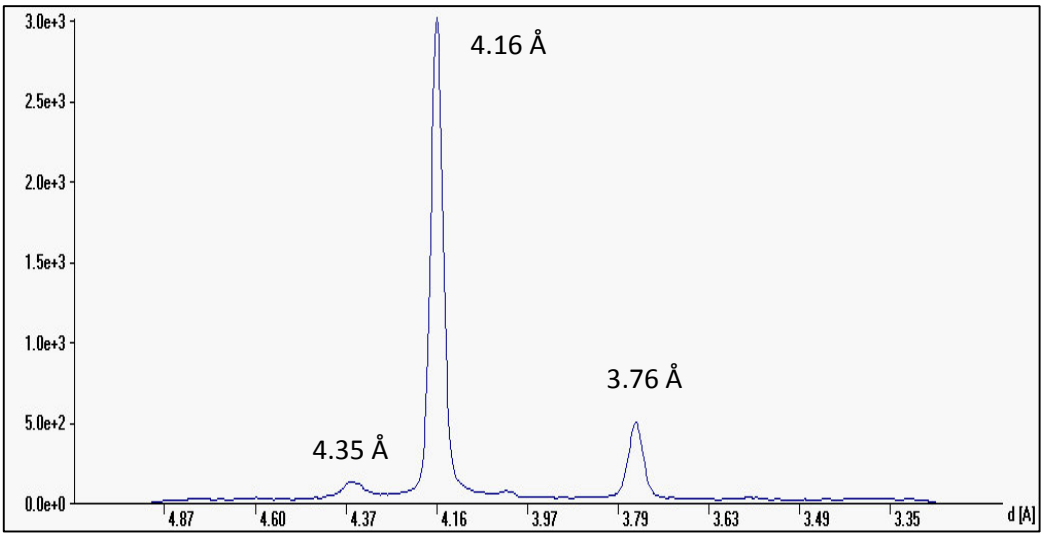

Figure 28. WAXS of pure stearic acid.

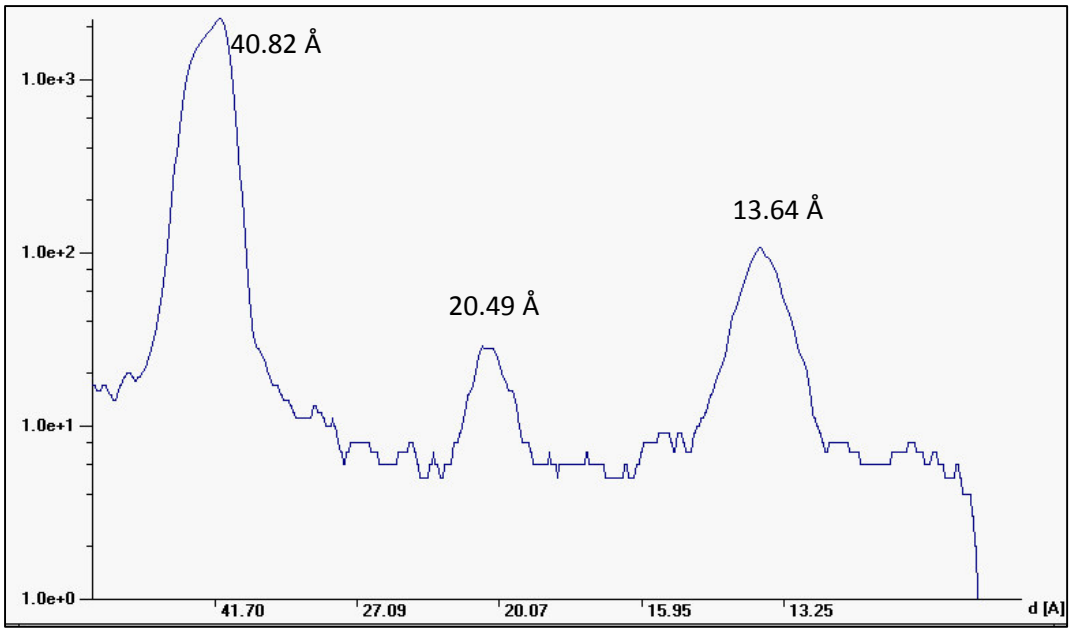

Figure 29. SAXS of pure stearic acid.

1.1 Storage of mixtures of Dynasan® 116 or Dynasan® 118 with Tween® 65

1.1.1 Dynasan® 116

After storage of samples containing mixtures of Dynasan® 116 and 10% to 30% (w/w) Tween® 65 at 25°C and 40°C, an extra signal was observed in SAXS after one month and four months, respectively. This extra signal occurs at 47.03 Å, equal to the signal of pure Tween® 65 at 47 Å. By increasing the amount of Tween® 65 to 40% and 50%, the extra signal was seen after one month storage at room temperature (Figure 32). This set of data shows that the occurring of the extra signal depends on the concentration of Tween® 65. Increased amounts of the emulsifier and storage temperature foster the extra signal.

Although Tween® 65 induces the transformation of α polymorph of Dynasan® 116 to β form, however to exclude that the additional 47.03 Å signal comes from the α polymorph of Dynasan® 116 (4.6 Å), additional DSC measurements have been undertaken. These results will be discussed in next chapter. SWAXS and DSC data show clearly the existence of the β form, therefore a strong indication of having a phase separation of lipid and emulsifier is present. In WAXS data, no significant evidence for phase separation can be observed, the signal of pure Tween® 65 is exactly overlapping with the signal of pure Dynasan® 116 and 118.

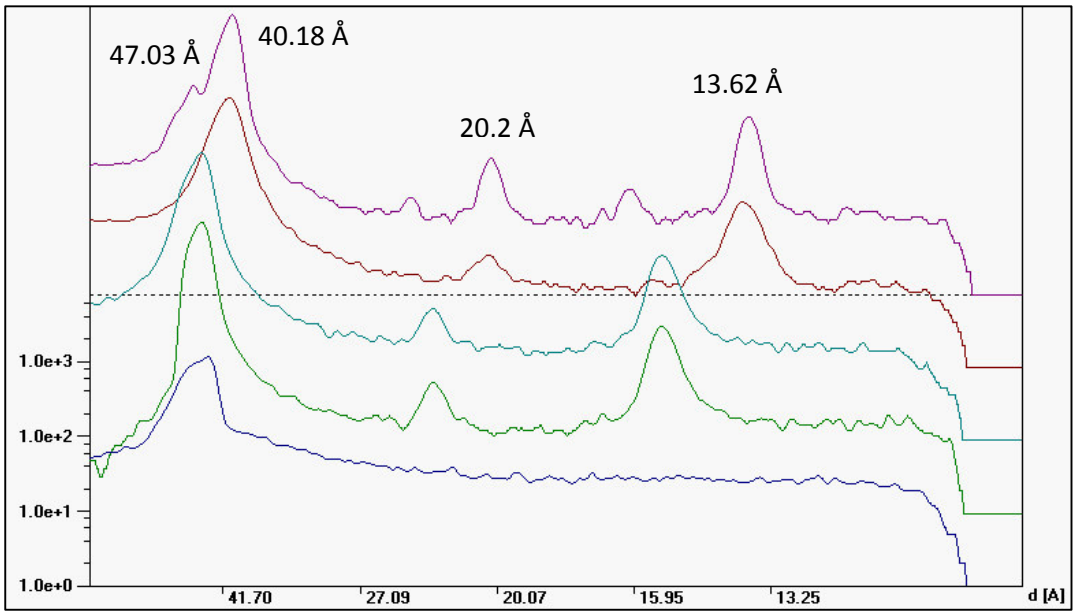

Figure 30. SAXS spectra of Dynasan® 116/10% Tween® 65 in comparison to pure substances after storing for one month.

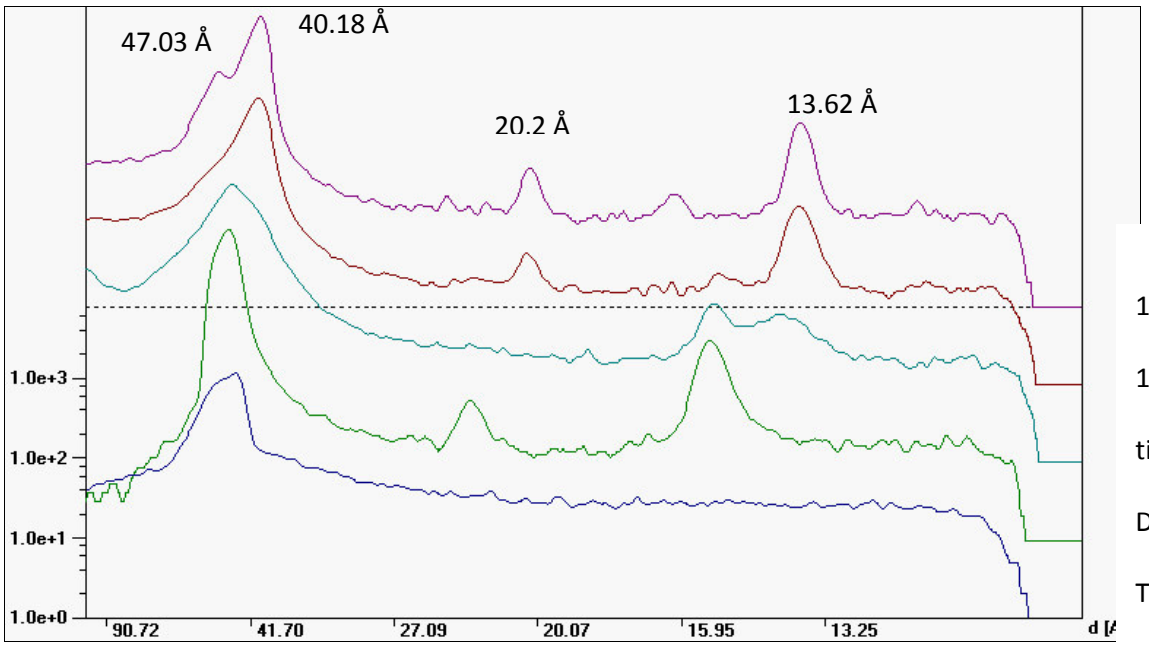

Figure 31. SAXS spectra of Dynasan® 116/30% Tween® 65 in comparison to pure substances after storing for one month.

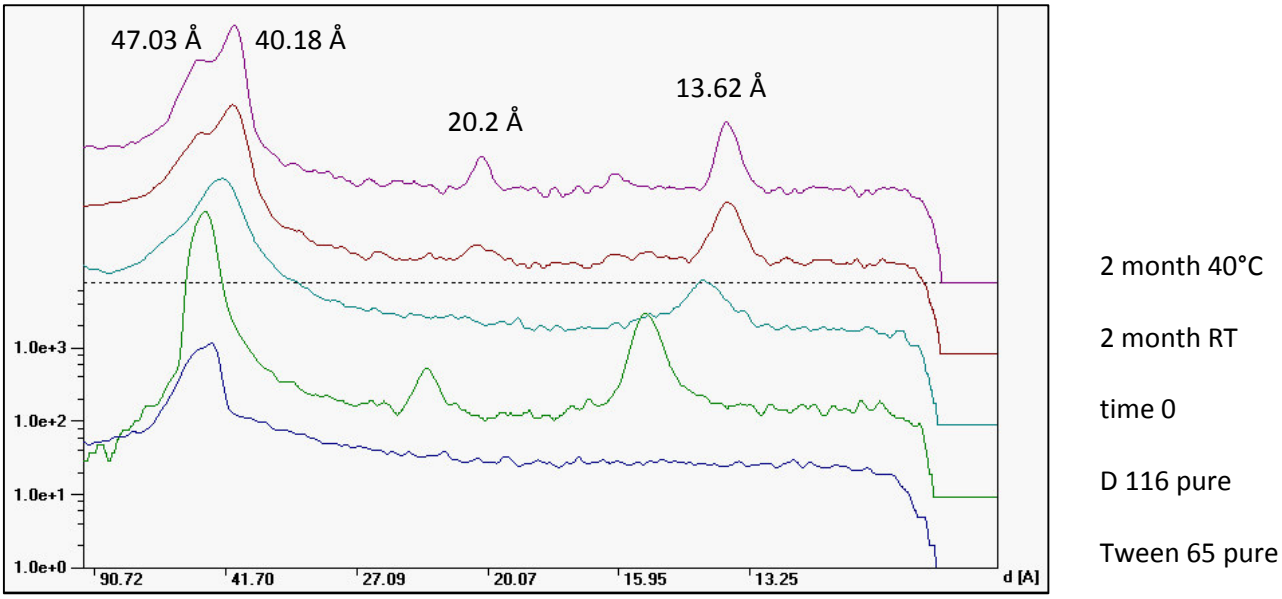

Figure 32. SAXS spectra of Dynasan® 116/50% Tween® 65 in comparison to pure substances after one month storage.

After storage of samples containing Dynasan® 116 and Tween® 65 for several months, the extra signal at 47.03 Å always occurs. Using lower amount of emulsifier, the extra signal can only be seen after storage at 40°C (Figure 33, 20% Tween® 65; Figure 34, 10% Tween® 65). If the amount of Tween® 65 is increased, the signal can also be observed after storage at room temperature, seen in Figure 35 (sample containing 40% Tween® 65) and Figure 36 (sample containing 50% Tween® 65).

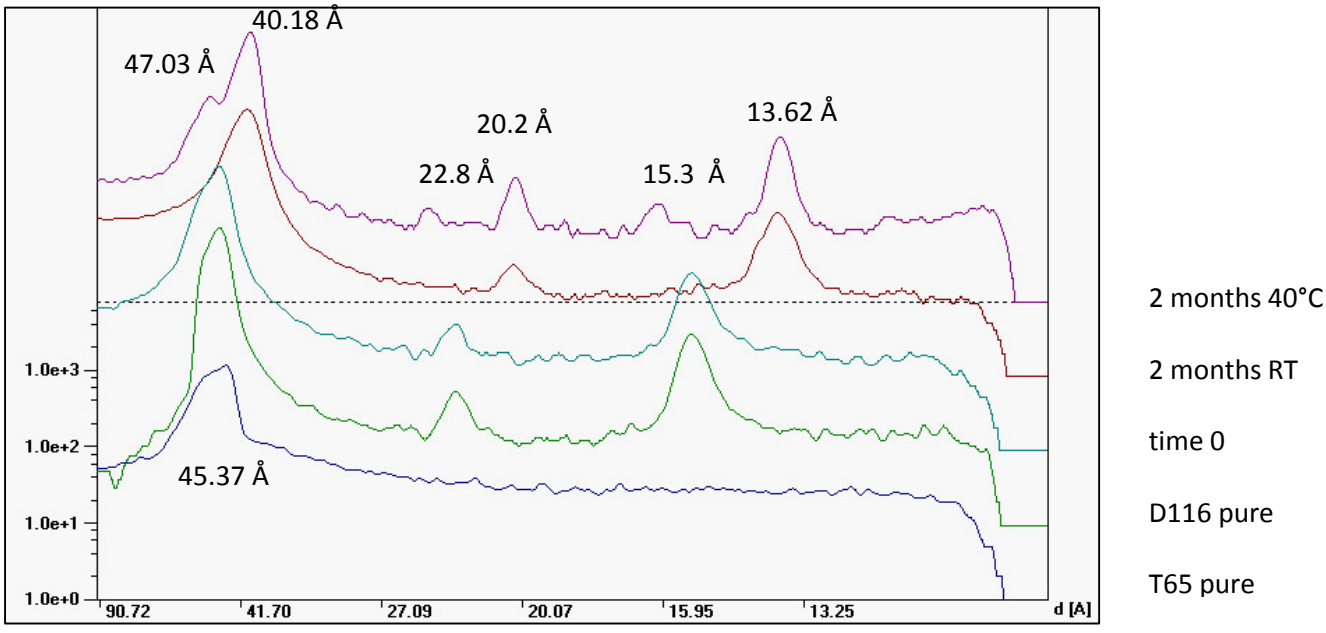

Figure 33. SAXS spectra of Dynasan® 116/20% Tween® 65 in comparison to pure substances after storing for two months.

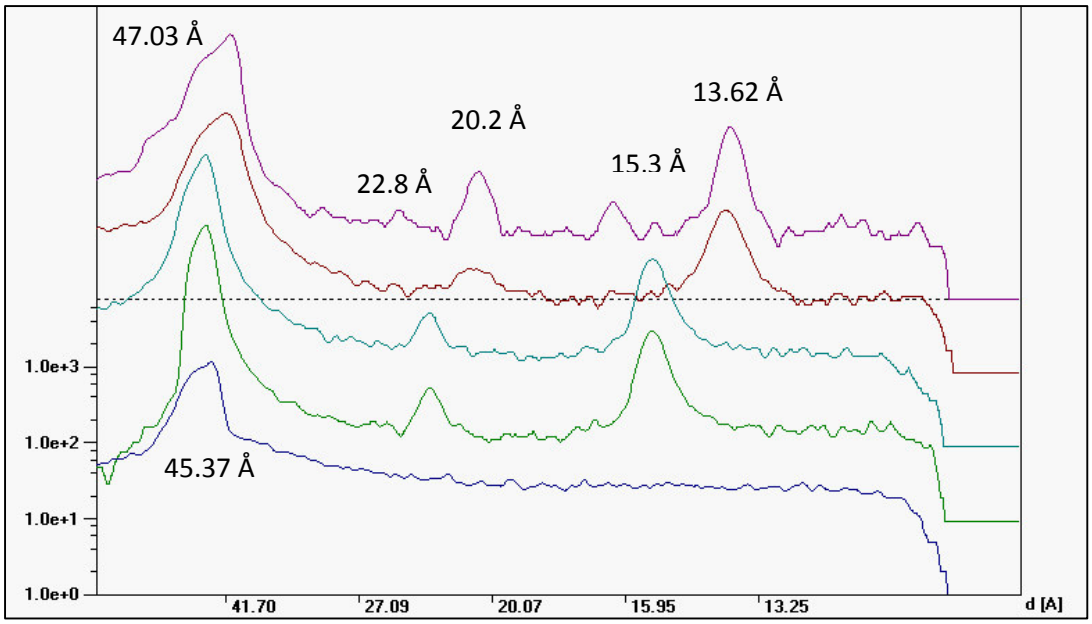

Figure 34. SAXS spectra of Dynasan® 116/10% Tween® 65 in comparison to pure substances after storing for four months.

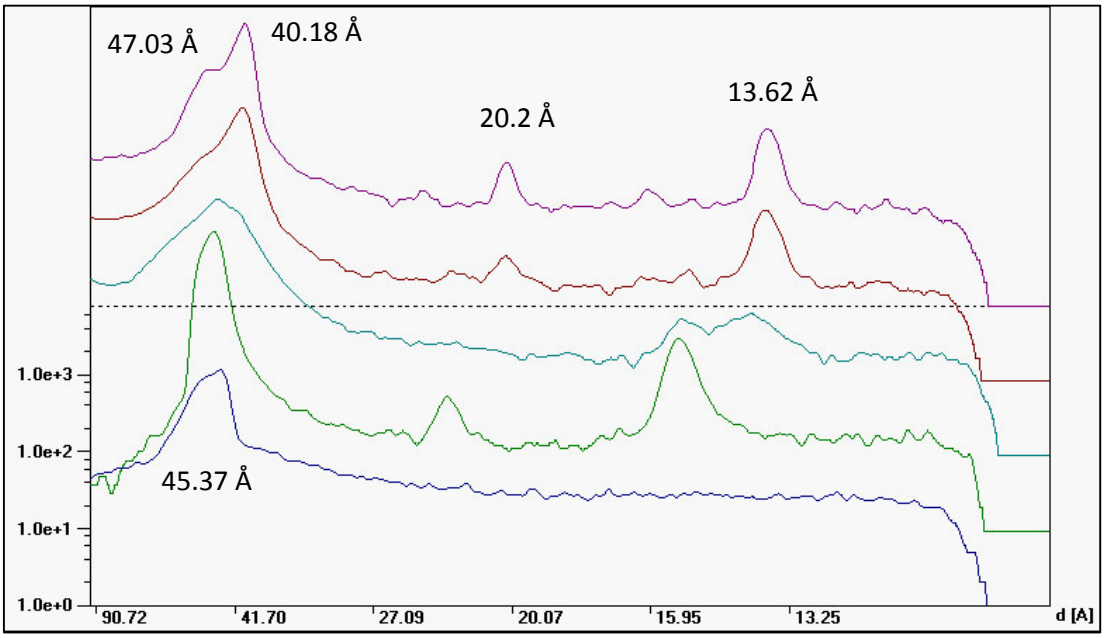

Figure 35. SAXS spectra of Dynasan® 116/40% Tween® 65 in comparison to pure substances after storing for two months.

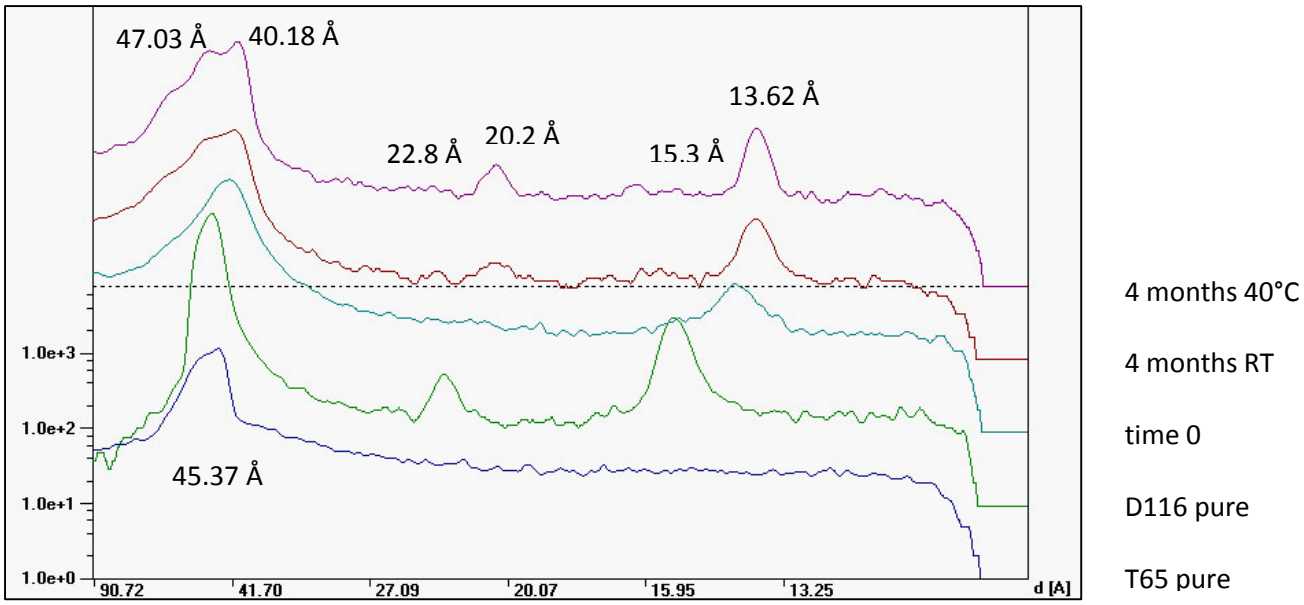

Figure 36. SAXS spectra of Dynasan® 116/50% Tween® 65 in comparison to pure substances after storing for four months.

1.1.2 Dynasan® 118

After one month storage of mixtures of Dynasan® 118 and Tween® 65 under room temperature and 40°C, no extra signal (similar to the extra signal of mixtures of Dynasan® 116 and Tween® 65) could be observed in SAXS. Figure 37 shows the SAXS spectra of a mixture of Dynasan® 118 and 10 % (w/w) Tween® 65. This can be due to the fact, that the extra signal of Tween® 65 (at 47.03 Å) is covered by the broad signal of Dynasan® 118 (at 50.7 Å).

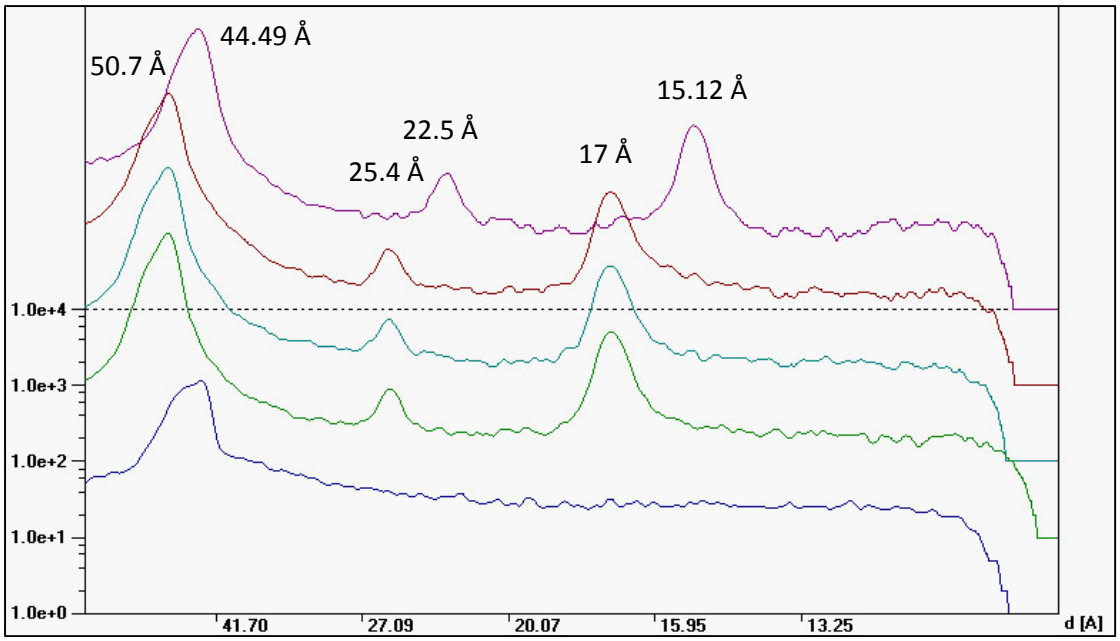

Figure 37. SAXS spectra of Dynasan® 118/10% Tween® 65 in comparison to pure substances after storing for one month.

1.2 Physical mixture

Additionally, physical mixtures of Dynasan®116:Tween® 65 and Dynasan®118:Tween® 65 with a ratio of 90:10 and 50:50, repectively, were prepared using a cryomill. The crystallinity of samples was investigated using SAXS measurements and the data was compared to the molten mixture of the same samples (Figure 38 to Figure 40). Using Dynasan®116, a clear extra signal at around 47 Å can be seen in comparison to the molten mixture, the same signal that occurs in molten samples after certain storage times and conditions. This can be monitored as another strong indicator for a phase separation of the stored samples. In samples containing Dynasan®118, this extra signal can also be seen, however it is not as clear as in the case of Dynasan® 116 and Tween® 65. Again the signal of Tween® 65 (at 47.03 Å) is covered by the broad signal of Dynasan® 118 at 50.7 Å).

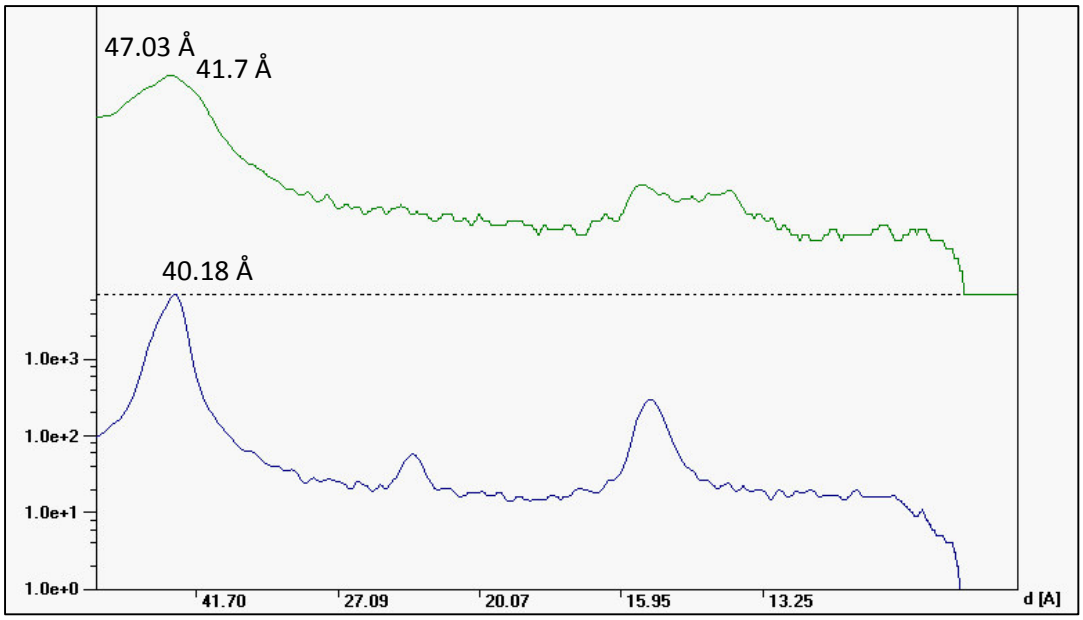

Figure 38. SAXS spectra of cryomilled Dynasan® 116/10% Tween® 65 in comparison to molten sample containing 10% Tween® 65.

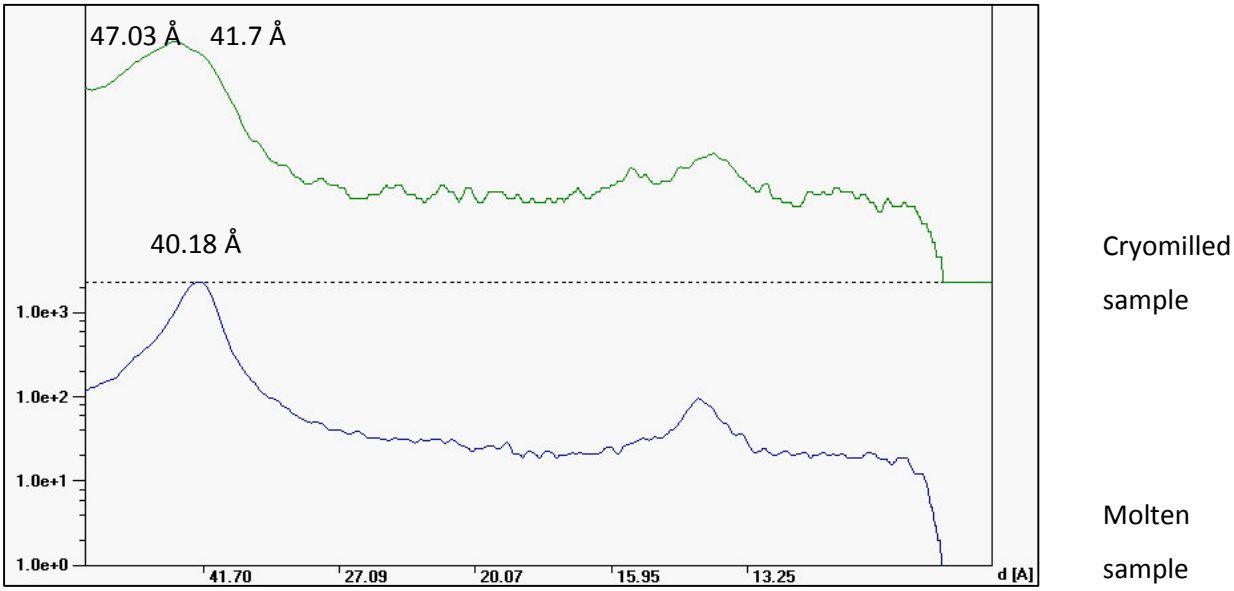

Figure 39. SAXS spectra of cryomilled Dynasan® 116/50% Tween® 65 in comparison to molten sample containing 50% Tween® 65.

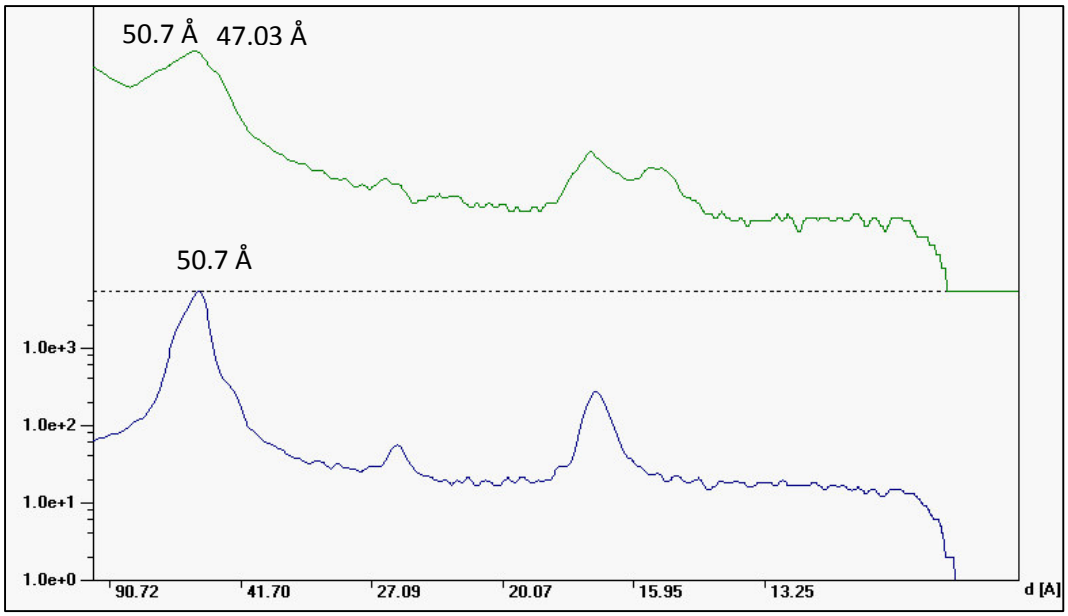

Figure 40. SAXS spectra of cryomilled Dynasan® 118/10% Tween® 65 in comparison to molten sample containing 10% Tween® 65.

Summing up, the extra signal at 47 Å occurs after storage of molten mixtures of Dynasan® 116 and Tween® 65 should be due to the phase separation in the lipid/emulsifier system. The obtained SAXS data on molten and physical mixtures support the assumption of phase separation. Further analytical methods have been used to confirm this assumption. This was especially important in the case of Dynasan®118 and Tween® 65, because of the overlapping of signals at SAXS range.

2. Differential Scanning Calorimetry

To confirm the results of the X-ray scattering, additional DSC measurements are performed. The same samples investigated via SWAXS are tested using DSC. Mixtures of Dynasan® and Tween® 65 are filled in pans and then stored at room temperature (20°C) and in the drying chamber at 40°C for six months. Table 6 shows the summary of the storage time and conditions to get the β polymorph. It is confirmed, that increasing amounts of Tween® 65 cause faster transformation from α to β. Pure Dynasan® 116 or 118 need thermal induction, for instance storage at 40°C, to transform α to β. Dynasan® 118 with longer carbon chain needs longer time to transform the α to β, comparing to Dynasan® 116. In the case of samples containing 40% of Tween® 65, the α form is immediately transformed to β, due to the existence of emulsifier. In comparison to SWASX measurements, the DSC measurements for Dynasan® 118 (samples containing 40% and 50% of Tween® 65) show faster transformation from α to β polymorph.

Ratio of Dynasan®118 in the mixture [%]	Ratio of Tween® 65 in the mixture [%]	β- form	Ratio of Dynasan ®116 in the mixture [%]	Ratio of Tween® 65 in the mixture [%]	β- form
100	0	1 month 40°C	100	0	1 month 40°C
90	10	1 month 40°C	90	10	1 month RT
80	20	1 month 40°C	80	20	1 month RT
70	30	n.d.	70	30	Time 0
60	40	Time 0	60	40	Time 0
50	50	Time 0	50	50	Time 0

Table 6. Storage time to get the β polymorph.

In Figure 41 to Figure 46, the DSC analysis of pure Dynasan® 116, Dynasan® 118 and Tween® 65 can be seen after preparation and after storage in different conditions for two and four months, respectively. The α polymorph of Dynasan® 116 melts at 44.7°C, while the β form melts at 66.4°C. In comparison, the α polymorph of Dynasan® 118 melts at 55.0°C, while the β form melts at 73,5°C [34].

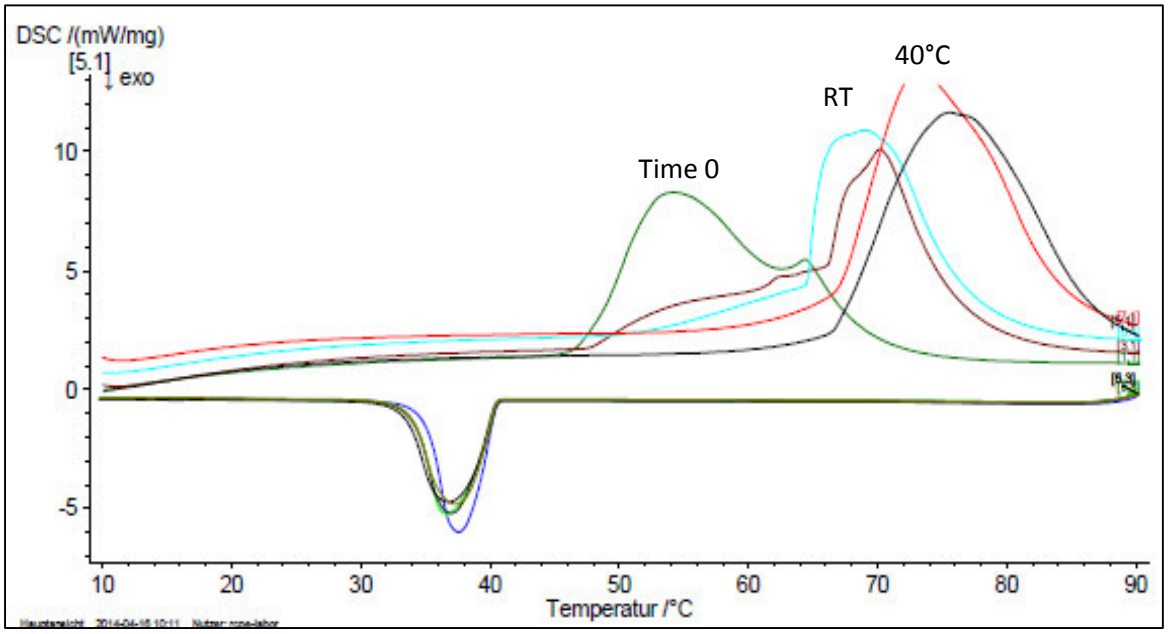

Figure 41. DSC analysis of pure Dynasan® 116 after two months storage.

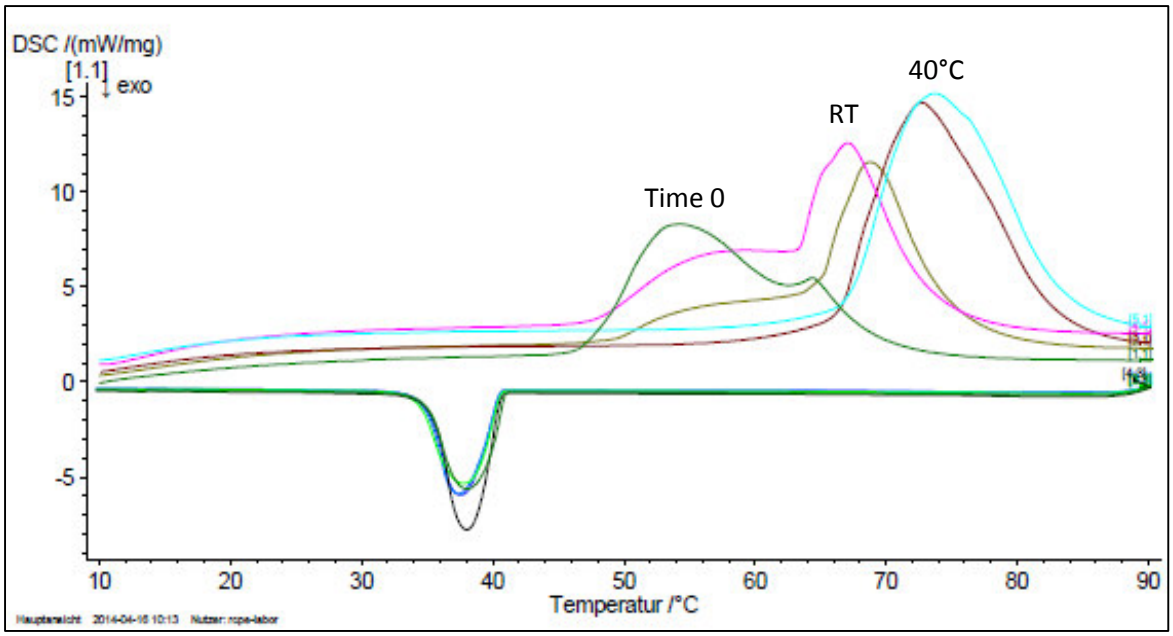

Figure 42. DSC analysis of pure Dynasan® 116 after four months storing.

In Figure 41 and Figure 42, it can be observed that pure Dynasan® 116 is in α directly after preparation. DSC measurements after two and four months storage at room temperature show the transition to β prime. Under accelerated conditions (40°C), the transformation to β happens after storage for one month. The same applies to pure Dynasan® 118, after preparing the α polymorph is screened. After storage at room temperature, the α signal is broader, indicating the transition to β prime form. After storage at 40°C a clear β form can be observed (Figure 43 and Figure 44).

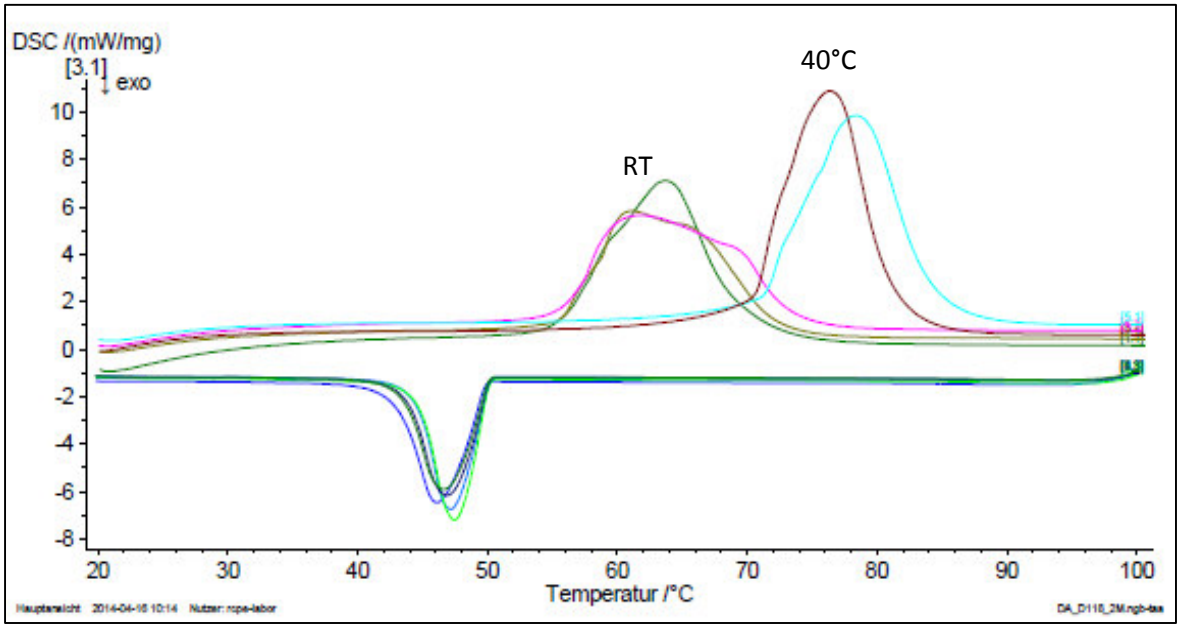

Figure 43. DSC analysis of pure Dynasan® 118 after two months storing.

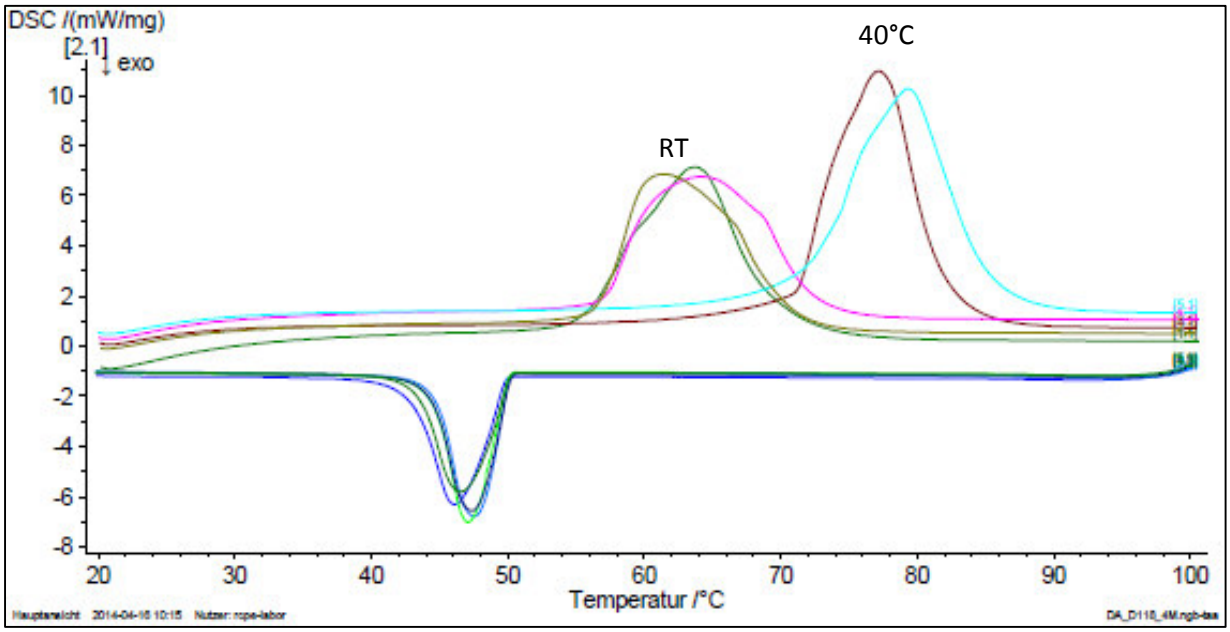

Figure 44. DSC analysis of pure Dynasan® 118 after four months storing.

Tween® 65 melts at around 30°C (Figure 44, inset 30 °C), as it can be seen in Figure 45 and Figure 46. After storing at 40°C, the recrystallization starts at higher temperatures.

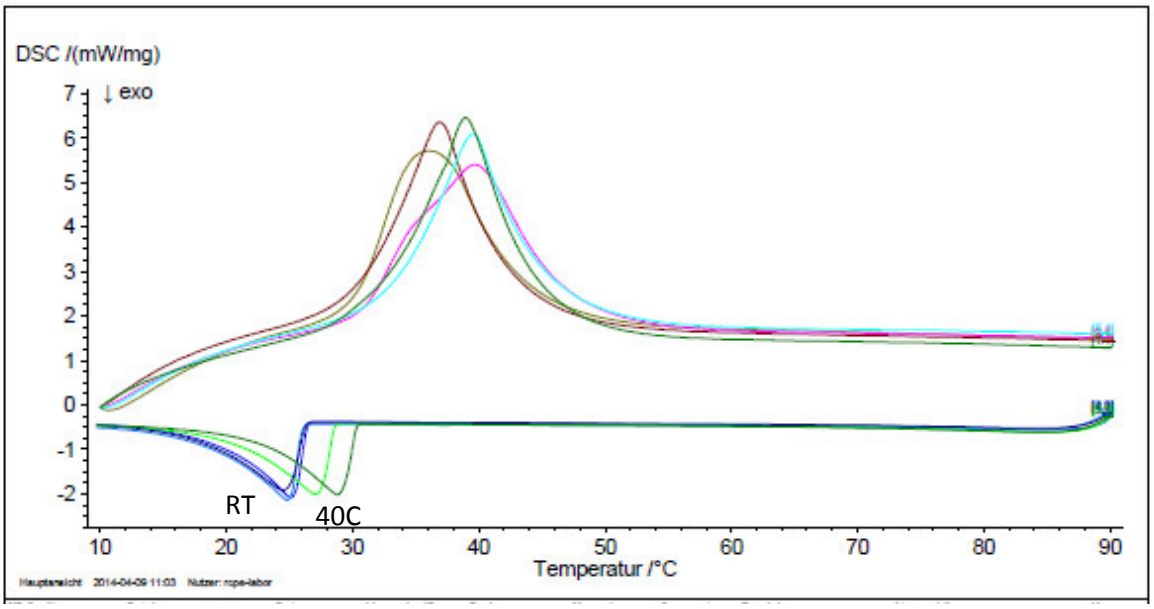

Figure 45. DSC analysis of pure Tween® 65 after two months storing.

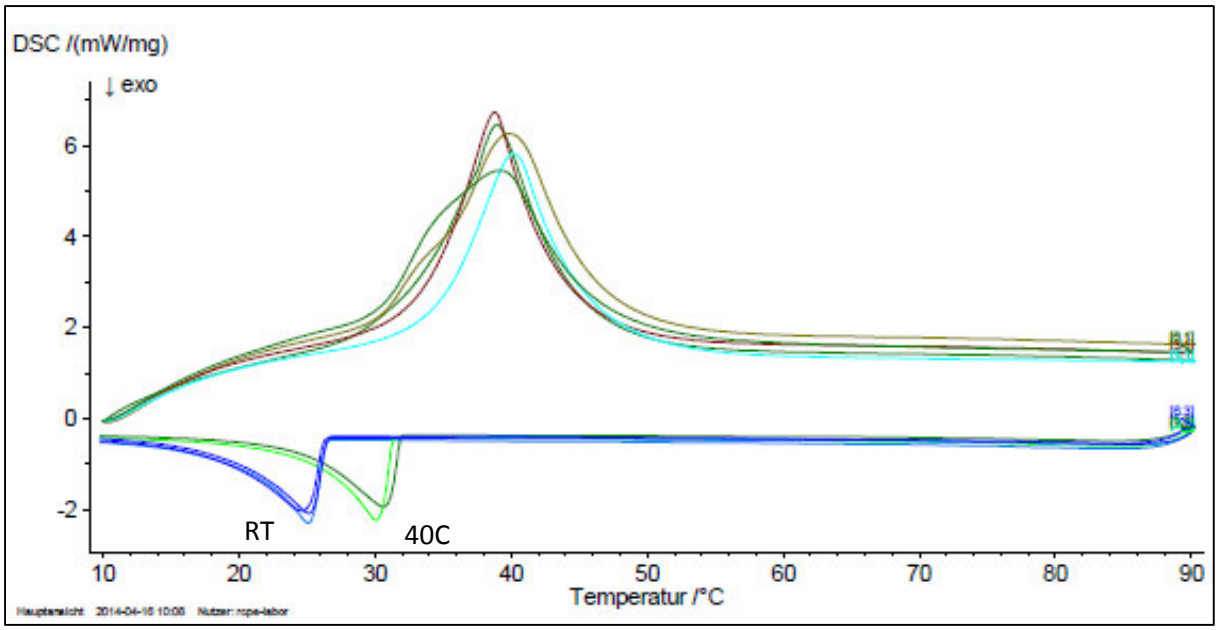

Figure 46. DSC analysis of pure Tween® 65 after four months storing.

To exclude the cleavage of stearic acid from the Tween® 65 molecule, this substance was also screened via DSC. As it can be seen in Figure 47, the melting of this substance starts at around 60°C, in comparison Tween® 65 has a melting point around 30°C. The DSC results confirm the SWAXS measurements and it can be concluded that there is no cleavage of stearic acid from the Tween® 65 molecule.

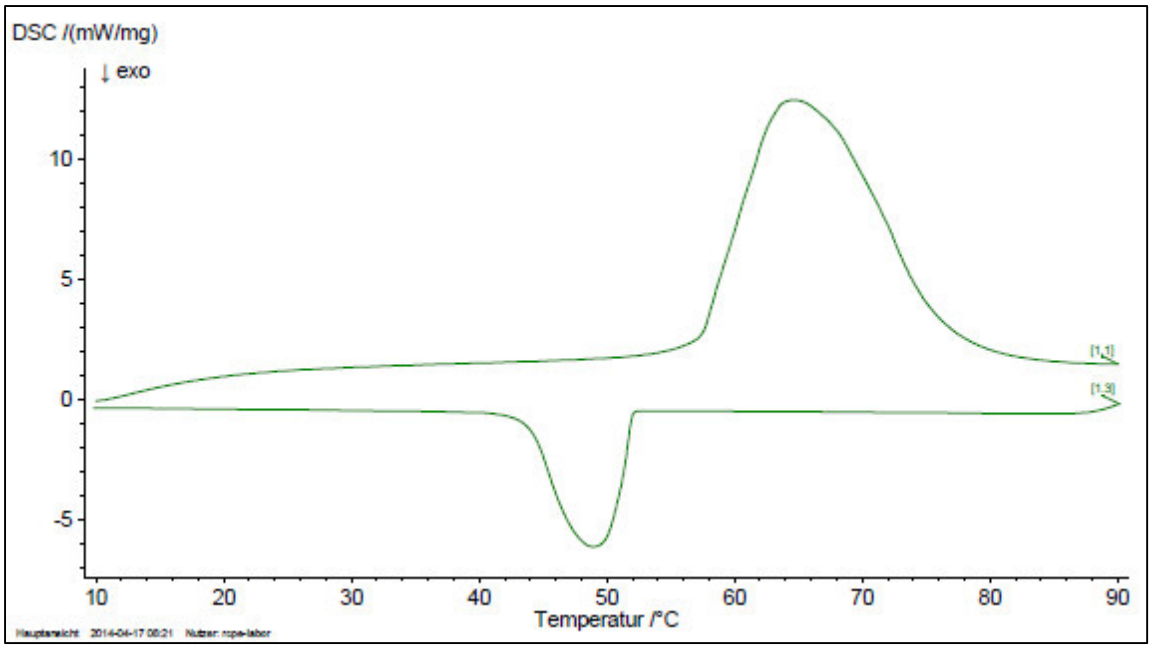

Figure 47. DSC analysis of pure stearic acid.

2.1 Storage of mixtures of Dynasan® 116 or Dynasan® 118 with Tween® 65

The DSC measurements of the samples consisting of Dynasan® 116 or Dynasan® 118 with Tween® 65 and analysized via SWAXS can be monitored here. It is clearly shown, that the additional signal observed in SWAXS after storage of samples is not due to the α polymorph. Figure 47 and 48 show the thermograms of pure Tween® 65, pure Dynasan® 116, and the mixture of Dynasan® 116 and 10% (w/w) and 50% (w/w)Tween® 65, respectively, freshly after preparation (Time 0) and after one month storage at room temperature (RT) and at 40°C. Figure 47 shows the β' polymorphism of the mixture of Dynasan 116 with 10% Tween® 65, which transforms to β in higher temperatures (40°C). Incraesing the ratio of Tween® 65 to 50%, the transformation to β occurs immediataley (Figure 49).

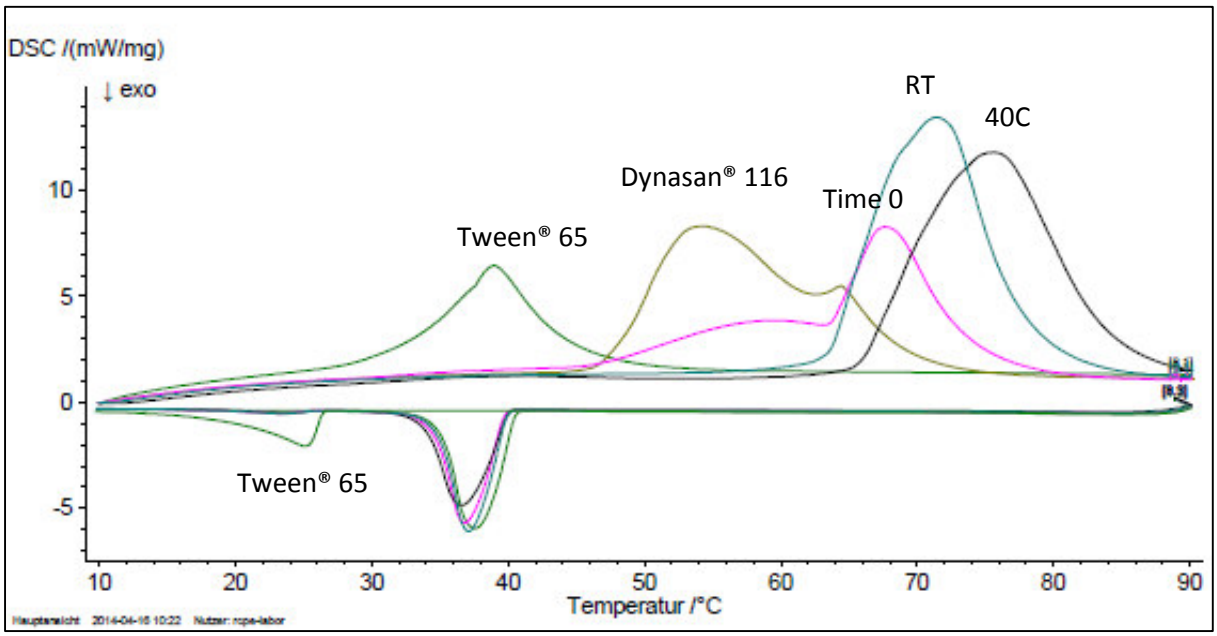

Figure 48. DSC measurement of the mixture of Dynasan® 116 and 10% (w/w) Tween® 65 after one month storage.

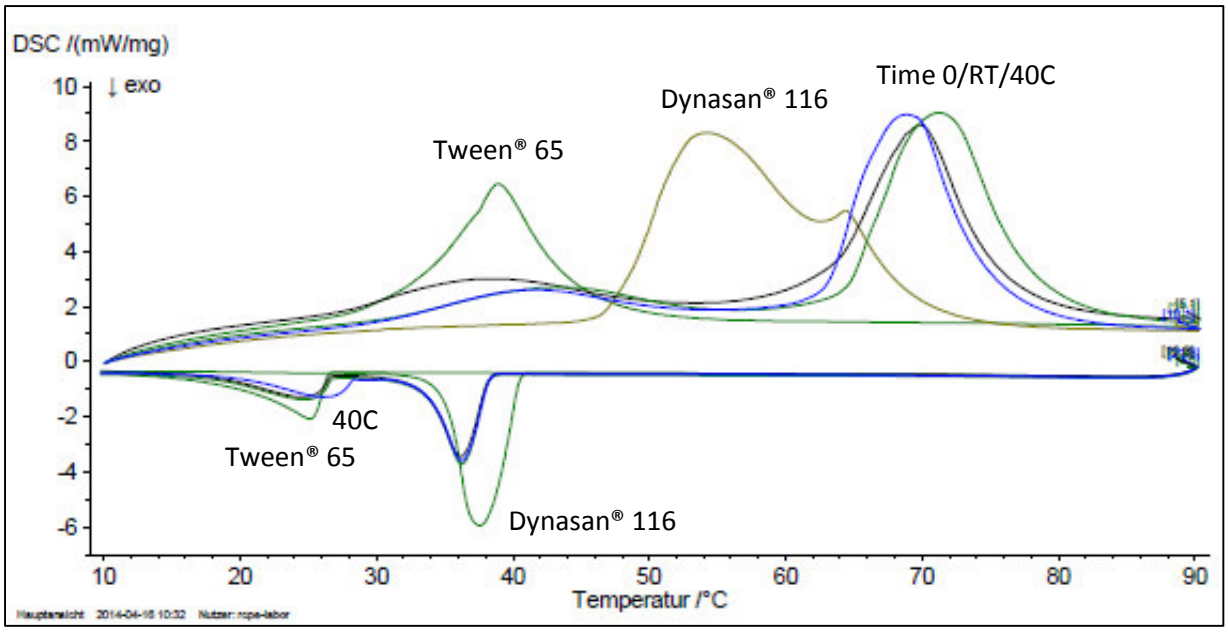

Figure 49. DSC measurement of the mixture of Dynasan® 116 and 50% (w/w) Tween® 65 after one month storage.

The same samples measured with SWAXS are investigated via DSC. It is clearly shown, that the additional signal observed in SWAXS (among all samples, from Dynasan® 116 and 10% (w/w) Tween® 65 to Dynasan® 116 and 50% (w/w) Tween® 65) cannot result from the α polymorph, as the DSC measurements and SWAXS clearly show the β or β prime form at time 0, respectively after storing at room temperature and/or 40°C. In the following Figure 50 to Figure 53), samples containing various amounts of Tween® 65, stored for two, respectively 4 months, are shown to clarify this result.

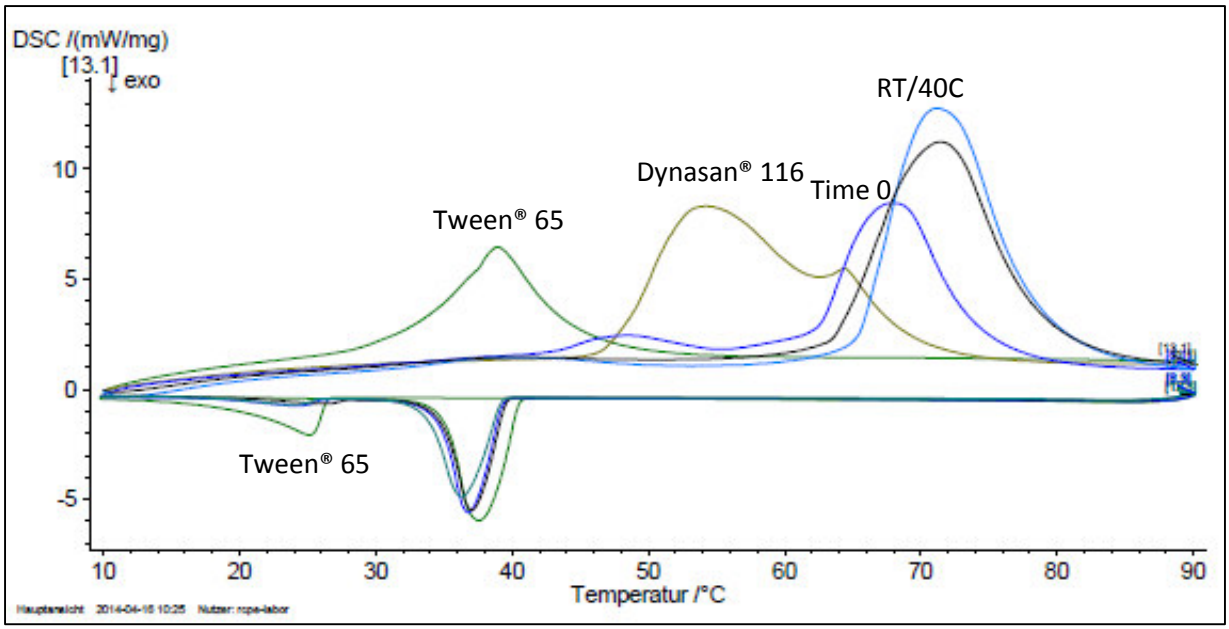

Figure 50. DSC measurement of the mixture of Dynasan® 116 and 20% (w/w) Tween® 65 after two month storage.

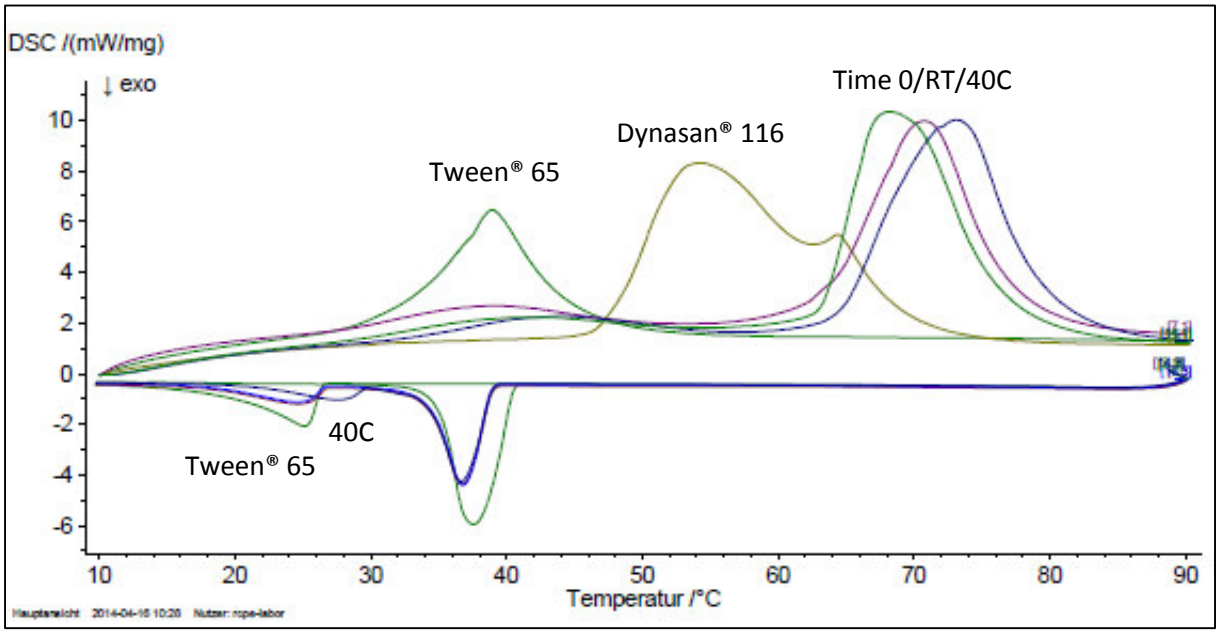

Figure 51. DSC measurement of the mixture of Dynasan® 116 and 40% (w/w) Tween® 65 after two month storage.

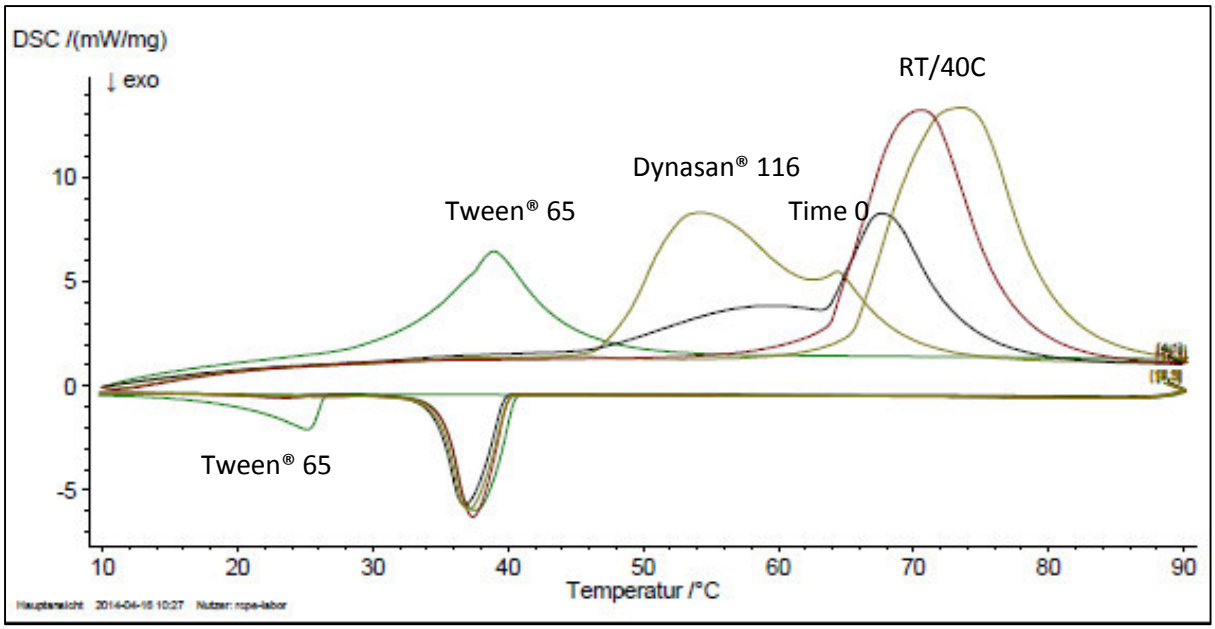

Figure 52.DSC measurement of the mixture of Dynasan® 116 and 10% (w/w) Tween® 65 after four month storage.

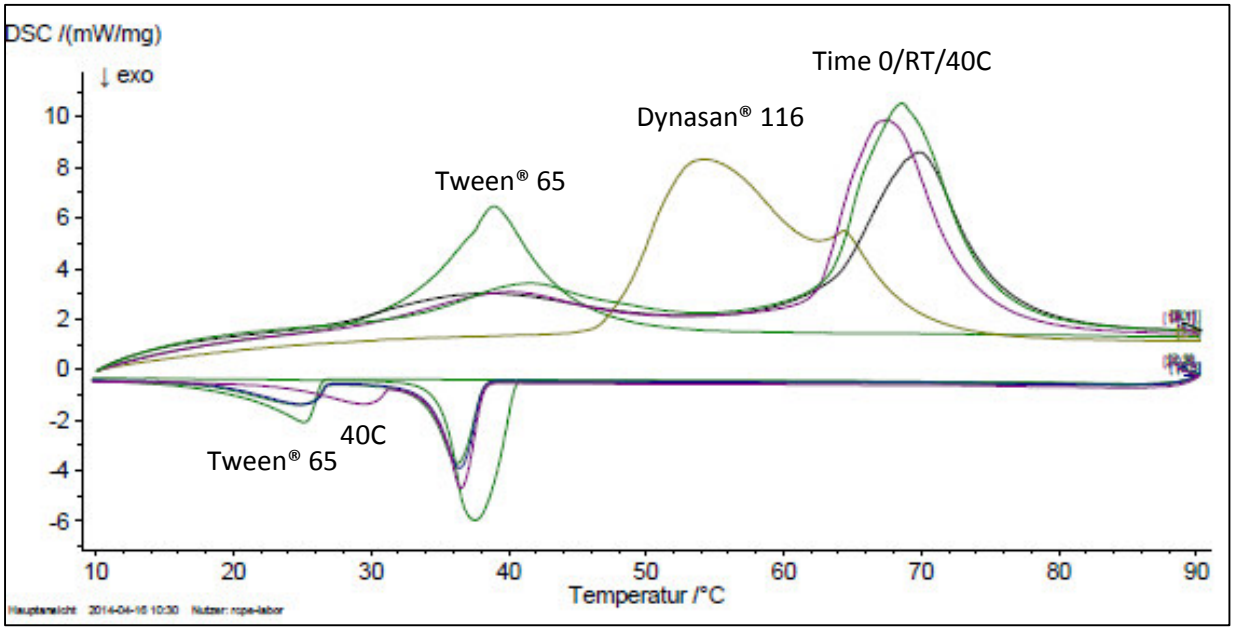

Figure 53. DSC measurement of the mixture of Dynasan® 116 and 50% (w/w) Tween® 65 after four month storage.

3. Contact angle measurement

Contact angle measurements were performed to investigate the phase separation more detailed. We assumed that having a smooth layer of API, coated with the mixture of Dynasan® and Tween® 65, the emulsifier would be located in the outer surface in the case of phase separation (and vs. for having a porous layer of API). Glass plain glass microscope slides and porous plates were used to imitate the smooth and porous layer of API, respectively and covered with different mixtures of lipid and emulsifier. Due to the different HLBs of lipids and Tween® 65 and different surface tensions between lipid and water or emulsifier and water, contact angle studies after preparation and after storage of samples can be used as a measure for phase separation.

3.1 Measurement on plain glass microscope slides

The results of the contact angle measurement directly after preparing the samples can be seen in Table 7, a regular drop can be observed in Figure 54. Both Dynasan® 116 and Dynasan® 118 have a high contact angle, which is due to their hydrophobic nature. Pure Tween® 65 has a contact angle of 25.5 (sd=±1), due to its hydrophilic behaviour (HLB value=10). Using mixtures of lipid and Tween 65, the higher the ratio of Tween® 65, the lower is the contact angle.

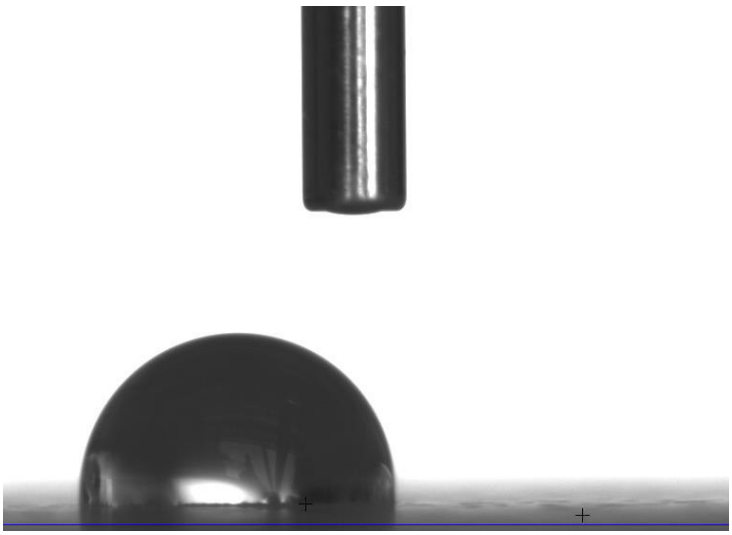

Figure 54. Regular drop during a contact angle measurement.

	Dynasan ® 116		Dynasan ® 118	
Amount of Tween® 65 [%]	Contact angle [°]	sd [±]	Contact angle [°]	sd [±]
0	107.7	2.5	110.6	2.0
10	104.9	1.3	101.5	2.3
20	101.3	2.0	102.1	2.2
30	64.0	1.9	55.3	2.5
40	56.1	1.3	53.2	1.7
50	53.7	2.0	54.4	1.8
100	25.5	1.0		

Table 7. Contact angle of the mixtures of Dynasan® 116 and Tween® 65 on plain glass microscope slides with water directly after preparing

3.1.1 Storage of samples

The prepared slides were stored at room temperature (25°C) and in a drying chamber at 40°C for one month. Afterwards the contact angle was measured again. The results are listed in Table 8 and 9 for Dynasan® 116 and 118, respectively, and compared with each other in Figures 56 to 59.

	Time 0	Dynasan ® 116 - room temperature		Dynasan ® 116 - 40°C	
Amount of Tween® 65 [%]	Contact angle [°]	Contact angle [°]	sd [±]	Contact angle [°]	sd [±]
0	107.7	112.8	6.1	153.2	6.1
10	104.9	155.4	6.7	151.6	6.1
20	101.3	151.9	7.6	126.6	5.5
30	64.0	72.5	2.9	54.6	2.1
40	56.1	65.1	3.9	47.3	1.5
50	53.7	61.0	1.4	45.9	1.6

Table 8. Contact angle of the mixtures of Dynasan ® 116 and Tween® 65 on plain glass microscope slides with water after one month storage.

Due to the heterogenous surface of samples, the reproducibility of measurements was not high enough. The contact angle of pure Dynasan® 116 does not change significantly after storage at room temperature (107.7° to 112.8°), but after storage at 40°C it increases up to 153.2°. Of note, that these measurements were very difficult, due to the extremely poor wettability of pure lipid. The

water drop does not fall down on the plate, as it can be observed in Figure 56, and adheres on the needle (Figure 57). The same phenomena occurs with 10% and 20% of Tween® 65 after storage at room temperature and with 10% after storage at 40°C (contact angles: 155.4°, 151.9° and 151.6°).
The increased contact angle of pure Dynasan 116 after storage at 40 °C can be due to the blooming effect. The transformation of α form to β after one month storage of pure Dynasan 116 at 40°C was shown with SWAXS data (Figures 19 and 20). This transformation is combined with morphological changes in the structure of lipid surface; the so-called blooming effect; which can additionally affect the wettability of surface and results in more increased contact angle [1].
Storage of samples containing 20% emulsifier at 40°C, the contact angle increases (126.6), but not as much as for the samples mentioned above. The contact angle of other samples (containing 30%-50 Tween 65) decreases clearly after storage at 40°C. With an amount of 30% Tween® 65 the contact angle dicreases from 72.5° to 54.6° (compared to 64.0° at time 0), with 40% of Tween® 65 it changes from 65.1° to 47.3° (compared to 56.1 at time 0), containing 50% of Tween® 65 the contact angle decreases from 61.0° to 45.9 (compared to 53.7 at time 0). This could be an indicator for a phase separation, more Tween® 65 in the surface leads to more wettability of the surface and decreased contact angles.

Comparing the results after different storage conditions shows that the addition of Tween® 65 to Dynasan® 116 up to 20%, the transformation of α polymorph to β may be partially due to the blooming effect, with higher values for contact angle. Increasing the amount of Tween® 65, the contact angle clearly decreases after storage at 40°C.

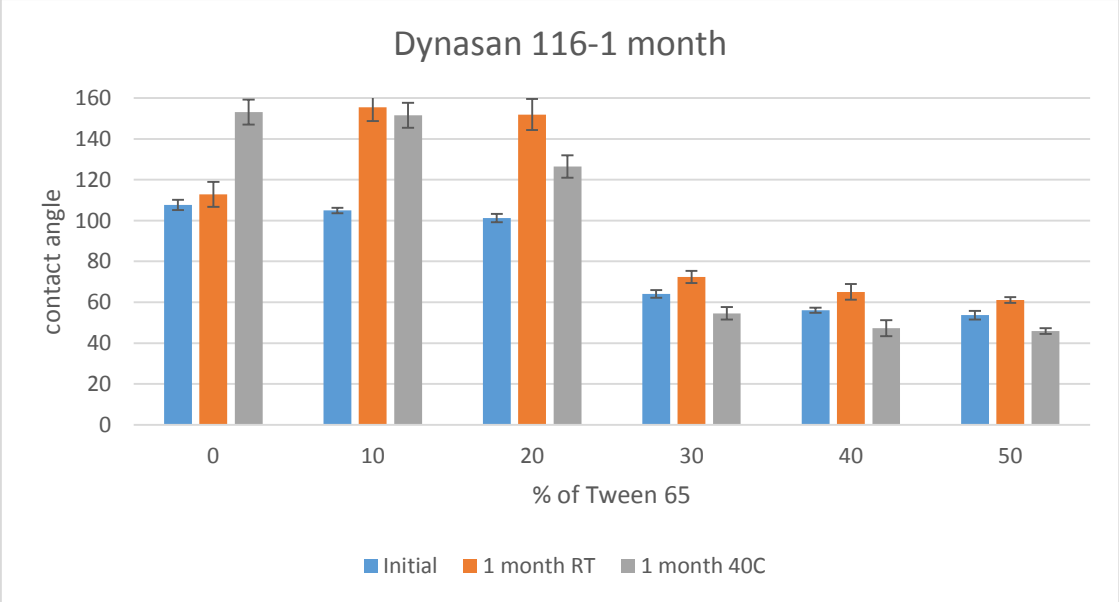

Figure 55. Diagram of contact angles of Dynasan® 116 and different amounts of Tween® 65 after one month of storage.

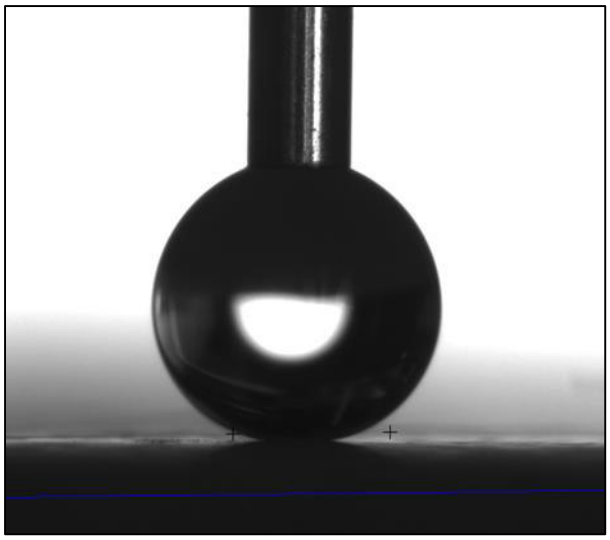

Figure 56. Water drop on the lipophilic surface.

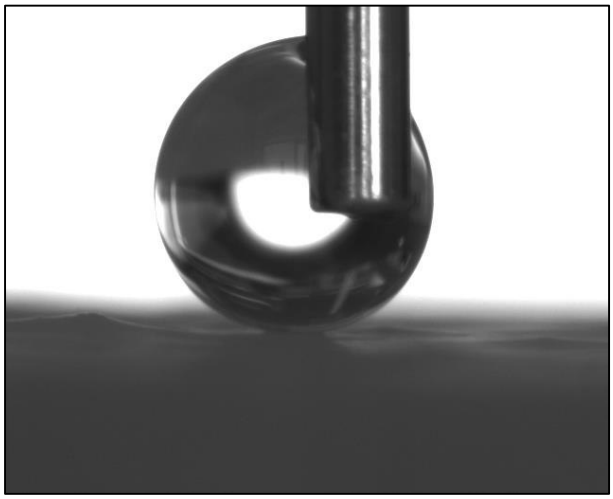

Figure 57. Water drop adheres at the needle.

	Time 0	**Dynasan ® 118 - room temperature**		**Dynasan ® 118 - 40°C**	
Amount of Tween® 65 [%]	Contact angle [°]	Contact angle [°]	sd [±]	Contact angle [°]	sd [±]
0	110.6	108.6	1.7	153.7	5.1
10	101.5	103.3	2.2	156.9	4.6
20	102.1	102.4	2.0	123.8	5.0
30	55.3	52.1	1.0	51.4	2.6
40	53.2	52.2	0.9	43.2	3.3
50	54.4	51.1	1.4	40.9	2.4

Table 9. Contact angle of the mixtures of Dynasan ® 118 and Tween® 65 with water after one month storage.

The contact angle for pure Dynasan ® 118 does not change significantly (110.6° to 108.6°) after storage at room temperature. After storage at 40°C, however, the same phenomena described for Dynasan ® 116, was also observed here. Storage of samples containing up to 20% Tween® 65 at 40°C resulted also in the increasing of contact angle. With an amount of 40% Tween® 65 the contact angle differs from 52.2 to 43.2 (compared to 53.2 at time 0) and samples containing 50% of Tween® 65 change from 51.1 to 40.8 (compared to 54.4 at time 0).

Again with lower amount of emulsifier the blooming effect prevails, the initial values are lower than the values after storage. Using 30% or more of Tween® 65, the contact angle decreases, which is maybe due to the phase separation.

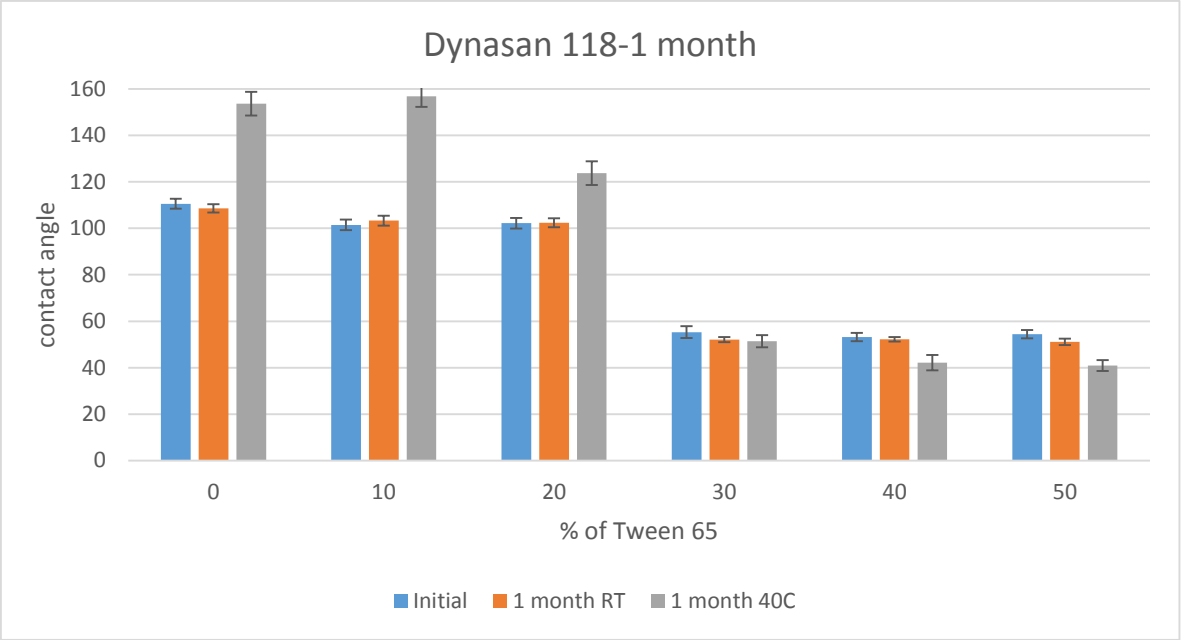

Figure 58. Diagram of contact angles of of Dynasan® 118 and different amounts of Tween® 65 after one month of storage.

The wettability of pure Tween® 65 after storage at room temperature could not be measured, the water drop disappears immediately as it can be observed in Figure 59.

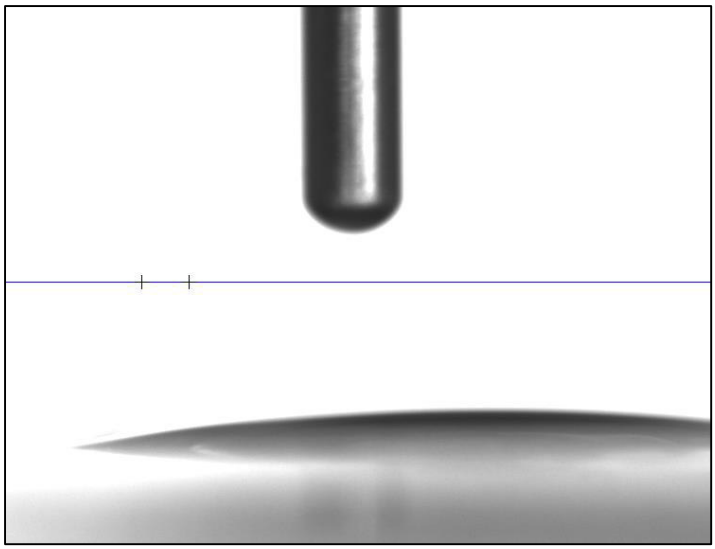

Figure 59. Contact angle measurement of pure Tween® 65 stored at room temperature.

Tables 10 and 11 show the contact angle of Dynasan® 116 and 118 with water, respectively, after 3 months storage at different conditions. In Figure 60 and Figure 61 the results of storage at room temperature or 40°C are compared.

	Time 0	**Dynasan® 116 - room temperature**		**Dynasan ® 116 - 40°C**	
Amount of Tween® 65 [%]	Contact angle [°]	Contact angle [°]	sd [±]	Contact angle [°]	sd [±]
0	107.7	110.5	5.1	-	-
10	104.9	-	-	-	-
20	101.3	138.7	7.7	128.8	6.8
30	64.0	68.9	1.8	50.3	2.1
40	56.1	60.6	4.0	46.4	1.1
50	53.7	59.1	2.3	43.4	1.7

Table 10. Results of the contact angle measurement after three months of storage for Dynasan ® 116.

The contact angle for pure Dynasan® 118 does not change significantly after storage at room temperature (110.6° at Time 0 to 108.6° after 3 months at room temperature), after storage at 40°C it was impossible to measure the contact angle. Samples containing 10% Tween® 65 could not also be measured after storage at 40°C and the drop adheres on the needle. After storing at room temperature, the contact angle changes from 101.4° at time 0 to 117.0°. For samples containing 20% Tween® 65, this phenomena slightly occurs after storage at room temperature (123.7° in comparison

to 102.1° at time 0), while after storing at 40°C the contact angle changes from 102.1° to 108.6°. Samples containing less Tween® 65 (0, 10 and 20%) show a higher standard deviation and the measurements were more difficult. As same as Dynasan 116, the samples containing ≥30 % (w/w) Tween 65 and stored at 40°C were affected more than the same samples stored at room temperature. As it can be seen in Figure 61, with an amount of 40% Tween® 65 the contact angle differs from 53.2° at Time 0 to 41.8° after three months storage at 40°C. Using 50% Tween 65, the contact angle with water decreased from 54.4° (time 0) to 40.7° after three months storage at 40°C.

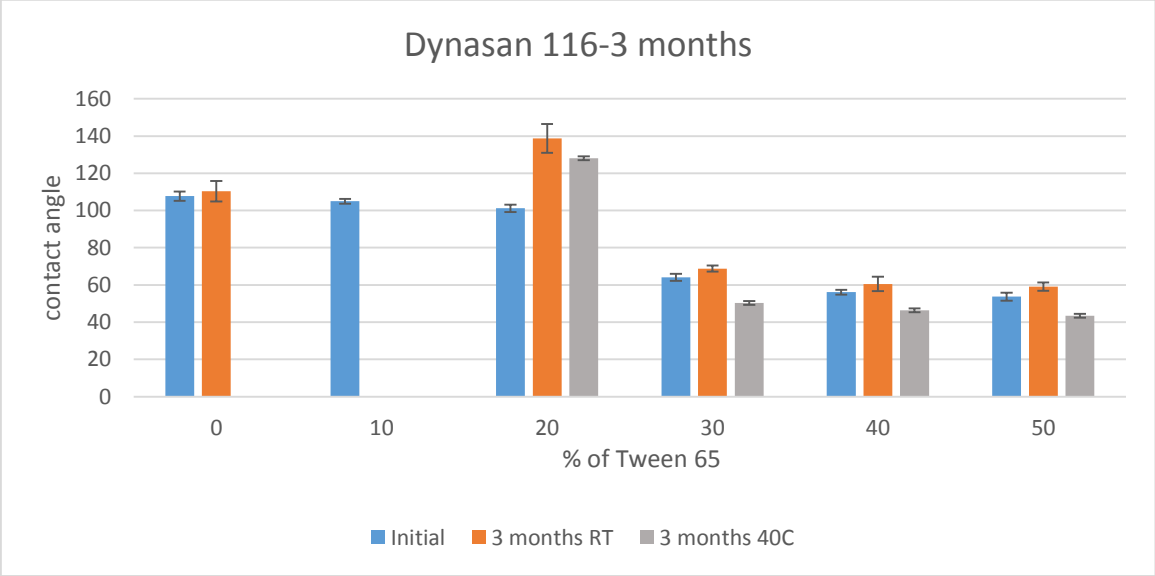

Figure 60. Diagram of contact angles of Dynasan® 116 and different amounts of Tween® 65 after three months of storage.

	Time 0	Dynasan ® 118 - room temperature		Dynasan ® 118 - 40°C	
Amount of Tween® 65 [%]	Contact angle [°]	Contact angle [°]	sd [±]	Contact angle [°]	sd [±]
0	110.6	108.6	3.9	-	-
10	101.5	117.0	6.6	-	-
20	102.1	123.7	4.1	108.6	4.1
30	55.3	51.4	2.3	45.7	2.3
40	53.2	50.4	2.5	41.8	1.8
50	54.4	49.7	2.5	40.7	2.4

Table 11. Results of the contact angle measurement after three months of storage for Dynasan ® 118.

The contact angle for pure Dynasan ® 118 does not change significantly after storage at room temperature (110.6° at Time 0 to 108.6 after 3 months at room temperature), after storage at 40°C it was impossible to measure the contact angle. Samples containing 10% Tween® 65 could not also be measured after storage at 40°C and the drop adheres on the needle. After storing at room temperature, the contact angle changes from 101.4 at time 0 to 117.0. For samples containing 20% Tween® 65, this phenomena slightly occurs after storage at room temperature (123.7 in comparison to 102.1 at time 0), while after storing at 40°C the contact angle changes from 102.1 to 108.6. Samples containing less Tween® 65 (0, 10 and 20%) show a higher standard deviation and the measurements were more difficult. As same as Dynasan 116, the samples containing ≥30 % (w/w) Tween 65 and stored at 40°C were affected more than the same samples stored at room temperature. As it can be seen in Figure 61, with an amount of 40% Tween® 65 the contact angle differs from 53.2° at Time 0 to 41.8° after three months storage at 40°C. Using 50% Tween 65, the contact angle with water decreased from 54.4° (time 0) to 40.7° after three months storage at 40°C.

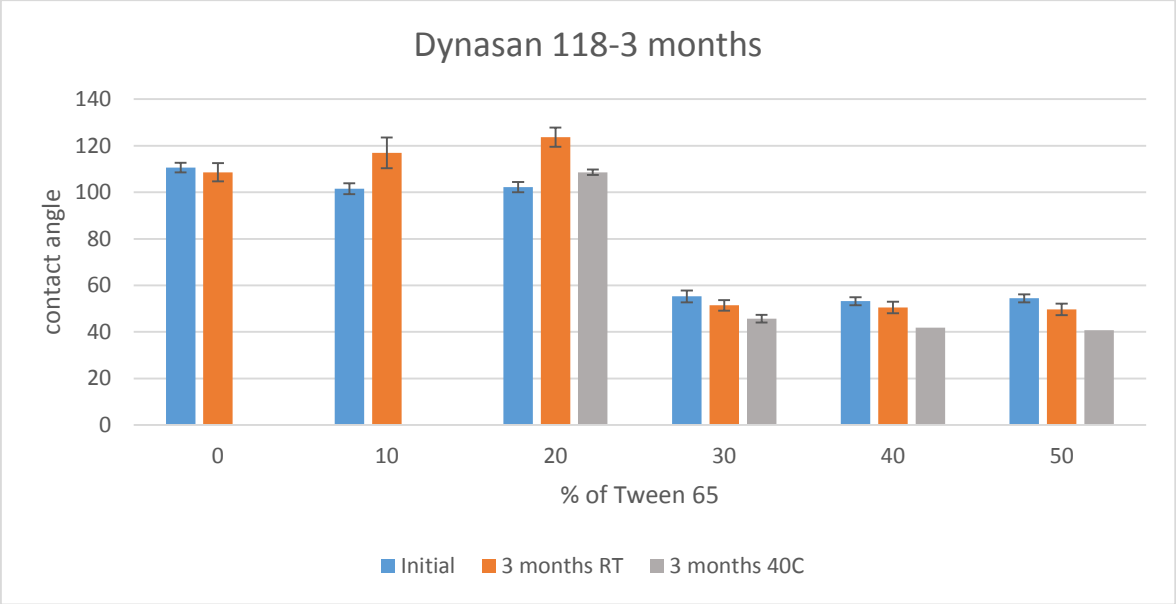

Figure 61. Diagram contact angles of Dynasan® 118 and different amounts of Tween® 65 after three months of storage.

To conclude, the results strongly indicate a phase separation, the plain glass microscope slides representing the smoothed surface API show a clear decrease of the contact angle after storing at 40°C in comparison to storage at room temperature.

3.2 Measurement on porous plate

The results of the contact angle measurement directly after preparing the samples can be seen in Table 12. In comparison to the plain glass microscope slides, the contact angle is slightly decreased with higher standard deviations, which is due to the rougher surface of the sample, as it can be clearly seen in Figure 62. Increasing the amount of Tween® 65 resulted in the more hydrophilic surface with better wettability and thus reducing in the contact angle with water.

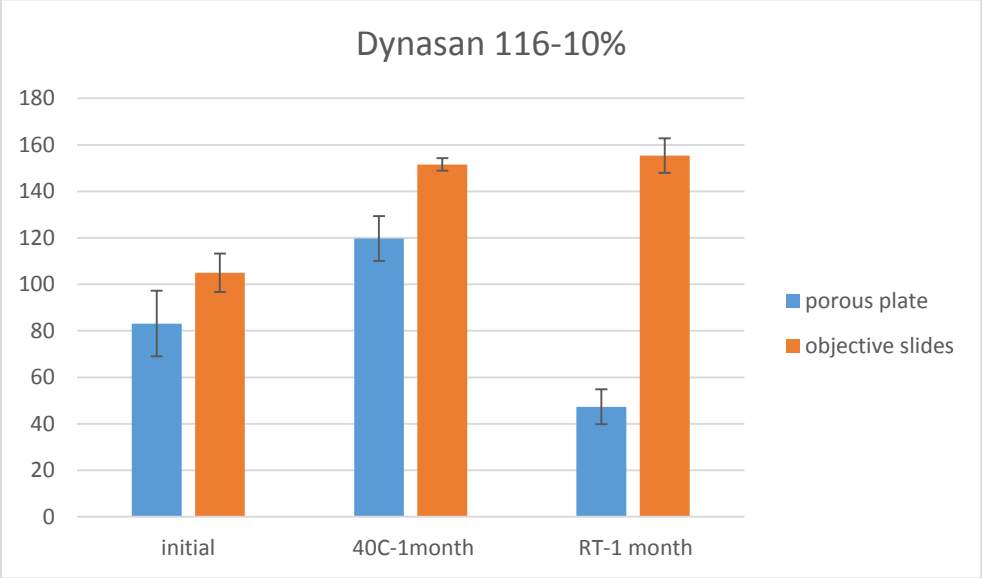

Figure 62. Comparison of contact angles of Dynasan® 116 containing 10% Tween® 65 measured on a porous plate and plain glass microscope slides.

	Dynasan ® 116		**Dynasan ® 118**	
Amount of Tween® 65 [%]	Contact angle	Standard deviation	Contact angle	Standard deviation
10	83.1	8.24	91.8	2.3
50	68.1	2.7	47.3	3.5

Table 12. Results of the contact angle measurement of mixtures of Dynasan® and Tween® on a porous plate directly after preparing.

3.2.1 One month storage

We assumed that in the case of phase separation, the contact angle should be increased after one month of storage due to the porous surface. The results of the measurements after one month are listed in Table 13 and Table 14-.Of note, that the measurements were difficult with low reproducibility (high standard deviations), which is due to the rough surface of the porous plates in combination with the increased lipophilicity of the surface.

For Dynasan® 116 containing 10% of Tween® 65, the contact angle is increasing from 83.1° to 119.9° and 125.8° after storage at 40°C and room temperature, respectively. Samples containing 50% emulsifier change from 68.1° to 112.6° after storing at 40°C, and to 108.6° after storing at room temperature. The same tendency can be observed using Dynasan® 118. For samples consisting of 10% Tween® 65, the contact angle increases from 91.8° to 102.6° after storing at room temperature. It was not possible to measure the contact angle after one month storage at 40°C, the water drop adhered to the needle, which indicates very high lipophilicity of the sample. For samples containing 50% emulsifier, the angle differs from 47.3° to 119.8° after storing at 40°C, respectively to 84.0° after storage at room temperature. This significant increase of the contact angle confirms the theory of having a phase separation in the lipid/emulsifier mixture. According to the porous surface, the emulsifier penetrates the pores, less emulsifier in the surface leads to worse wettability, as a consequence the contact angle increases.

	Dynasan ® 116 - room temperature		**Dynasan ® 116 - 40°C**		**Time 0**
Amount of Tween® 65 [%]	Contact angle	Standard deviation	Contact angle	Standard deviation	Contact angle
10	125.8	14.1	119.9	19.2	83.1
50	108.6	9.6	112.6	7.5	68.1

Table 13. Results of the contact angle measurement of mixtures of Dynasan® and Tween® 65 on a porous plate after one month of storage for Dynasan ® 116.

	Dynasan ® 118 - room temperature		Dynasan ® 118 - 40°C		Time 0
Amount of Tween® 65 [%]	Contact angle	Standard deviation	Contact angle	Standard deviation	Contact angle
10	102.6	5.1	-	-	91.8
50	84.0	7.7	119.8	8.0	47.3

Table 14. Results of the contact angle measurement of mixtures of Dynasan® and Tween® on a porous plate after one month of storage for Dynasan® 118.

Summing up, the results strongly indicate a phase separation, the plain glass microscope slides representing the smooth surface of API crystals show a decrease of the contact angle after storing at 40°C, while using the porous plate, representing porous systems like granules, leads to an increase of the contact angle after storage under the same condition.

4. FT-IR

The FT-IR measurements were used to investigate the coating material. The measurements were undertaken at time 0 and then the samples were stored at room temperature and in the drying chamber at 40°C for three months. The spectra of pure Dynasan® and Tween® 65 can be observed in Figure 63 to Figure 65.

Within the spectrum of Dynasan® 118, the $-CH_2$ and $-CH_3$ groups (2914 cm^{-1}, 2848 cm^{-1}, 1471 cm^{-1}) and the side chains (721 cm^{-1}) can be seen as well as the ester groups (1729 cm^{-1}, 1050-1300 cm^{-1}). The region below 1500 cm^{-1} is the so called fingerprint region, it is unique for every structure. In Figure 64, the spectrum of pure Dynasan® 116 is shown. It has nearly the same signals as Dynasan® 118, these two structures only differ in the length of the side chains, so again the $-CH_2$ and $-CH_3$ groups (2915 cm^{-1}, 2848 cm^{-1}, 1467 cm^{-1}, 1380 cm^{-1}), the side chains (721 cm^{-1}) and the ester groups (1736 cm^{-1}, 1050-1300 cm^{-1}) can be observed. In comparison, pure Tween® 65, seen in Figure 65, shows additional signals for the OH-group in the region between 3600 cm^{-1} and 3200 cm^{-1} and ether groups at 1098 cm^{-1} (C-O-C). These areas are of interest, as the samples containing different amounts of Tween® 65 can be distinguished. The other signals are similar do these of the Dynasan® 118 and 116, the $-CH_2$ and $-CH_3$ groups (2916 cm^{-1}, 1466 cm^{-1}), the side chains (721 cm^{-1}) and the ester groups (1736 cm^{-1}, 1050-1300 cm^{-1}) occur by Tween 65 as well.

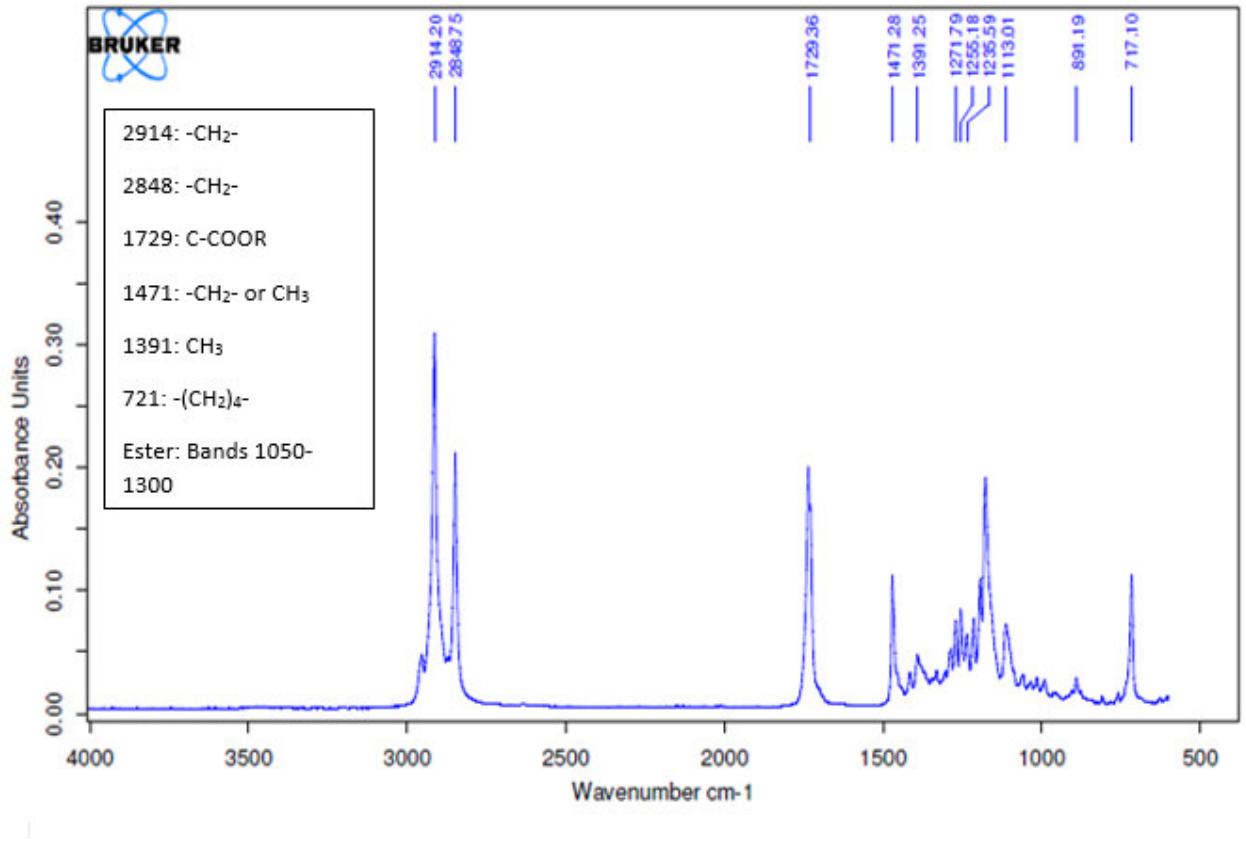

Figure 63. FT-IR spectrum of pure Dynasan® 118.

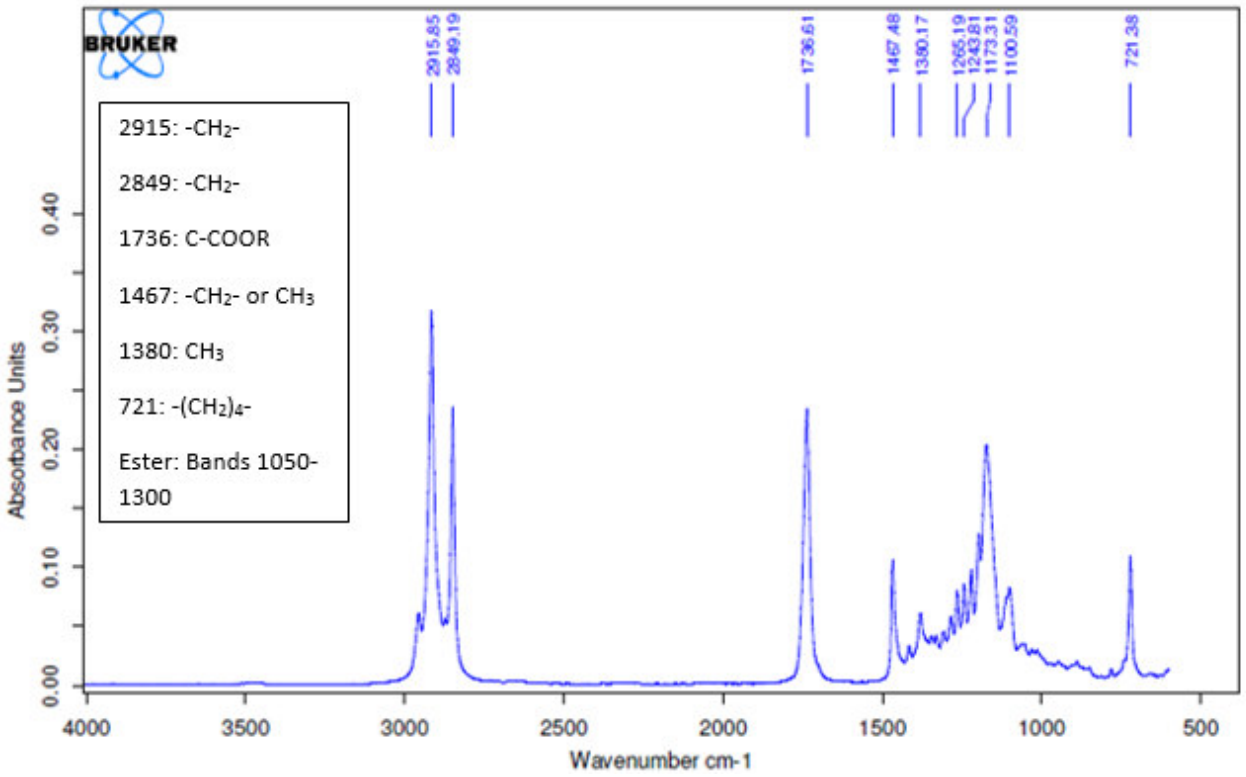

Figure 64. FT-IR spectrum of pure Dynasan® 116

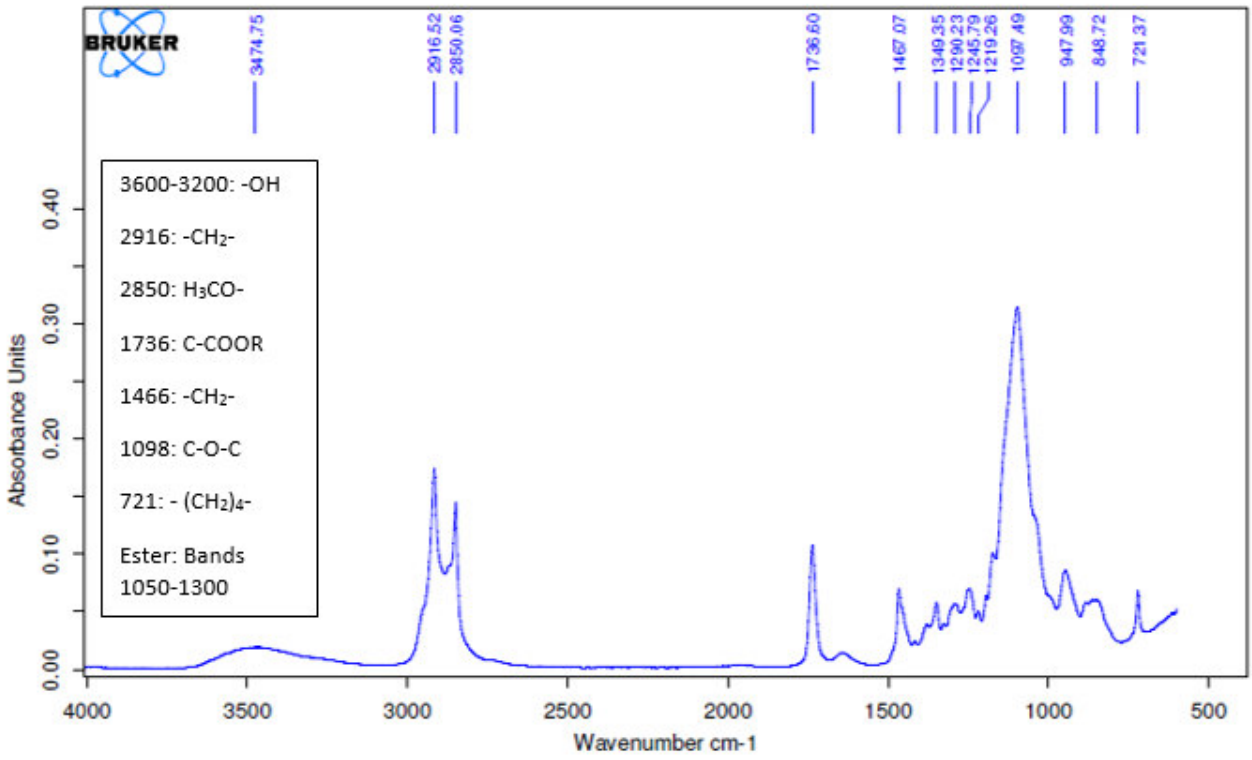

Figure 65. FT-IR spectrum of pure Tween® 65

4.1 Dynasan® 116

In the following figures (66 and 67), pure Dynasan® 116 and pure Tween® 65 are compared to different mixtures of both substances after storage. The obtained data is evaluated using SIMCA, in a SNV corrected spectrum, the wave number between 1055 cm^{-1} and 1115 cm^{-1} is studied. In this region the ether bond provides a difference between various samples. Figure 66, shows the spectra of samples containg 10% Tween 65 and stored under different conditions. No difference in the spectra of samples stored at room temperature and 40°C can be seen. In Figure 67, samples containing 50% Tween® 65 can be observed, but again no difference in the spectra can be seen. However, these samples show an additional signal at around 1087 cm^{-1}, compared to the samples measured immediately after preparation (Time 0). This could be attributable to changes in the polymorphism. All samples containing Dynasan® 116 and Tween® 65 (10%-50%) are in β polymorphism after one month of storing, whether the storing happens at room temperature or 40°C, so differences in the spectra's can be seen.

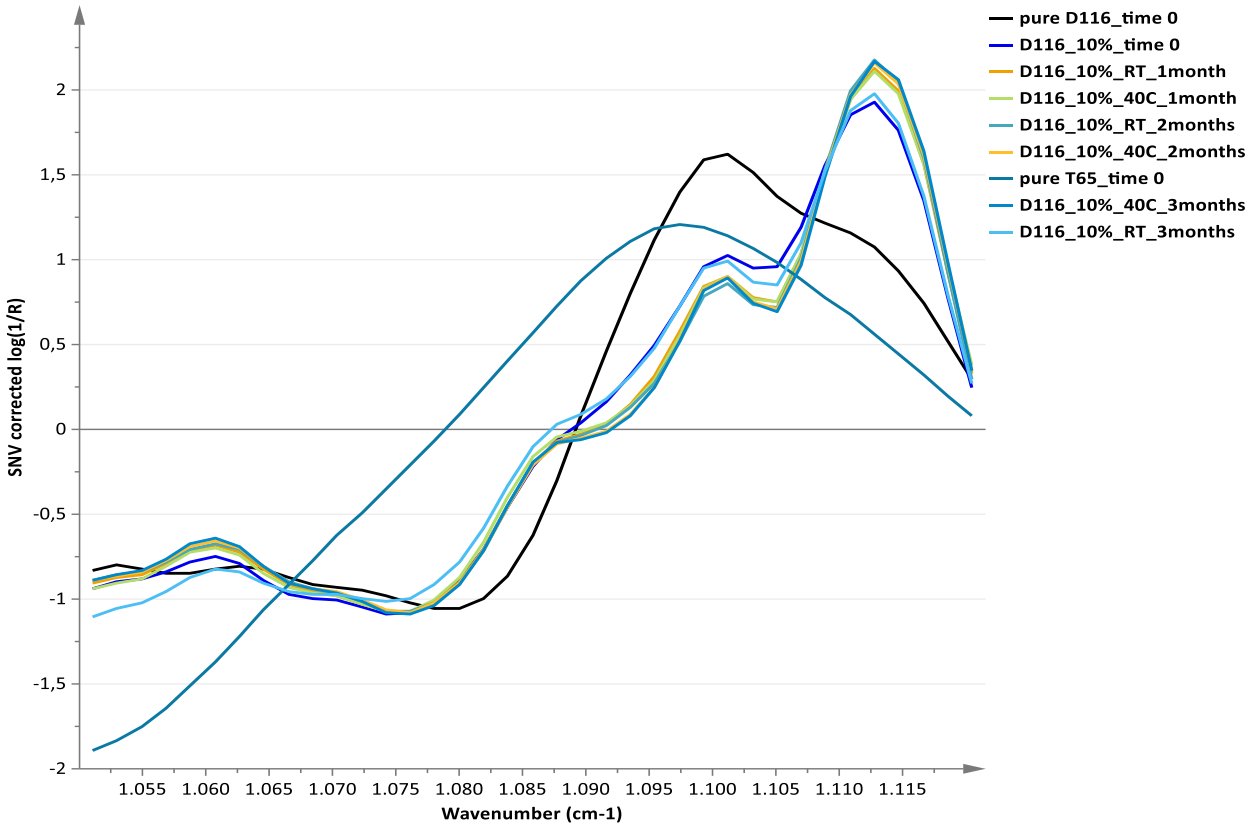

Figure 66. SNV spectra of samples containing 10% Tween® 65 and Dynasan 116.

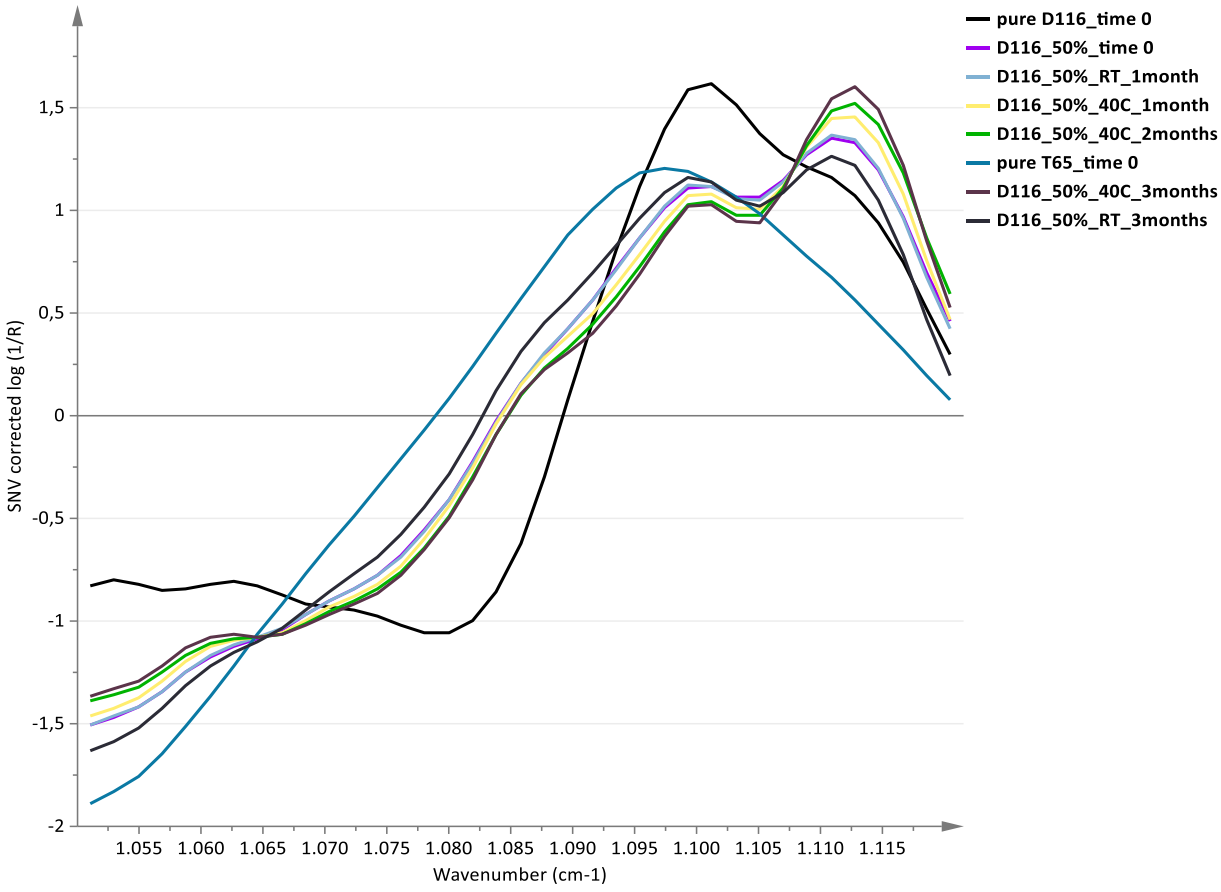

Figure 67. SNV spectra of samples containing 50% Tween® 65 and Dynasan 116.

4.2 Dynasan® 118

In the following figures, the spectra of pure Dynasan® 118 and pure Tween® 65 are compared to different mixtures of both substances after storage. The obtained data is evaluated using SIMCA, in a SNV corrected spectra, the wavenumber between 1055 cm^{-1} and 1115 cm^{-1} is studied. In this region there is a difference between the ether bonds of various samples. In Figure 68, samples containing 10% Tween® 65 can be seen. A clear difference between the samples stored at room temperature and 40°C can be observed. Samples stored at 40°C show an extra signal at a wave number of around 1087 cm^{-1}, compared to samples stored at room temperature. Furthermore, a signal at 1102 cm^{-1} is shifted to 1112 cm^{-1} and has a higher intensity. It must be said that samples stored at room temperature nearly show the same spectra as the sample measured at time 0. The same phenomena occurs with samples containing 20% and 30% of emulsifier (Figure 69, 30% Tween® 65). But again this effect could arise due to the polymorphic forms of Dynasan® 118. In Figure 70, pure Dynasan® 118 can be observed at different storage conditions. It can be clearly seen, that after storing at 40°C (β-polymorph) a different spectrum occurs in comparison to the samples at time 0 and stored at room temperature (α polymorph). Again, in samples containing 10% Tween® 65, a clear difference according to storage conditions can be seen, this samples are in α polymorph at time 0 and after storage at room temperature and in β polymorph after storage at 40°C.

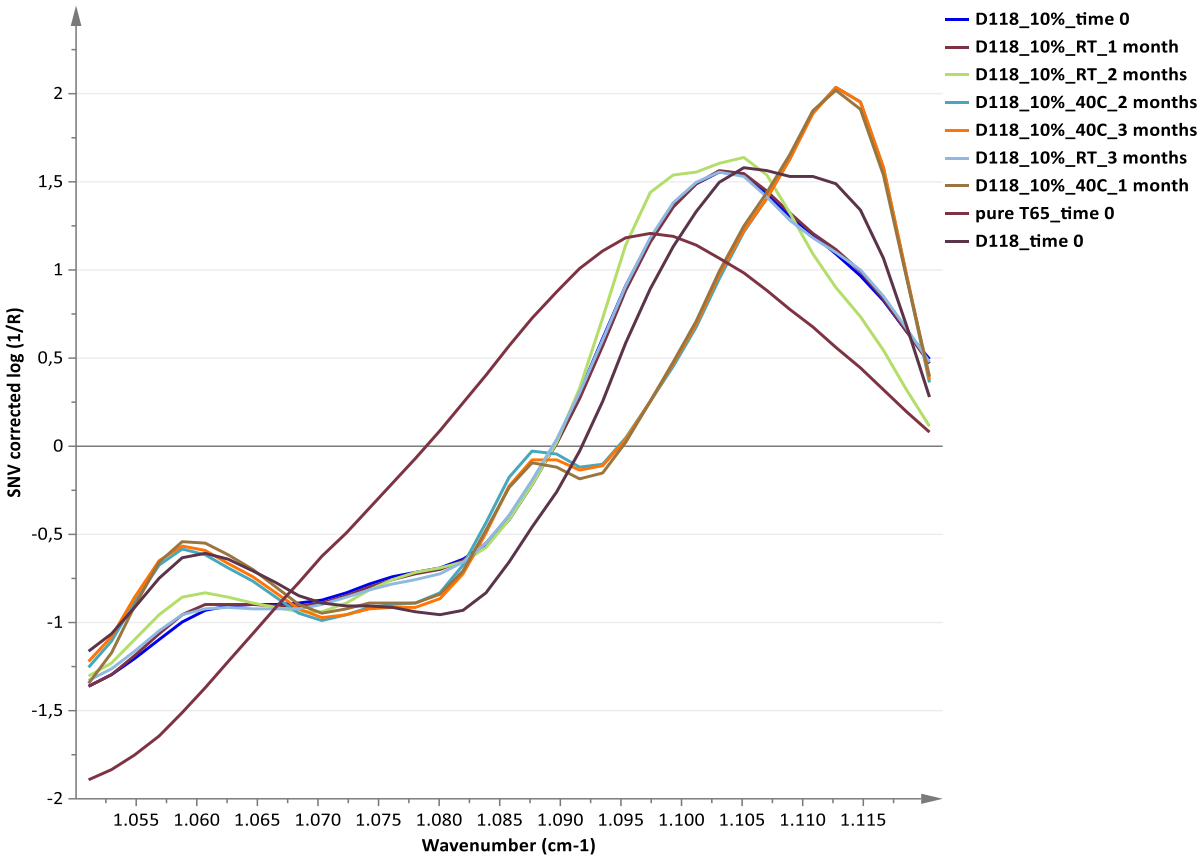

Figure 68. SNV spectra of samples containing 10% Tween® 65 and Dynasan 118.

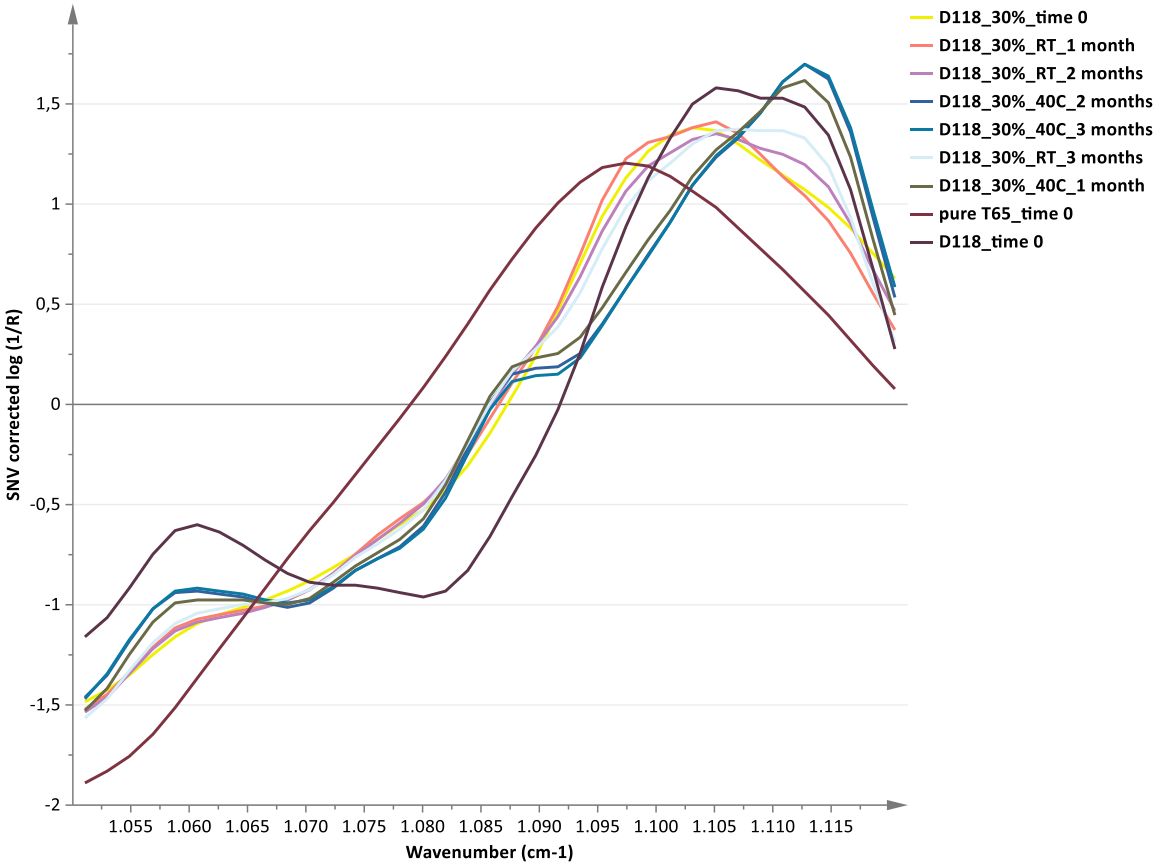

Figure 69. SNV spectra of samples containing 30% Tween® 65 and Dynasan 118.

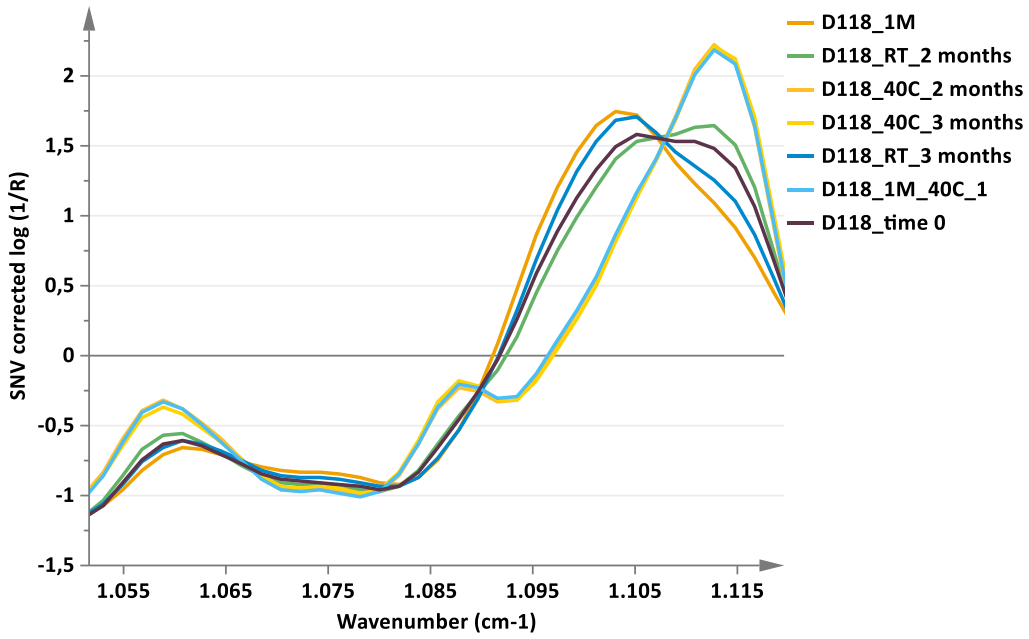

Figure 70. SNV spectra of pure Dynasan® 118 after different storing conditions.

If the amount of emulsifying agent is increased up to 40% or 50%, the extra signal also slightly appears after storage at room temperature. In this case, the shifted signal becomes very broad, the intensity is still decreased compared to samples stored at 40°C (Figure 71, 50% Tween® 65). Again, this could occur due to the polymorphic forms of Dynasan® 118, samples containing 40% or 50% Tween® 65 are in β polymorph after storage at room temperature and 40°C.

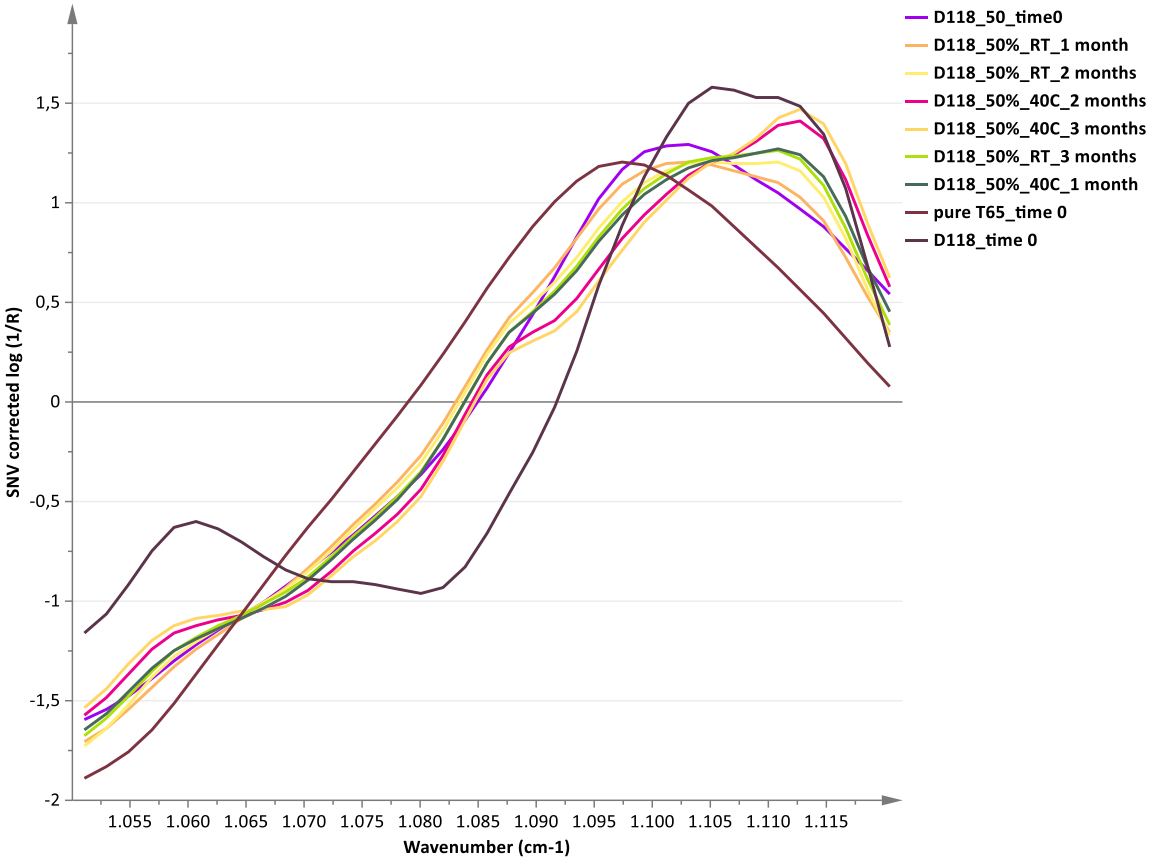

Figure 71. SNV spectra of samples containing 50% Tween® 65 and Dynasan® 118.

Summing up, FT-IR measurements could not use as a reference for phase separation. However it was possible to use them as an additional tool to confirm the changes in the polymorphism due to the changes in the amount of Tween 65 or different storage conditions.

V. Conclusion

This thesis deals with the assessment of properties of coating material containing tristearin or tripalmitin (Dynasan® 116 and Dynasan® 118, respectively) with different amounts of polysorbate 65 (Tween® 65) after preparation and after storage at different conditions. Changes in the polymorphism of lipids and phase separation after storage at room temperature and 40°C were studied using X-ray scattering, DSC, FT IR and the measurement of the contact angle of samples with water.

The obtained results can be used as a strong indication for phase separation of the coating after storage. The X-ray scattering of mixtures of lipid and Tween® 65 showed an extra signal at the area of pure Tween® 65 signal, depending on the concentration of Tween® 65 and storage conditions. With low amounts of emulsifier, this extra signal could only be observed after storage at 40°C. By increasing the amount of Tween® 65 to 50% (w/w), the extra signal could also be observed after storage at room temperature.

The contact angle measurements of the coated plain glass microscope slides with lipid or mixtures of lipid and Tween® 65 showed a clear increase of wettability after storing at 40°C. The plain glass microscope slides represent a smooth surface of API crystals and in this case a phase separation leads to an increased amount of emulsifier in the surface. In contrast, the contact angle of the coated porous plate, that imitates a rough surface (such as granules), significantly increased after storage. According to the porosity of the surface, it has been suggested that after a phase separation the emulsifier penetrates to the pores and lipid remains at the surface and leads to reduced wettability.

The FT-IR measurements show an extra signal and signal shifting due to the polymorphic transformation of Dynasan® 116 and Dynasan® 118. According to the damage of the surface during measurements, this method was not suitable for assessment of phase separation.

Bibliography

[1] K. Sato, “Crystallization behaviour of fats and lipids — a review,” *Chem. Eng. Sci.*, vol. 56, no. 7, pp. 2255–2265, Apr. 2001.

[2] K. Sato and T. Kuroda, “Kinetics of melt crystallization and transformation of tripalmitin polymorphs,” *J. Am. Oil Chem. Soc.*, 1987.

[3] M. Ollivon and R. Perron, “Measurements of enthalpies and entropies of unstable crystalline forms of saturated even monoacid triglycerides,” *Thermochim. Acta*, vol. 53, 1982.

[4] G. H. Charbonnet and W. . Singleton, “Thermal properties of fats and oils. VI. Heat capacity, heats of fusion and transition, and entropy of trilaurin, trimyristin, tripalmitin, and tristearin,” *J. Am. Oil Chem. Soc.*, 1947.

[5] R. Voigt, *Pharmazeutische Technologie*. Deutscher Apotheker Verlag, 2010.

[6] P. D. Hede, *Fluid Bed Particle Processing*. BookBoon, 2006.

[7] S. S. Behzadi, S. Toegel, and H. Viernstein, “Innovations in coating technology.,” *Recent Pat. Drug Deliv. Formul.*, vol. 2, no. 3, pp. 209–30, Jan. 2008.

[8] R. Turton, G. I. Tardos, and B. J. Ennis, *Flat-panel Display Technologies: Japan, Russia, Ukraine, and Belarus*. .

[9] R. Turton and X. X. Cheng, “The scale-up of spray coating processes for granular solids and tablets,” *Powder Technol.*, vol. 150, no. 2, pp. 78–85, Feb. 2005.

[10] (Cited 2013 Oct 14) available at

“http://www.glatt.com/cm/de/verfahrenstechniken/coating/spruehcoaten-in-der-wirbelschicht.html.” .

[11] “Practical aspects of encapsulation technologies,” 2002.

[12] (Cited 2013 Oct 4) available at

“http://www.glatt.com/cm/en/process-technologies/coating/fluid-bed-coating.html.” .

[13] V. Jannin and Y. Cuppok, “Hot-melt coating with lipid excipients,” *Int. J. Pharm.*, vol. 026, Oct. 2012.

[14] O. Glatter and O. Kratky, *Small Angle X-ray Scattering*. Academic Press Inc. (London) LTD, 1982.

[15] M. a Graewert and D. I. Svergun, “Impact and progress in small and wide angle X-ray scattering (SAXS and WAXS).,” *Curr. Opin. Struct. Biol.*, vol. 23, no. 5, pp. 748–54, Oct. 2013.

[16] G. Höhne, W. Hemminger, and H.-J. Flammersheim, *Differential Scanning Calorimetry*. Springer, 2003.

[17] (Cited 2014 Feb 11) available at

"http://www.kruss.de/services/education-theory/glossary/contact-angle/." .

[18] (Cited 2014 Feb 11) available at

"http://membranes.edu.au/wiki/index.php/Contact_Angle." .

[19] B. Schrader, *Infrared and Raman Spectroscopy: Methods and Applications*. VCH, 1995.

[20] M. Schmid, *Arzneistoff-und Arzneimittelanalytik*. Institut für Pharmazeutische Wissenschaften, Bereich Pharmazeutische Chemie, 2010.

[21] (Cited 2014 Feb 12) available at

"http://mmrc.caltech.edu/FTIR/FTIRintro.pdf." .

[22] R. White, *Chromatography/Fourier Transform Infrared Spectroscopy and its Applications*. Marcel Dekker Inc.

[23] (Cited 2014 Apr 17) available at

"http://www.retsch.com/products/milling/ball-mills/mixer-mill-cryomill/function-features/." .

[24] B. Aikin and C. Juhas, "Improvements in cryomill processing."

[25] (Cited 2013 Oct 14) available at

"http://www.pharmawiki.ch/wiki/index.php?wiki=Acetylcystein." .

[26] (Cited 2013 Oct 14) available at

"http://www.pharmxplorer.at/pharmxp/px/index1.php." .

[27] *European Pharmacopoeia 5.0.* Deutscher Apothekerverlag, 2005.

[28] (Cited 2013 Oct 14) available at

"http://de.academic.ru/dic.nsf/dewiki/1121281." .

[29] (Cited 2013 Oct 14) available at

"http://www.lebensmittellexikon.de/p0002340.php." .

[30] (Cited 2013 Oct 15) available at

"http://webbook.nist.gov/cgi/cbook.cgi?ID=C555431&Mask=8." .

[31] (Cited 2013 Oct 15) available at

"http://www.chemicalbook.com/ChemicalProductProperty_DE_CB9163652.htm." .

[32] M. Kellens, W. Meeussen, R. Gehrke, and H. Reynaers, “Synchrotron radiation investigations of the polymorphic transitions of saturated monoacid triglycerides . Part 1 " Tripalmitin and tristearin,” *Sci. Elsevier*, vol. 58, pp. 131–144, 1991.

[33] O. O. Mykhaylyk and C. M. Martin, “Effect of unsaturated acyl chains on structural transformations in triacylglycerols,” *Eur. J. Lipid Sci. Technol.*, vol. 111, no. 3, pp. 227–235, Mar. 2009.

[34] H.-D. Belitz, W. Grosch, and P. Schieberle, *Food Chemistry*. Springer, 2004.

VI. Appendix

List of Illustrations

[1] K. Sato, “Crystallization behaviour of fats and lipids — a review,” *Chem. Eng. Sci.*, vol. 56, no. 7, pp. 2255–2265, Apr. 2001.

[9] R. Turton and X. X. Cheng, “The scale-up of spray coating processes for granular solids and tablets,” *Powder Technol.*, vol. 150, no. 2, pp. 78–85, Feb. 2005.

[12] (Cited 2013 Oct 4) available at

“http://www.glatt.com/cm/en/process-technologies/coating/fluid-bed-coating.html.” .

[14] O. Glatter and O. Kratky, *Small Angle X-ray Scattering*. Academic Press Inc. (London) LTD, 1982.

[17] (Cited 2014 Feb 4) available at

“http://www.kruss.de/services/education-theory/glossary/contact-angle/.” .

[20] (Cited 2013 Feb 12) available at

“http://mmrc.caltech.edu/FTIR/FTIRintro.pdf.” .

[21] (Cited 2013 Apr 17) available at

“http://www.retsch.com/products/milling/ball-mills/mixer-mill-cryomill/function-features/.” .

[22] (Cited 2013 Oct 4) available at

“http://www.pharmawiki.ch/wiki/index.php?wiki=Acetylcystein.” .

[24] (Cited 2013 Oct 4) available at

“http://de.academic.ru/dic.nsf/dewiki/1121281.” .

[26] (Cited 2013 Oct 4) available at

"http://webbook.nist.gov/cgi/cbook.cgi?ID=C555431&Mask=8." .

[27] (Cited 2013 Oct 4) available at

"http://www.chemicalbook.com/ChemicalProductProperty_DE_CB9163652.htm." .

Table of equations

Equation 1: 11
Equation 2: 12
Equation 3: 13
Equation 4: 14
Equation 5: 18

Table of figures

Figure 1. Triacylglycerol molecule. 2
Figure 2. Polymorphism of a triacylglycerol molecule. [1] 2
Figure 3. Chain length structure. [1] 3
Figure 4. Molecular structures and Gibbs energy (*G*)-temperature relation of Dynasan® 116. 3
Figure 5. Schematic diagram of a fluid bed coating equipment (top spray) 6
Figure 6. Formation of a coated particle during a coating process. 8
Figure 7. A small and a bigger spherical particle 10
Figure 8. Different types of scattering curves 11
Figure 9. Contact angle of different samples. 18
Figure 10. Diagram of the contact angle. 19
Figure 11. Setup of a Fourier-Spectrometer. 21
Figure 12. Picture of a Retsch® cryomill. 22
Figure 13. Chemical structure of N-Acetylcysteine 23
Figure 14. Chemical structure of Tween® 65 24
Figure 15. Chemical structure of Dynasan® 118 25
Figure 16. Chemical structure of Dynasan® 116 26
Figure 17. WAXS Spectra of pure Dynasan ® 116 after 1 and 2 months. 32
Figure 18. SAXS Spectra of pure Dynasan ® 116 after 1 and 2 months. 32
Figure 19. WAXS Spectra of pure Dynasan ® 116 after 3 and 4 months. 33

Figure 20. SAXS Spectra of pure Dynasan ® 116 after 3 and 4 months. 33
Figure 21. WAXS Spectra of pure Dynasan ® 118 after 1 and 2 months. 34
Figure 22. SAXS Spectra of pure Dynasan ® 118 after 1 and 2 months. 34
Figure 23. WAXS Spectra of pure Dynasan ® 118 after 3 and 4 months. 35
Figure 24. SAXS Spectra of pure Dynasan ® 118 after 3 and 4 months. 35
Figure 25. WAXS Spectra of pure Tween ® 65 and after 1 and 2 months storage at room temperature and 40°C. 36
Figure 26. SAXS Spectra of pure Tween ® 65 and after 1 and 2 months storage at room temperature and 40°C. 36
Figure 27. SAXS Spectra of pure Tween ® 65 and after 3 and 4 months storage at room temperature and 40°C. 37
Figure 28. WAXS of pure stearic acid. 37
Figure 29. SAXS of pure stearic acid. 38
Figure 30. SAXS spectra of Dynasan® 116/10% Tween® 65 in comparison to pure substances after storing for one month. 39
Figure 31. SAXS spectra of Dynasan® 116/30% Tween® 65 in comparison to pure substances after storing for one month. 39
Figure 32. SAXS spectra of Dynasan® 116/50% Tween® 65 in comparison to pure substances after one month storage. 40
Figure 33. SAXS spectra of Dynasan® 116/20% Tween® 65 in comparison to pure substances after storing for two months 40
Figure 34. SAXS spectra of Dynasan® 116/10% Tween® 65 in comparison to pure substances after storing for four months. 41
Figure 35. SAXS spectra of Dynasan® 116/40% Tween® 65 in comparison to pure substances after storing for two months 41
Figure 36. SAXS spectra of Dynasan® 116/50% Tween® 65 in comparison to pure substances after storing for four months. 42
Figure 37. SAXS spectra of Dynasan® 118/10% Tween® 65 in comparison to pure substances after storing for one month. 43
Figure 38. SAXS spectra of cryomilled Dynasan® 116/10% Tween® 65 in comparison to molten sample containing 10% Tween® 65. 44
Figure 39. SAXS spectra of cryomilled Dynasan® 116/50% Tween® 65 in comparison to molten sample containing 50% Tween® 65. 44
Figure 40. SAXS spectra of cryomilled Dynasan® 118/10% Tween® 65 in comparison to molten sample containing 10% Tween® 65. 45

Figure 41. DSC analysis of pure Dynasan® 116 after two months storage. 46
Figure 42. DSC analysis of pure Dynasan® 116 after four months storing. 47
Figure 43. DSC analysis of pure Dynasan® 118 after two months storing. 47
Figure 44. DSC analysis of pure Dynasan® 118 after four months storing. 48
Figure 45. DSC analysis of pure Tween® 65 after two months storing. 48
Figure 46. DSC analysis of pure Tween® 65 after four months storing. 49
Figure 47. DSC analysis of pure stearic acid. 49
Figure 48. DSC measurement of the mixture of Dynasan® 116 and 10% (w/w) Tween® 65 after one month storage. 50
Figure 49. DSC measurement of the mixture of Dynasan® 116 and 50% (w/w) Tween® 65 after one month storage. 51
Figure 50. DSC measurement of the mixture of Dynasan® 116 and 20% (w/w) Tween® 65 after two month storage. 52
Figure 51. DSC measurement of the mixture of Dynasan® 116 and 40% (w/w) Tween® 65 after two month storage. 52
Figure 52.DSC measurement of the mixture of Dynasan® 116 and 10% (w/w) Tween® 65 after four month storage. 53
Figure 53. DSC measurement of the mixture of Dynasan® 116 and 50% (w/w) Tween® 65 after four month storage. 53
Figure 54. Regular drop during a contact angle measurement. 54
Figure 55. Diagram of contact angles of Dynasan® 116 and different amounts of Tween® 65 after one month of storage. 56
Figure 56. Water drop on the lipophilic surface. 57
Figure 57. Water drop adheres at the needle. 57
Figure 58. Diagram of contact angles of of Dynasan® 118 and different amounts of Tween® 65 after one month of storage. 58
Figure 59. Contact angle measurement of pure Tween® 65 stored at room temperature. 59
Figure 60. Diagram of contact angles of Dynasan® 116 and different amounts of Tween® 65 after three months of storage. 60
Figure 61. Diagram contact angles of Dynasan® 118 and different amounts of Tween® 65 after three months of storage. 61
Figure 62. Comparison of contact angles of Dynasan® 116 containing 10% Tween® 65 measured on a porous plate and plain glass microscope slides. 62
Figure 63. FT-IR spectrum of pure Dynasan® 118. 65
Figure 64. FT-IR spectrum of pure Dynasan® 116 65

Figure 65. FT-IR spectrum of pure Tween® 65 66
Figure 66. SNV spectra of samples containing 10% Tween® 65 and Dynasan 116. 67
Figure 67. SNV spectra of samples containing 50% Tween® 65 and Dynasan 116. 67
Figure 68. SNV spectra of samples containing 10% Tween® 65 and Dynasan 118. 69
Figure 69. SNV spectra of samples containing 30% Tween® 65 and Dynasan 118. 69
Figure 70. SNV spectra of pure Dynasan® 118 after different storing conditions. 70
Figure 71. SNV spectra of samples containing 50% Tween® 65 and Dynasan® 118. 71

Table of tables

Table 1. Melting points of Dynasan® 116. 4
Table 2. Melting points and corresponding enthalpies of fusion. 4
Table 3. The investigated samples of Dynasan® 116, Dynasan® 118 and Tween® 65 27
Table 4. DSC conditions for Dynasan® 116 and Dynasan® 118. 29
Table 5. Dynasan® 116 & 118: Transformation of α-from to β as response to temperature and adding emulsifier (Tween® 65) 31
Table 6. Storage time to get the β polymorph. 46
Table 7. Contact angle of the mixtures of Dynasan® 116 and Tween® 65 on plain glass microscope slides with water directly after preparing 55
Table 8. Contact angle of the mixtures of Dynasan ® 116 and Tween® 65 on plain glass microscope slides with water after one month storage. 55
Table 9. Contact angle of the mixtures of Dynasan ® 118 and Tween® 65 with water after one month storage. 57
Table 10. Results of the contact angle measurement after three months of storage for Dynasan ® 116. 59
Table 11. Results of the contact angle measurement after three months of storage for Dynasan ® 118. 60
Table 12. Results of the contact angle measurement of mixtures of Dynasan® and Tween® on a porous plate directly after preparing. 62
Table 13. Results of the contact angle measurement of mixtures of Dynasan® and Tween® 65 on a porous plate after one month of storage for Dynasan ® 116. 63
Table 14. Results of the contact angle measurement of mixtures of Dynasan® and Tween® on a porous plate after one month of storage for Dynasan® 118. 64

List of abbrevations

ADI: Acceptable Daily Intake

API: Active Pharmaceutical Ingredient

DSC: Differential Scanning Calorimetry

DSCs: Differential Scanning Calorimeters

EGA: Evolved Gas Analysis

FT-IR: Fourier-Transform Infrared spectroscopy

ICTAC: International Confederation for Thermal Analysis and Calorimetry

IR: Infrared spectroscopy

IUPAC: International Union of Pure and Applied Chemistry

LD: Letale Dosis

NAC: N-Acetylcysteine

NAPQI: N-acetyl-p-benzoquinone imine)

RT: room temperature

SAXS: Small angle X-ray scattering

TAG: Triacylglycerol

TG: Thermogravimetry

WAXS: Wide angle X-ray scattering